Arthritis & Rheumatology
Vol. 77, No. 3, March 2025, pp 283–297
DOI 10.1002/art.43028

American College of Rheumatology
Empowering Rheumatology Professionals

Targeting Long Noncoding RNA H19 in Subchondral Bone Osteocytes and the Alleviation of Cartilage Degradation in Osteoarthritis

Rongliang Wang,[1] Babak Mehrjou,[2] Dorsa Dehghan-Banian,[3] Belle Yu Hsuan Wang,[4] Qiangqiang Li,[1] Shuai Deng,[5] Chuanhai Liu,[6] Zhe Zhang,[7] Yanlun Zhu,[6] Haixing Wang,[3] Dan Li,[2] Xiaomin Lu,[3] Jack Chun Yiu Cheng,[8] Michael Tim Yun Ong,[9] Hon Fai Chan,[6] Gang Li,[3] Paul K. Chu,[2] and Wayne Yuk Wai Lee[10]

Objective. Emerging evidence suggests long noncoding RNA H19 is associated with osteoarthritis (OA) pathology. However, how H19 contributes to OA has not been reported. This study aims to investigate the biologic function of H19 in OA subchondral bone remodeling and OA progression.

Methods. Clinical joint samples and OA animal models induced by surgical destabilization of the medial meniscus (DMM) were used to verify the causal relationship between osteocyte H19 and OA subchondral bone and cartilage changes. MLO-Y4 osteocyte cells subjected to fluid shear stress were used to verify the mechanism underlying H19-mediated mechanoresponse. Finally, the antisense oligonucleotide (ASO) against H19 was delivered to mice knee joints by magnetic metal–organic framework (MMOF) nanoparticles to develop a site-specific delivery method for targeting osteocyte H19 for OA treatment.

Results. Both clinical OA subchondral bone and wildtype mice with DMM-induced OA exhibit aberrant higher subchondral bone mass, with more H19 mice expressing osteocytes. On the contrary, mice with osteocyte-specific deletion of H19 are less vulnerable to DMM-induced OA phenotype. In MLO-Y4 cells, H19-mediated osteocyte mechanoresponse through PI3K/AKT/GSK3 signal activation by EZH2-induced H3K27me3 regulation on protein phosphatase 2A inhibition. Targeted inhibition of H19 (using ASO-loaded MMOF) substantially alleviates subchondral bone remodeling and OA phenotype.

Conclusion. In summary, our results provide new evidence that the elevated H19 expression in osteocytes may contribute to aberrant subchondral bone remodeling and OA progression. H19 appears to be required for the osteocyte response to mechanical stimulation, and targeting H19 represents a new promising approach for OA treatment.

INTRODUCTION

Osteoarthritis (OA) is a common joint disease characterized by the degradation of articular cartilage, synovial inflammation, and bone remodeling.[1] Many risk factors are reported to incur or exacerbate OA development, such as aging, sex, obesity, and inherent genetic alterations; however, its etiology and pathogenesis remain elusive, and there is yet no disease-modifying drug

This work was mainly supported by the General Research Fund (reference 24121622), University Grants Committee, Hong Kong SAR; and partly by Area of Excellence (reference AoE/M-402/20) and Matching Grant Scheme, University Grants Committee, Hong Kong SAR; the "Start-up Fund" of The Chinese University of Hong Kong; a Rising Star Award provided by the American Society for Bone and Mineral Research; the Center for Neuromusculoskeletal Restorative Medicine (reference CT1.1), Health@InnoHK program, Innovation Technology Commission, Hong Kong SAR.

[1]Rongliang Wang, PhD, Qiangqiang Li, PhD: Department of Orthopaedics and Traumatology, Faculty of Medicine, Prince of Wales Hospital, The Chinese University of Hong Kong, Shatin, Hong Kong SAR, China; Li Ka Shing Institute of Health Sciences, The Chinese University of Hong Kong, Shatin, Hong Kong SAR, China; SH Ho Scoliosis Research Laboratory, Joint Scoliosis Research Center of the Chinese University of Hong Kong and Nanjing University, The Chinese University of Hong Kong, Shatin, Hong Kong SAR, China; and State Key Laboratory of Pharmaceutical Biotechnology, Division of Sports Medicine and Adult Reconstructive Surgery, Nanjing Drum Tower Hospital, The Affiliated Hospital of Nanjing University Medical School, Nanjing, China; [2]Babak Mehrjou, PhD, Dan Li, PhD, Paul K. Chu, PhD: Department of Physics, Department of Materials Science and Engineering, Department of Biomedical Engineering, City University of Hong Kong, Tat Chee Avenue, Kowloon, Hong Kong SAR, China; [3]Dorsa Dehghan-Banian, PhD, Haixing Wang, PhD, Xiaomin Lu, MSc, Gang Li, MBBS, D. Phil: Department of Orthopaedics and Traumatology, Faculty of Medicine, Prince of Wales Hospital, The Chinese University of Hong Kong, Shatin, Hong Kong SAR, China, and Li Ka Shing Institute of Health Sciences, The Chinese University of Hong Kong, Shatin, Hong Kong SAR, China; [4]Belle Yu Hsuan Wang, PhD: Department of Orthopaedics and Traumatology, Faculty of Medicine, Prince of Wales Hospital, The Chinese University of Hong Kong, Shatin, Hong Kong SAR, China; Li Ka Shing Institute of Health Sciences, The Chinese University of Hong Kong, Shatin, Hong Kong SAR, China; and Center for Neuromusculoskeletal Restorative Medicine, CUHK InnoHK Centres, Hong Kong Science Park, Hong Kong SAR, China; [5]Shuai Deng, PhD: Institute for Tissue Engineering and Regenerative Medicine, The Chinese University of Hong Kong, Shatin, Hong Kong SAR, China,

available to slow or reverse OA progression.[2] As one of the critical factors, mechanical loading was reported to exert anticatabolic and anabolic effects on cartilage, resulting in abnormal subchondral bone remodeling.[3] Therefore, reducing loading and/or blocking mechanotransduction in responsive joint tissues has been postulated to modify OA progression.

Subchondral bone remodeling is an important feature of OA pathology that is regarded as an aberrant mechanosensitive response upon injury during OA progression. Such alteration plays a vital role in cartilage degradation.[4] The resultant stiffer subchondral bone in late-stage OA could transmit more shear stresses to overlying cartilage, leading to cartilage splitting and fibrillation.[5] As a result, the disintegration of the subchondral bone physical boundary along OA progression results in more risk exposure in the cartilage environment, including vasculature, oxygen, nutrients, and cytokines.[1] Osteocytes constitute 90% to 95% of the total bone cells and play a major role in sensing and transmitting mechanical stimulation owing to their wide distribution throughout the bone matrix and their complex interconnected lacunocanalicular network.[6] Hence, osteocytes can respond to mechanical signals and secret soluble factors to regulate both osteoclast and osteoblast activities.[7] The intercellular communication required for such a feat is achieved by the production of biomolecules such as prostaglandins (produced by cyclooxygenase 2 [COX-2]), osteoprotegerin (OPG), RANKL, and dentin matrix protein 1 (DMP1).[8] Although some of these biomarkers have been reported to be associated with OA progression,[9–11] the role of osteocytes in OA subchondral bone remains elusive.

Long noncoding RNAs (lncRNAs) is a type of transcript having more than 200 nucleotides without protein encoding function.[12] Several lncRNAs have been found to be associated with OA severity and influence the functions of cells derived from OA joint tissues in vitro. The plausible roles of lncRNAs in various OA phenotypic changes, such as cartilage degradation, synovial inflammation, dysfunction of subchondral bone homeostasis, and meniscus injury, are yet to be elucidated.[13] lncRNA H19 (H19) is the first reported mammalian lncRNA and has been widely studied in different human diseases. Recent evidence primarily indicates an association between H19 and the cartilage and synovium changes in OA without a clear relationship.[14,15] In addition, H19 is involved in maintaining bone quality through regulation of osteoblast differentiation, bone regeneration, and bone metabolism.[16] Notably, H19 has been shown to influence the osteogenic differentiation capacity of bone marrow–derived mesenchymal stromal cells under tensile stimulation.[17] With these, it is reasonable for us to hypothesize that H19 may be able to influence subchondral bone remodeling in OA, particularly in response to altered mechanical alignment, thus potentially contributing to the progression of cartilage erosion and other pathologic changes.

Nanoparticles have been extensively used to deliver drugs and genes to tissue sites of interest for various purposes with no exemption in the OA research field.[18] Recently, the metal–organic frameworks (MOFs) have emerged as a promising tool for gene delivery with high loading capacity, good protection against biologic degradation, and excellent biocompatibility.[19] Furthermore, the modification of physiochemical properties on MOFs, for example, conjugation with the metallic nodes, organic linkers, and other compounds, enables their response to exogenous stimuli, such as a magnetic field for target delivery, thus facilitating localization at specific sites of interest and prolonged release applications.[20] In this study, to explore the translational value of targeting H19 for OA treatment, we developed a specific gene-delivery system by combining Fe_3O_4 nanoparticles and MOFs to form magnetic MOFs (MMOFs) and to transport anti-H19 antisense oligonucleotides (ASOs) to subchondral bone osteocytes in the presence of an external magnetic field for in vivo functional evaluation.

and Key Laboratory for Regenerative Medicine, Ministry of Education, School of Biomedical Sciences, Faculty of Medicine, The Chinese University of Hong Kong, Hong Kong SAR, China; [6]Chuanhai Liu, MD, Yanlun Zhu, PhD, Hon Fai Chan, PhD: Center for Neuromusculoskeletal Restorative Medicine, CUHK InnoHK Centres, Hong Kong Science Park, Hong Kong SAR, China; Institute for Tissue Engineering and Regenerative Medicine, The Chinese University of Hong Kong, Shatin, Hong Kong SAR, China; and Key Laboratory for Regenerative Medicine, Ministry of Education, School of Biomedical Sciences, Faculty of Medicine, The Chinese University of Hong Kong, Hong Kong SAR, China; [7]Zhe Zhang, PhD: Department of Orthopaedics and Traumatology, Faculty of Medicine, Prince of Wales Hospital, The Chinese University of Hong Kong, Shatin, Hong Kong SAR, China; Li Ka Shing Institute of Health Sciences, The Chinese University of Hong Kong, Shatin, Hong Kong SAR, China; and SH Ho Scoliosis Research Laboratory, Joint Scoliosis Research Center of the Chinese University of Hong Kong and Nanjing University, The Chinese University of Hong Kong, Shatin, Hong Kong SAR, China; [8]Jack Chun Yiu Cheng, MBBS, MD, Department of Orthopaedics and Traumatology, Faculty of Medicine, Prince of Wales Hospital, The Chinese University of Hong Kong, Shatin, Hong Kong SAR, China, and SH Ho Scoliosis Research Laboratory, Joint Scoliosis Research Center of the Chinese University of Hong Kong and Nanjing University, The Chinese University of Hong Kong, Shatin, Hong Kong SAR, China; [9]Michael Tim Yun Ong, MBChB, MSc: Department of Orthopaedics and Traumatology, Faculty of Medicine, Prince of Wales Hospital, The Chinese University of Hong Kong, Shatin, Hong Kong SAR, China; [10]Wayne Yuk Wai Lee, PhD: Department of Orthopaedics and Traumatology, Faculty of Medicine, Prince of Wales Hospital, The Chinese University of Hong Kong, Shatin, Hong Kong SAR, China; Li Ka Shing Institute of Health Sciences, The Chinese University of Hong Kong, Shatin, Hong Kong SAR, China; SH Ho Scoliosis Research Laboratory, Joint Scoliosis Research Center of the Chinese University of Hong Kong and Nanjing University, The Chinese University of Hong Kong, Shatin, Hong Kong SAR, China; and Center for Neuromusculoskeletal Restorative Medicine, CUHK InnoHK Centres, Hong Kong Science Park, Hong Kong SAR, China.

Drs R. Wang and Mehrjou contributed equally to this work.

Additional supplementary information cited in this article can be found online in the Supporting Information section (http://onlinelibrary.wiley.com/doi/10.1002/art.43028).

Author disclosures and graphical abstract are available at https://onlinelibrary.wiley.com/doi/10.1002/art.43028.

Address correspondence via email to Wayne Yuk Wai Lee, PhD, at waynelee@cuhk.edu.hk; to Paul K. Chu, PhD, at paul.chu@cityu.edu.hk; or to Gang Li, MBBS, D. Phil, at gangli@cuhk.edu.hk

Submitted for publication October 13, 2023; accepted in revised form September 13, 2024.

MATERIALS AND METHODS

A detailed description of the procedures and specific materials used for micro–computed tomography (micro-CT) analysis, histology and immunohistochemistry, fluorescence in situ hybridization (FISH), MLO-Y4 cell culture, fluid shear stress (FSS), RNA sequencing and analysis, real-time quantitative reverse transcription polymerase chain reaction, Western blot, synthesis of MMOF, in vitro ASO release assay, and in vivo biodistribution is provided in the Supplementary Methods.

Collection of clinical samples. Recruitment of patients was under strict guidance of clinical ethics approval from the Joint Chinese University of Hong Kong-New Territories East Cluster Clinical Research Ethics Committee (CREC-2013.248) and in compliance with the Declaration of Helsinki. Informed consent was obtained before surgery from all patients and their guardians. The subchondral bone tissue samples used in the study were collected from patients with knee OA undergoing joint replacement surgery (five women and seven men with an average ± SD age of 72.75 ± 5.817 years). Then the regions of interest were divided into different parts with a saw blade and subjected to different processing procedures to preserve the sample quality for RNA extraction and histologic and micro-CT analyses. Exclusion criteria were as follows: (1) patients with a history of surgical treatments or severe OA lesions of the lateral compartment or patellofemoral compartment, metabolic arthritis, joint infections, or mechanical pain caused by meniscal tears; (2) patients with malignancy, diabetes, or other severe diseases in the previous five years; and (3) patients with pathologic fractures, concomitant polytrauma or high-energy mechanism of injury.

Animals. The animal use and the experimental protocols were reviewed and approved by the Animal Experimentation Ethics Committee of The Chinese University of Hong Kong (ethical approval number 20-268-MIS). Osteocyte-specific deletion of H19 was obtained by crossing $H19^{fl/fl}$ mice (project number XM200616, Nanjing Biomedical Research Institute of Nanjing University) with transgenic mice expressing Cre recombinase under the control of the Dmp1 gene promoter (strain #: 023047, Jackson Laboratory). Dmp1-Cre^{+} $H19^{fl/fl}$ mice (referred to as conditional knockout [cKO] mice) and control Dmp1-Cre^{-} $H19^{fl/fl}$ (referred to as Flox mice) were used in the subsequent experiments. All mice were on a 100% C57BL/6 background. The primers for genotyping are listed in Supplementary Table 1.

Male C57BL/6 mice and Flox and cKO mice of around 12 weeks old were subjected to destabilization of the medial meniscus (DMM) surgery. From day 1 to day 3 post operation, the mice received buprenorphine (0.3 mg/kg of body weight) daily. The mice were allowed free to food, water, and cage activities after the operation.

In vivo therapeutic efficacy. After one week of DMM surgery, the C57BL/6 mice were randomly divided into six groups. Over a period of seven consecutive weeks, the mice received different treatments: ASO, MMOF, ASO-loaded MMOF at a dosage of 5 mg/kg, or phosphate buffered saline as vehicle control with concurrent six-hour magnetic field exposure once a week. Another group with ASO-loaded MMOF administration without magnetic field exposure served as the control group for magnetic cotreatment. Mice with a sham operation served as the positive control. To apply the external magnetic field, a 5 × 2 × 1–cm magnet was placed beside the targeted knee joint. Before magnetic field exposure, the mice were anesthetized using a mixture of ketamine and xylazine and maintained under isoflurane anesthesia throughout the six-hour period to ensure immobility. Three days after the last administration, the mice were killed to collect their knee joints and major organs for analysis.

Statistical analysis and data availability statement. All data are presented as mean ± SD, and n represents the number of tissue preparations, cells, or animals. In vitro experiments were performed in triplicates. Paired two-tailed Student's *t*-test was used for comparison between injured and uninjured groups of human bone samples. Unpaired two-tailed Student's *t*-test was used for comparison between two groups when data were normally distributed. One-way analysis of variance with relevant post hoc tests was used for multigroup comparisons. A P value of 0.05 was considered to be statistically significant using the GraphPad Prism software. The raw data that support the findings of this study will be openly available on publication in the GEO database (GSE254053).

RESULTS

Identification of H19 in subchondral bone alteration of OA. Subchondral bone tissues were collected from patients with OA undergoing total knee replacement surgery. The medial condyle side with severe cartilage erosion was labeled as injured, and the lateral condyle side with relatively intact cartilage was labeled as uninjured for internal control comparison (Figure 1A). Micro-CT showed a remarkable increase in the bone volume fraction in subchondral bone underneath the injured cartilage (Figure 1B, Supplementary Figure 1A and B). Notably, the expression level of the mechanical responsive proteins COX-2, OPG, and DMP1 in subchondral bone osteocytes was upregulated in the injured group (Figure 1B and C). In addition, FISH staining of H19 indicated a significantly higher ratio of H19-positive osteocytes in the subchondral bone of the injured group than that in the uninjured group (Figure 1B and C), which was further confirmed with a high expression level of *H19* observed in the subchondral bone of the injured group (Figure 1D). In the OA mouse model, OA phenotype was successfully developed in the knee joint with the meniscus

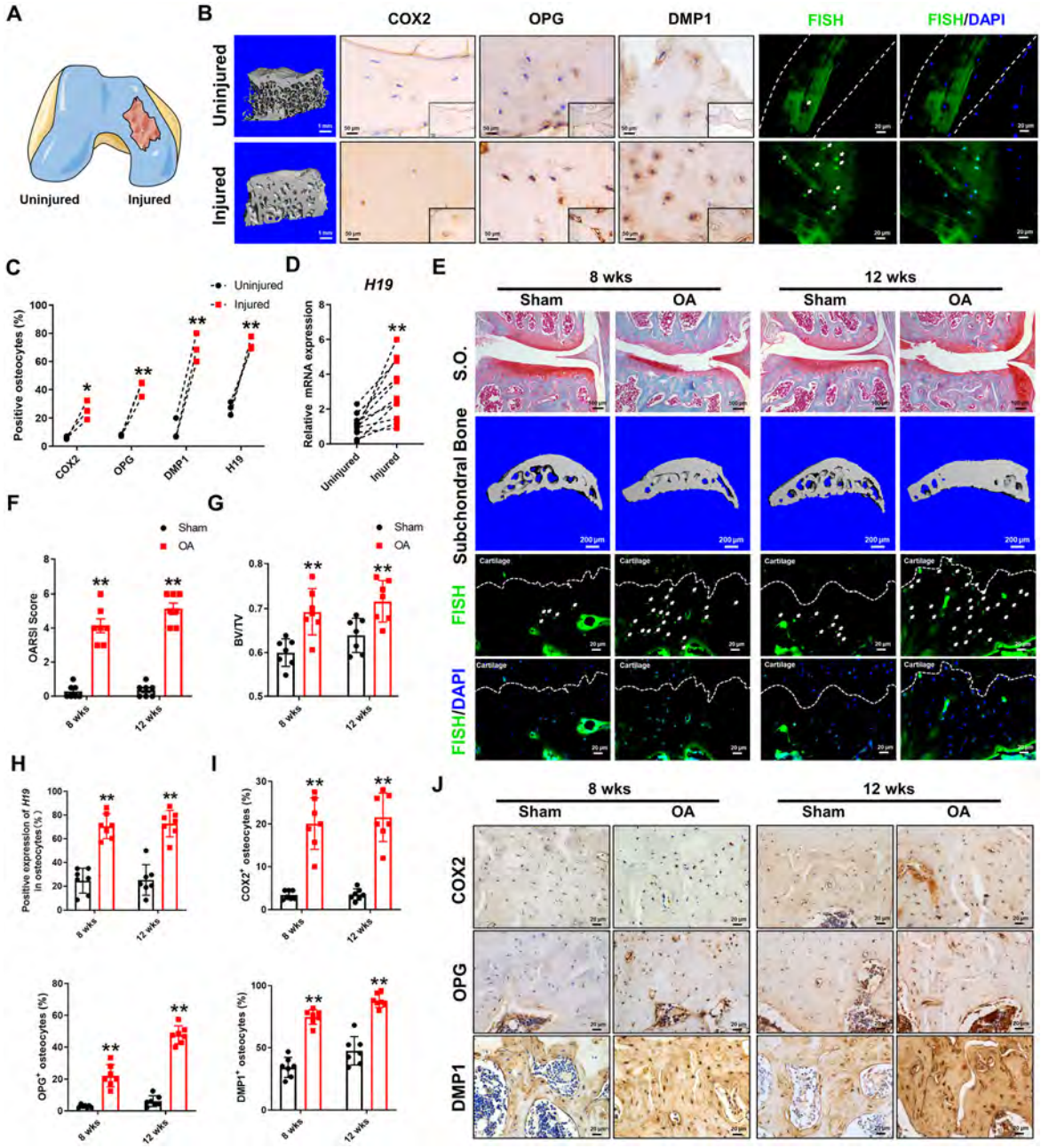

Figure 1. Elevated osteocyte H19 in subchondral bone during OA development. (A) Schematic illustration of the subchondral bone source from human OA samples. (B) Representative micro-CT 3D reconstruction of human OA subchondral bone; IHC staining for COX-2, OPG, and DMP1; and FISH staining of osteocytes counterstained with DAPI in human OA subchondral bone from the uninjured and injured groups (scale bar = 20 μm). (C) Quantification of the number for COX-2, OPG, DMP1, and H19-positive osteocytes in human OA subchondral bone. n = 3 in each group. (D) The expression of *H19* in human OA subchondral bone from the uninjured and injured groups was assessed by qPCR. n = 12 in each group. (E) Representative S.O. staining of knee joints (scale bar = 100 μm), micro-CT 3D reconstruction of subchondral bone (scale bar = 200 μm), FISH staining of osteocytes counterstained with DAPI (scale bar = 20 μm) in subchondral bone from C57BL/6 mice subjected to sham or DMM operation for 8 and 12 weeks. Quantitation of OA severity by (F) OARSI scores, (G) subchondral bone parameter (BV/TV), and (H) the percentage number for H19-positive osteocytes in subchondral bone for C57BL/6 mice subjected to sham or DMM operation for 8 and 12 weeks. n = 7 in each group. (I) The percentage number for COX-2-, OPG-, and DMP1-positive osteocytes in subchondral bone for C57BL/6 mice subjected to sham or DMM operation for 8 and 12 weeks. n = 7 in each group. (J) Representative IHC staining of subchondral bone for COX-2, OPG, and DMP1 in osteocytes from C57BL/6 mice subjected to sham or DMM operation for 8 and 12 weeks. n = 7 in each group (scale bar = 20 μm). *$P < 0.05$; **$P < 0.01$. 3D, three-dimensional; BV/TV, bone volume fraction; COX-2, cyclooxygenase 2; DMM, destabilization of the medial meniscus; DMP1, dentin matrix protein 1; FISH, fluorescence in situ hybridization; IHC, immunohistochemistry; micro-CT, micro–computed tomography; OA, osteoarthritis; OARSI, Osteoarthritis Research Society International; OPG, osteoprotegerin; qPCR, quantitative reverse transcription polymerase chain reaction; S.O., safranin O/fast green.

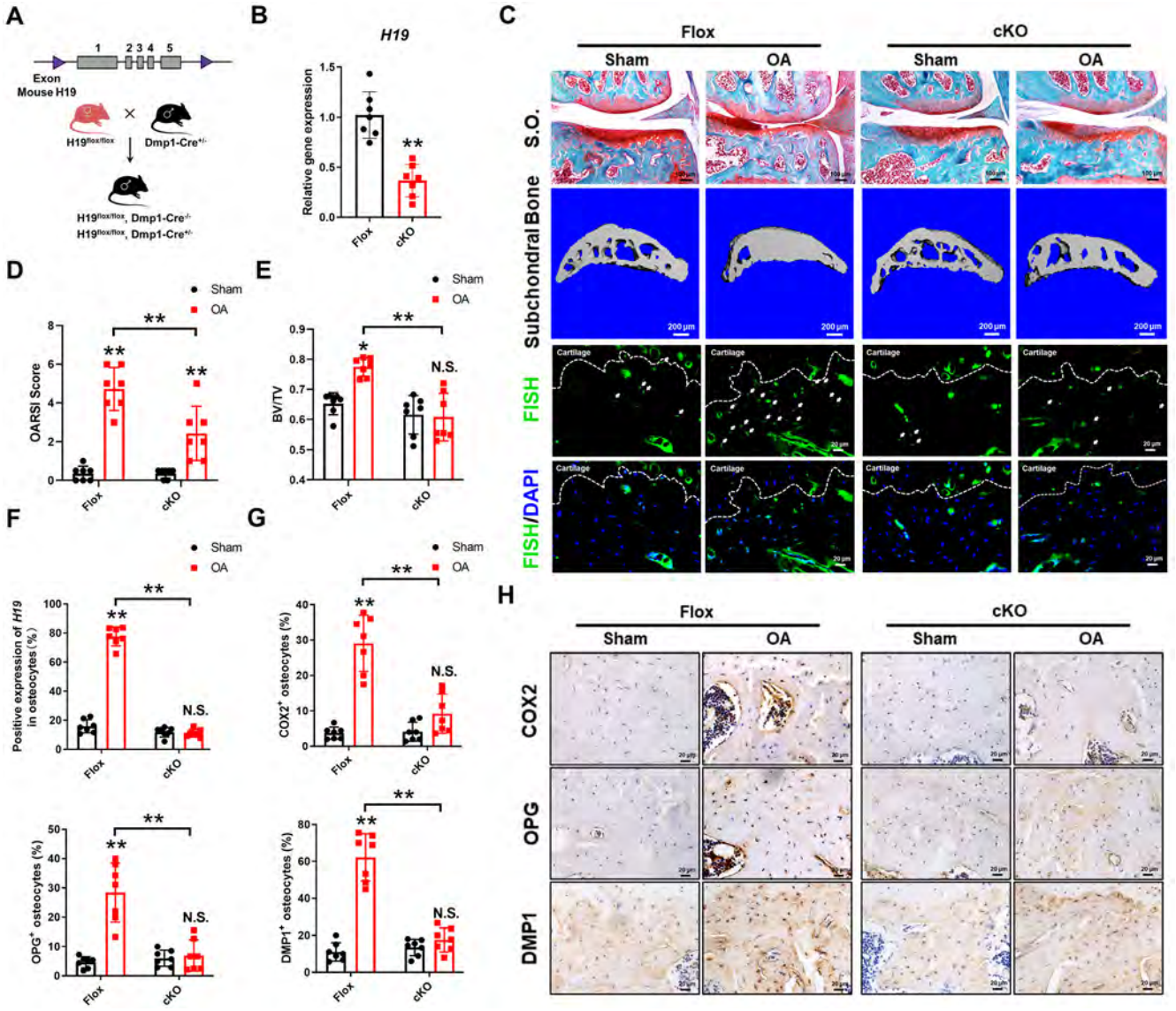

Figure 2. Mice with H19 deficiency are resistant to OA progression and subchondral bone remodeling. (A) Breeding strategy for generation of the osteocyte-specific H19 cKO mice. (B) The expression of *H19* in osteocyte-rich bone tissues of three-month-old male Flox and cKO mice was assessed by qPCR. n = 7 in each group. (C) Representative S.O. staining of knee joints (scale bar = 100 μm), micro-CT 3D reconstruction of subchondral bone (scale bar = 200 μm), and FISH staining of osteocytes counterstained with DAPI (scale bar = 20 μm) in subchondral bone from Flox and cKO mice subjected to sham or DMM operation for eight weeks. (D) Quantitation of OA severity by OARSI scores for three-month-old male Flox and cKO mice subjected to sham or DMM operation for eight weeks. n = 7 in each group. (E) Quantitation subchondral bone parameter (BV/TV) for three-month-old male Flox and cKO mice subjected to sham or DMM operation for eight weeks. n = 7 in each group. (F) Quantitation of the percentage number for H19-positive osteocytes in subchondral bone from Flox and cKO mice subjected to sham or DMM operation for eight weeks. n = 7 in each group. (G) The percentage number for COX-2-, OPG-, and DMP1-positive osteocytes in subchondral bone for three-month-old male Flox and cKO mice subjected to sham or DMM operation for eight weeks. n = 7 in each group. (H) Representative IHC staining of subchondral bone for COX-2, OPG, and DMP1, in osteocytes from Flox and cKO mice subjected to sham or DMM operation for eight weeks (scale bar = 20 μm). $^{*}P < 0.05$; $^{**}P < 0.01$. 3D, three-dimensional; BV/TV, bone volume fraction; cKO, conditional knockout; COX-2, cyclooxygenase 2; DMM, destabilization of the medial meniscus; DMP1, dentin matrix protein 1; FISH, fluorescence in situ hybridization; IHC, immunohistochemistry; micro-CT, micro–computed tomography; N.S., no significance; OA, osteoarthritis; OARSI, Osteoarthritis Research Society International; OPG, osteoprotegerin; qPCR, quantitative reverse transcription polymerase chain reaction; S.O., safranin O/fast green. Color figure can be viewed in the online issue, which is available at http://onlinelibrary.wiley.com/doi/10.1002/art.43028/abstract.

removed as shown by extensive lesion of articular cartilage and increased thickness of the subchondral bone at 8 and 12 weeks after DMM surgery (Figure 1E–G and Supplementary Figure 1C). Similar to human OA specimens, the expression of H19, COX-2, OPG, and DMP1 was found to be significantly up-regulated in mice OA joint, particularly in the osteocytes of the subchondral bone region (Figure 1H–J and Supplementary Figure 1D and E). These results suggest that osteocyte H19

expression is up-regulated and associated with abnormal structural changes in response to mechanical stress in OA subchondral bone.

cKO of osteocyte H19 in osteocytes mitigates cartilage damage and subchondral bone sclerosis in OA mouse model. To investigate the effect of osteocyte H19 on OA, we generated osteocyte H19 cKO mice by crossing the $H19^{fl/fl}$ mice (Flox) with the Dmp1-Cre transgenic mice (Figure 2A), which had significantly lower *H19* expression in osteocyte-enriched bone tissues (Figure 2B). At 12 weeks old, the H19 cKO mice were comparable to control Flox mice in terms of size, body weight, and bone quality (Supplementary Figure 2A–D). The knockout efficiency was verified by FISH staining in the trabecular and cortical bone tissues (Supplementary Figure 2E). The Flox mice showed degenerative cartilage damage and subchondral bone sclerosis at eight weeks post DMM surgery, whereas the cKO mice were found nearly invulnerable to DMM-induced cartilage and subchondral bone changes (Figure 2C and 2D and 2E and Supplementary Figure 2F). As expected, the degree of H19 up-regulation in subchondral bone osteocytes diminished in cKO mice (Figure 2C and F), associated with notable decreased protein expression of COX-2, OPG, and DMP1 in the subchondral bone osteocytes (Figure 2G and H). These results provide supporting evidence that H19 up-regulation in subchondral bone osteocytes can promote OA development and subchondral bone alteration.

H19-mediated mechanoresponse in MLO-Y4 cells. To explore the molecular mechanism underlying H19-mediated osteocyte mechanotransduction in OA, we first employed FSS stimulation on MLO-Y4 cells to mimic the mechanical stimulations that osteocytes experience in vivo[21] (Figure 3A). In line with previous studies, the application of FSS on MLO-Y4 cells resulted in the up-regulation of *Ptgs2*, *Tnfrsf11b*, the *Opg/Rankl* ratio, and *Dmp1* Figure 3B. Of note, prior H19 overexpression enhanced the response of MLO-Y4 cells toward FSS-induced up-regulations of these mechanoresponsive genes Figure 3B and Supplementary Figure 3A.[22] In contrast, knockdown of H19 by ASO reduced the mechanoresponse of MLO-Y4 cells to FSS-mediated up-regulation of *Ptgs2*, *Tnfrsf11b*, the *Opg/Rankl* ratio, and *Dmp1* (Figure 3C and Supplementary Figure 3B and C). Then bulk RNA sequencing analysis was conducted to compare ASO-treated and control MLO-Y4 cells upon FSS stimulation to determine the potential underlying mechanism. In brief, the 451 differentially expressed genes were found with expression level change more than 1.5 times in ASO-treated cells upon FSS stimulation. Twenty-six percent of genes were associated with environment information processing according to Kyoto Encyclopedia of Genes and Genomes (KEGG) pathway classification (Figure 3E). Of note, signal transduction was the most enriched one (53.8%), and a gene set enrichment analysis identified that most of the up-regulated genes were related to phosphatidylinositol 3-kinase (PI3K)/protein kinase B (AKT) signaling (Figure 3D and F and Supplementary Figure 3D). Consistent with previous results and RNA sequencing data in which PI3K/AKT signaling activation was involved in osteocyte-mediated intracellular mechanotransduction,[23] phosphorylation of AKT and glycogen synthase kinase 3 (GSK3) increased significantly upon concurrent FSS stimulation and H19 overexpression (Figure 3G). With H19 knockdown, FSS stimulation failed to activate the AKT/GSK3 signaling pathway in MLO-Y4 cells (Figure 3H and Supplementary Figure 3E). The pretreatment of LY290042, a PI3K inhibitor, prevented the up-regulation of H19 on AKT/GSK3 pathway activation and targeted expression of mechanotransduction (Figure 3I and Supplementary Figure 3F). Our data suggest that H19 participates as an enhancer of the PI3K/AKT/GSK3 signaling pathway in the mechanoresponse of osteocytes.

H19-mediated mechanoresponse and mechanotransduction via protein phosphatase 2A regulation. To further investigate the downstream target of H19 on mechanotransduction in osteocytes, we compared the differentially expressed genes related to the PI3K/AKT/GSK3 signaling pathway in ASO-treated and control MLO-Y4 cells upon FSS stimulation. Among the candidate signaling genes dysregulated by H19 reduction, *Ppp2r1a* and *Ppp2r5d* belong to the subunit genes of protein phosphatase 2A (PP2A) complex enzymes (Figure 4A), which is reported to be an important and ubiquitously expressed phosphatase for dephosphorylating AKT.[24] H19 overexpression or depletion, independent of FSS stimulation, influenced *Ppp2r1a* and *Ppp2r5d* expression in osteocytes (Figure 4B and C and Supplementary Figure 3G). To elucidate the role of PP2A in H19-mediated osteocyte mechanotransduction, the cells were pretreated with either DT-601 (PP2A activator) or okadaic acid (OKA; PP2A inhibitor) to interfere with PP2A before FSS stimulation. In the presence of DT-601, the up-regulated expression of *Ptgs2*, *Tnfrsf11b*, the *Opg/Rankl* ratio, and *Dmp1* in response to FSS stimulation and H19 overexpression was abolished (Figure 4D), whereas OKA restored the down-regulated expression of these marker genes caused by H19 knockdown despite the FSS stimulation (Figure 4E and Supplementary Figure 3H). In addition, the AKT/GSK3 signaling pathway activated by H19 overexpression was suppressed by DT-601 (Figure 4F). In contrast, OKA treatment promoted activation of the AKT/GSK3 signaling pathway even in H19 deficiency (Figure 4G and Supplementary Figure 3I). These results indicate that the regulatory effect of H19 on osteocyte mechanotransduction via the AKT/GSK3 signaling pathway can be mediated by PP2A.

To explore the interactions between H19 and PP2A, we first determined the protein expression level of PPP2R1A and PPP2R5D in osteocytes after overexpression or knockdown of

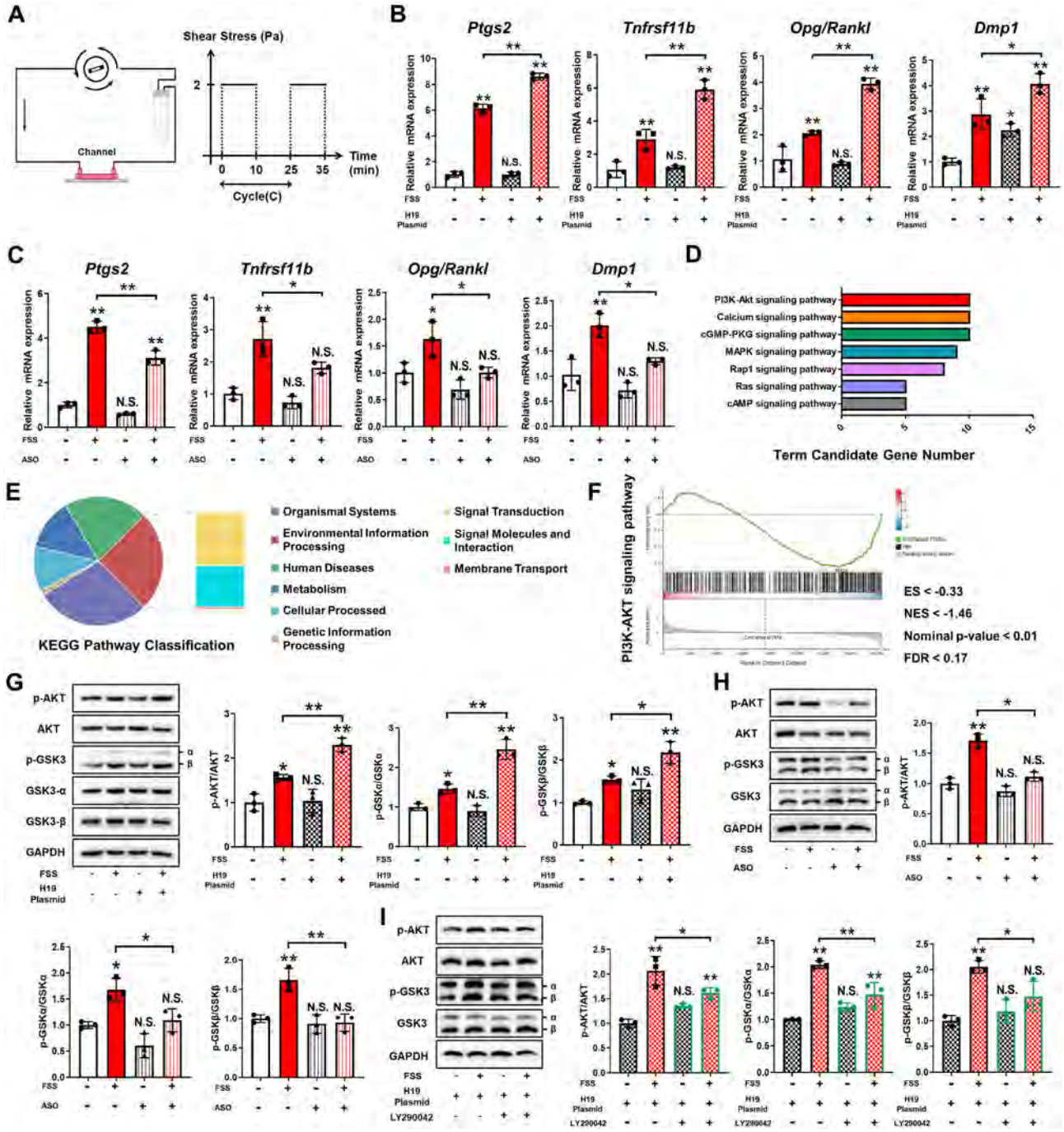

Figure 3. H19-mediated osteocyte mechanoresponse via PI3K/AKT/GSK3 signaling. (A) Schematic illustration showing the in vitro FSS mode. (B) The expression of *Ptgs2*, *Tnfrsf11b*, the *Opg/Rankl* ratio, and *Dmp1* was assessed by qPCR in control or H19-overexpressed MLO-Y4 cells under FSS conditions. n = 3 per group. (C) The expression of *Ptgs2*, *Tnfrsf11b*, the *Opg/Rankl* ratio, and *Dmp1* was assessed by qPCR in control or H19-silenced MLO-Y4 cells under FSS conditions. n = 3 per group. (D) KEGG analysis of the pathway candidate gene number and (E) classification from DEGs in MLO-Y4 cells transfected with control and ASO after FSS stimulation. n = 4 per group. (F) GSEA showing the enrichment of PI3K/AKT signaling pathways in MLO-Y4 cells transfected with control and ASO after FSS stimulation. n = 4 per group. (G) The protein levels of AKT/GSK3 signaling in control or H19-overexpressed MLO-Y4 cells were analyzed by Western blot under FSS conditions. n = 3 per group. (H) The protein levels of AKT/GSK3 signaling in control or H19-silenced MLO-Y4 cells were analyzed by Western blot under FSS conditions. n = 3 per group. (I) The protein levels of AKT/GSK3 signaling in H19-overexpressed MLO-Y4 cells were analyzed by Western blot under FSS conditions with or without pretreatment of LY290042 (10 μM) for 30 minutes. n = 3 per group. $^{*}P < 0.05$; $^{**}P < 0.01$. AKT, protein kinase B; ASO, antisense oligonucleotide; DEG, differentially expressed gene; ES, enrichment score; FDR, false discovery rate; FSS, fluid shear stress; GSEA, gene set enrichment analysis; GSK3, glycogen synthase kinase 3; KEGG, Kyoto Encyclopedia of Genes and Genomes; mRNA, messenger RNA; NES, normalized enrichment score; N.S., no significance; PI3K, phosphatidylinositol 3-kinase; qPCR, quantitative reverse transcription polymerase chain reaction. Color figure can be viewed in the online issue, which is available at http://onlinelibrary.wiley.com/doi/10.1002/art.43028/abstract.

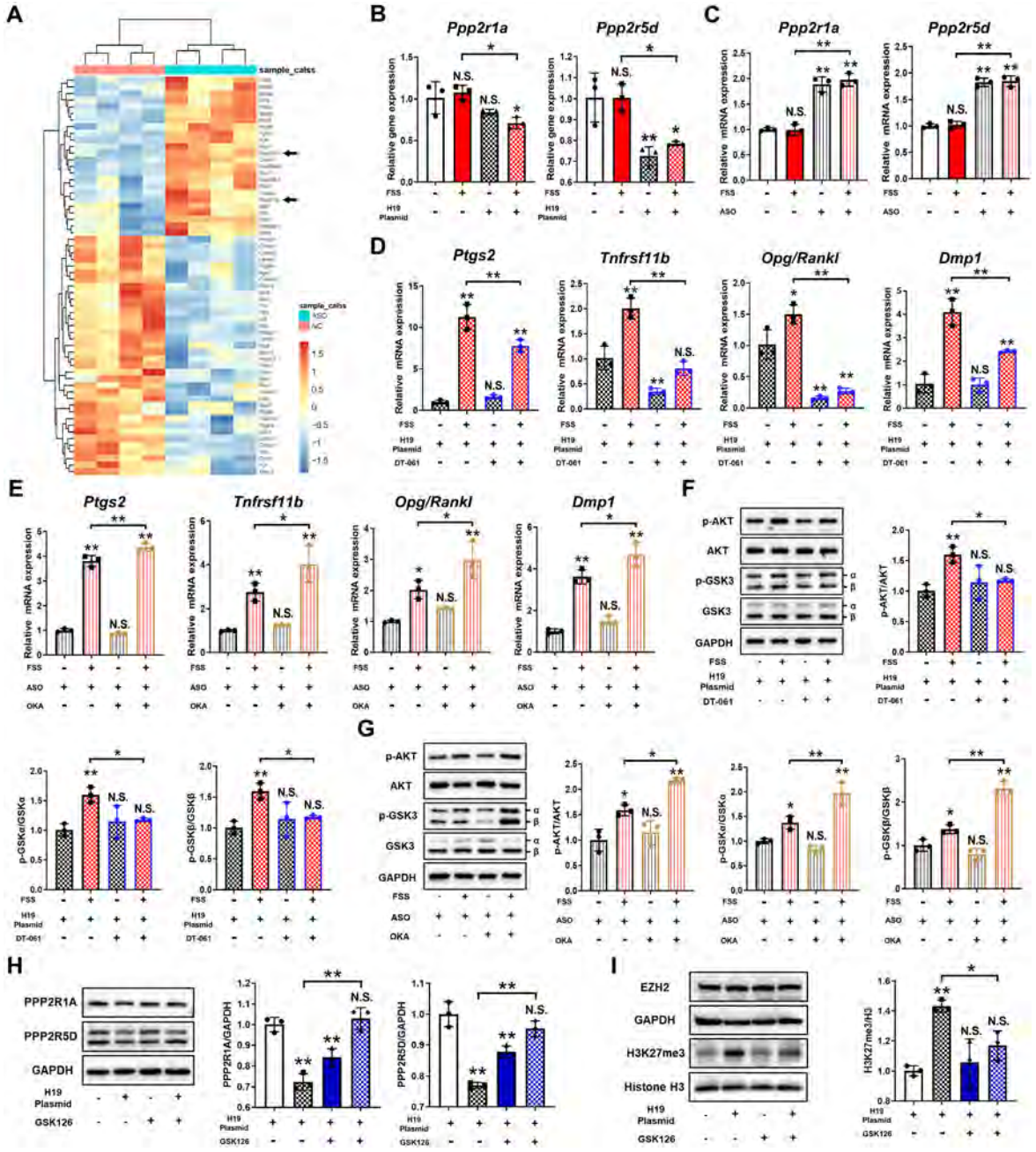

Figure 4. H19-mediated osteocyte mechanoresponse and mechanotransduction via PP2A regulation. (A) Heatmap representing DEGs of PI3K/AKT signaling pathways in MLO-Y4 cells transfected with control and ASO after FSS stimulation. n = 4 per group. The expression of *Ppp2r1a* and *Ppp2r5d* in (B) H19-overexpressed and (C) H19-silenced MLO-Y4 cells was assessed by qPCR under FSS conditions. n = 3 per group. (D) The expression of *Ptgs2*, *Tnfrsf11b*, the *Opg/Rankl* ratio, and *Dmp1* in H19-overexpressed MLO-Y4 cells was assessed by qPCR under FSS conditions with or without pretreatment of DT-061 (10 μM) for 30 minutes. n = 3 per group. (E) The expression of *Ptgs2*, *Tnfrsf11b*, the *Opg/Rankl* ratio, and *Dmp1* in H19-silenced MLO-Y4 cells was assessed by qPCR under FSS conditions with or without pretreatment of OKA (10 n*M*) for 30 minutes. n = 3 per group. (F) The protein levels of AKT/GSK3 signaling in H19-overexpressed MLO-Y4 cells were analyzed by Western blot under FSS conditions with or without pretreatment of DT-061 (10 μM) for 30 minutes. n = 3 per group. (G) The protein levels of AKT/GSK3 signaling in H19-silenced MLO-Y4 cells were analyzed by Western blot under FSS conditions with or without pretreatment of OKA (10 nM) for 30 minutes. n = 3 per group. (H) The protein levels of EZH2 and H3K27me3 were analyzed by Western blot in control or H19-overexpressed MLO-Y4 cells with or without GSK126 (6 μM) treatment for 24 hours. n = 3 per group. (I) The protein levels of PPP2R1A and PPP2R5D were analyzed by Western blot in control or H19-overexpressed MLO-Y4 cells with or without GSK126 (6 μM) treatment for 24 hours. n = 3 per group. *$P < 0.05$; **$P < 0.01$. AKT, protein kinase B; ASO, antisense oligonucleotide; DEG, differentially expressed gene; FSS, fluid shear stress; GSK3, glycogen synthase kinase 3; mRNA, messenger RNA; N.S., no significance; OKA, okadaic acid; PI3K, phosphatidylinositol 3-kinase; PP2A, protein phosphatase 2A; qPCR, quantitative reverse transcription polymerase chain reaction. Color figure can be viewed in the online issue, which is available at http://onlinelibrary.wiley.com/doi/10.1002/art.43028/abstract.

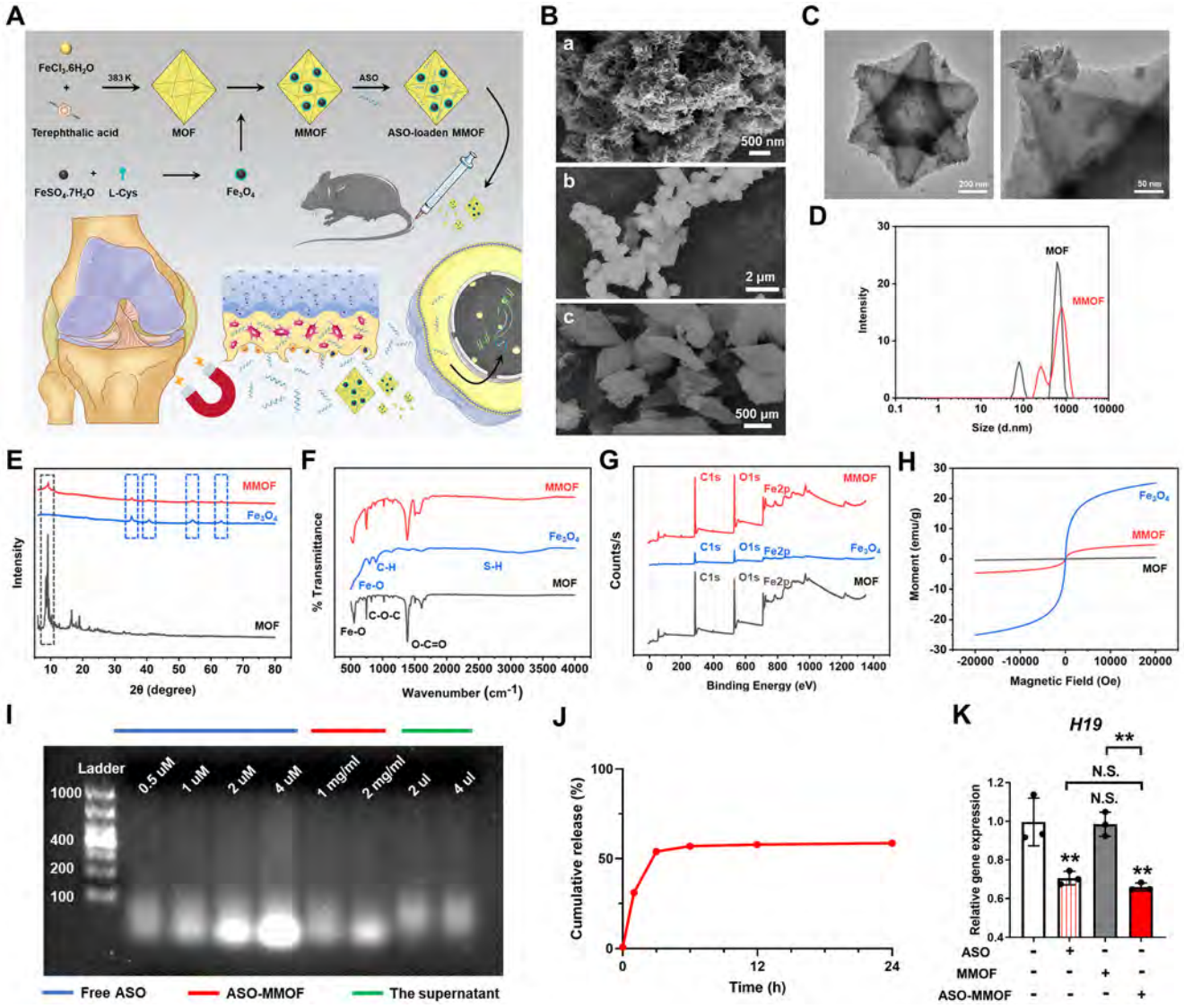

Figure 5. Characterization of MMOF. (A) Schematic illustration for MMOF synthesis. (B) Representative SEM images of (a) Fe_3O_4 (scale bar = 500 nm), (b) MOF (scale bar = 2 μm), and (c) MMOF (scale bar = 500 μm). (C) Representative TEM images of MMOF (scale bar = 200 nm and 50 nm). (D) DLS of MOF and MMOF. The size ranges of MOF with two polydispersity indexes were not affected by the addition of Fe_3O_4. (E) XRD spectra of Fe_3O_4, MOF, and MMOF. Characteristic peaks ascribed to Fe_3O_4 or MOF were marked with blue or black boxes, respectively. (F) FTIR spectra of Fe_3O_4, MOF, and MMOF. Characteristic absorption peaks of chemical bonds to Fe_3O_4 or MOF were marked in blue or black, respectively. (G) Full XPS spectra of Fe_3O_4, MOF, and MMOF. Characteristic spectra of O1s, C1s, and Fe2p of the Fe3O4, MOF, and MMOF were marked in blue, black, or red, respectively. (H) The hysteresis loop of Fe_3O_4, MOF, and MMOF. MOF exhibited magnetic behavior by the addition of Fe_3O_4. (I) DNA gel electrophoresis of ASO-loaded MMOF. The signal of ASO from MMOF (2 mg/mL) was comparable with that from the free ASO (1 μM). (J) Cumulative in vitro ASO release profile of MMOF. (K) The expression of *H19* was assessed by qPCR in MLO-Y4 cells treated with control, ASO, MMOF, and ASO-loaded MMOF. n = 3 per group. $^*P < 0.05$; $^{**}P < 0.01$. ASO, antisense oligonucleotide; DLS, dynamic light scattering; FTIR, Fourier transform infrared spectroscopy; MOF, metal–organic framework; MMOF, magnetic metal–organic framework; N.S., no significance; qPCR, quantitative reverse transcription polymerase chain reaction; SEM, scanning electron microscope; TEM, transmission electron microscopetransmission electron microscope; XPS, x-ray photoelectron spectroscopy; XRD, X-ray diffraction. Color figure can be viewed in the online issue, which is available at http://onlinelibrary.wiley.com/doi/10.1002/art.43028/abstract.

H19. H19 overexpression reduced the protein level of PPP2R1A and PPP2R5D, whereas H19 knockdown induced their protein levels (Supplementary Figure 4A and B), indicating that H19 might be able to negatively regulate the expression of PP2A. Given that H19 was found predominantly in the nuclei of osteocytes (Supplementary Figure 4C) and it was previously reported that EZH2, commonly known as a methyltransferase, could be recruited by H19 and induce trimethylation of lysine (K) at position 27 of histone H3 (H3K27me3),[25] we speculated that EZH2 inhibition might be involved in H19-mediated suppression of PP2A. The inducement of H3K27me3 was confirmed in MLO-Y4 cells by H19 overexpression, which could be significantly inhibited by GSK126 (a selective EZH2 methyltransferase inhibitor) (Figure 4H). Intriguingly, our findings show that EZH2

methyltransferase inhibition increased PPP2R1A and PPP2R5D expressions in a concentration-dependent manner (Supplementary Figure 4D). Furthermore, inhibiting EZH2 could suppress the inhibitory effect of H19 on PPP2R1A and PPP2R5D expressions (Figure 4I). Collectively, our findings suggest the plausible regulatory role of EZH2 via the PP2A-associated signaling pathway on H19-mediated osteocyte mechanotransduction.

Targeting H19 by MMOF nanoparticles. To confirm the H19 potential as a therapeutic target for OA treatment through modulation of subchondral bone remodeling, we designed an MMOF nanoplatform (Figure 5A) to deliver anti-H19 ASO in a controlled manner to the target and to augment its effectiveness when compared with that of systemic injection of ASO alone. Scanning Electron Microscope (SEM) and Transmission Electron Microscope (TEM) were employed to observe the morphology of the synthesized nanoparticles, and the distribution of Fe_3O_4 nanoparticles on the MOF surface was observed (Figure 5B and C). The addition of Fe_3O_4 did not significantly affect the size range of MOF nanoparticles (Figure 5D). The synthesized MOF had Brunauer Emmett Teller (BET) and Langmuir surface areas of around 282 m^2/g and 635 m^2/g, respectively, with a 0.394-cm^3/g pore volume, whereas the presence of iron oxide in MMOF decreased the BET and Langmuir surface area and pore volume to 25.8 m^2/g, 220 m^2/g, and 0.098 cm^3/g, respectively (Supplementary Figure 5J and K). Furthermore, the zeta potential of MMOF was lower (9.7 mV) than that of MOF (around 17 mV) because of the presence of Fe_3O_4 (–6.21 mV) on its surface. After introducing ASO, the zeta potential shifted to a negative value (–3.95 mV) because the synthesized oligonucleotides normally had negative charge,[26,27] and this result proved that ASO was successfully loaded into the particles. The chemical structure of the synthesized powders was studied by X-ray diffraction (XRD) and Fourier transform infrared spectroscopy, which indicated successful synthesizing of Fe_3O_4, MOF, and MMOF (Figure 5E and F). To further analyze their chemical states, the full spectra; the corresponding atomic percentage of Fe, C, and O; and high-resolution spectra of O1s, C1s, and Fe2p of the Fe_3O_4, MOF, and MMOF were acquired by x-ray photoelectron spectroscopy (Figure 5G, Supplementary Table 4, and Supplementary Figure 5A–I). From the full spectra and corresponding atomic contents, it was concluded that because of conjugation of Fe_3O_4 to MOF, the contents of Fe and O increased compared to that of MOF (Supplementary Information). Upon proving the successful synthesis of MMOF, its saturation magnetization value was measured to be 4.69 emu/g, whereas this value for MOF was 0.43 emu/g (Figure 5H), thus making the administrated MMOF able to be guided by the external magnetic field exposure (Supplementary Figure 5L). Taken together, MMOF was successfully made for subsequent experiments.

Next, the presence of the loaded ASO was verified by DNA gel electrophoresis on the supernatant and precipitate of the ASO-loaded MMOF. The precipitate exhibited the characteristic markers of free ASO, whereas free ASO was barely detected from the supernatant, indicating that the ASO was successfully conjugated to the MMOF (Figure 5I) with a loading ratio of 2.185% (weight/weight%) (Supplementary Figure 6A). The ASO release profile indicated that 54% of the ASO released within the first three hours whereas the release percentage reached its maximum (57%) after six hours upon incubation in the releasing medium (Figure 5J). Furthermore, efficient inhibition of *H19* expression in osteocytes upon the in vitro supplementation of MMOF revealed the capability of MMOF in the delivery of the ASO to the cells with suitable bioavailability (Figure 5K).

In vivo treatment of MMOF. In vivo fluorescence imaging was employed to verify the efficient MMOF accumulation in the knee joints under magnetic field exposure. The fluorescence intensity of Indocyanine Green (ICG)-labeled MMOF was predominately accumulated in the target knee joint exposed to the external magnetic field, whereas the contralateral side without magnetic field exposure showed a weak fluorescence signal (Figure 6A and B). The efficient knee joint accumulation of ASO-loaded MMOF upon magnetic field exposure six hours post injection was confirmed because the fluorescence signals in these samples were significantly higher in the knee joint when compared to those without magnetic stimulation across the studied period (Figure 6C and Supplementary Figure 6B). Because MMOF can be retained in the joint for a longer time once exposed to the magnetic field, they have a delayed circulation to other organs upon exposure to the magnetic field. Ex vivo images of the excised organs and knee joints after 24 hours of MMOF injection showed a remarkable fluorescence signal in the liver and kidney, indicating a possible toxicity accumulation for other organs in the subsequent treatment (Figure 6D and Supplementary Figure 6C).

The therapeutic effectiveness of ASO-loaded MMOF was evaluated with a DMM-induced OA mouse model. After eight weeks of treatment, cartilage degradation and subchondral bone sclerosis were significantly alleviated in mice receiving magnet-guided, ASO-loaded MMOF treatment. In the absence of a magnetic field, there was subtle improvement of Osteoarthritis Research Society International scores and subchondral bone sclerosis (Figure 6E–G and Supplementary Figure 6D). The FISH staining results confirmed that ASO-loaded MMOF treatment alone slightly decreased the distribution of osteocyte H19 in the subchondral bone region, whereas considerable inhibition of H19-positive osteocytes was observed once combined with a magnetic field (Figure 6E and H). Upon exposure to a magnetic field, MMOF injection significantly reduced the expression of COX-2, OPG, and DMP1 in OA subchondral bone osteocytes (Supplementary Figure 6E and F). Histologic analysis of the major

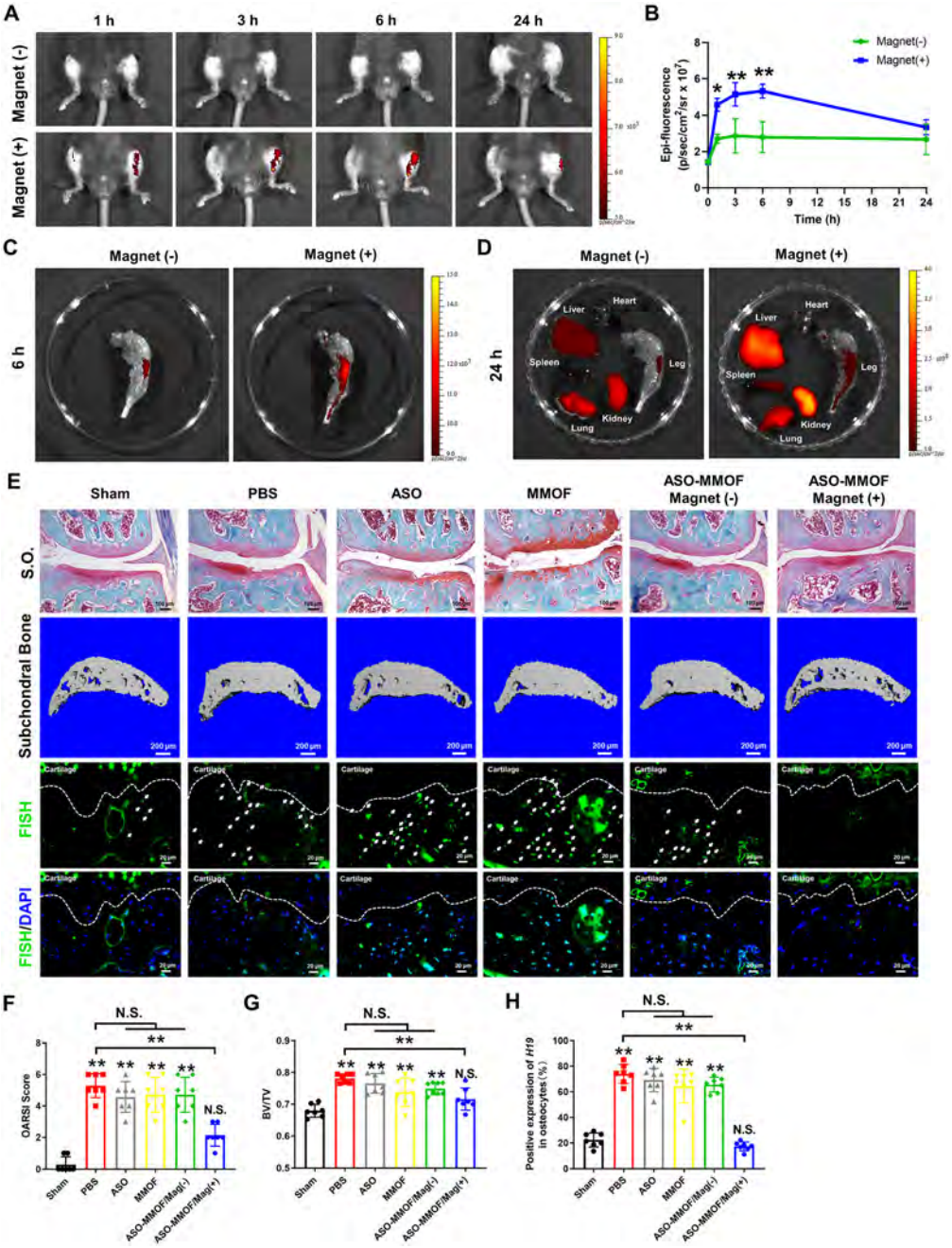

Figure 6. In vivo treatment of MMOF. (A) Fluorescence imaging and (B) fluorescence quantitative assessment in C57BL/6 mice post IV injection of ICG-labeled MMOF with or without six-hour external magnetic field exposure. n = 3 in each group. (C) Fluorescent images of isolated knee joints from C57BL/6 mice at six hours post IV injection of ICG-labeled MMOF with or without six-hour external magnetic field exposure. (D) Fluorescence images of isolated major organs and knee joints from C57BL/6 mice at 24 hours post IV injection of ICG-labeled MMOF with or without six-hour external magnetic field exposure. (E) Representative S.O. staining of knee joints (scale bar = 100 μm), micro-CT 3D reconstruction of subchondral bone (scale bar = 200 μm), and FISH staining of osteocytes counterstained with DAPI (scale bar = 20 μm) in subchondral bone from C57BL/6 mice following the indicated treatments. The mice received different treatments: ASO, MMOF, ASO-loaded MMOF at a dosage of 5 mg/kg or PBS as vehicle control with concurrent six-hour magnetic field exposure once a week. Another group with ASO-loaded MMOF administration without magnetic field exposure served as the control group for magnetic cotreatment. Mice with sham operation served as the positive control. Quantitation of OA severity by (F) OARSI scores, (G) subchondral bone parameter (BV/TV), and (H) the percentage number for H19-positive osteocytes in subchondral bone for C57BL/6 mice following the indicated treatments for seven consecutive weeks. n = 7 in each group. *$P < 0.05$; **$P < 0.01$. 3D, three-dimensional; ASO, antisense oligonucleotide; BV/TV, bone volume fraction; FISH, fluorescence in situ hybridization; ICG, Indocyanine Green; IV, intravenous; micro-CT, micro–computed tomography; MMOF, magnetic metal–organic framework; N.S., no significance; OA, osteoarthritis; OARSI, Osteoarthritis Research Society International; PBS, phosphate buffered saline; qPCR, quantitative reverse transcription polymerase chain reaction; S.O., safranin O/fast green. Color figure can be viewed in the online issue, which is available at http://onlinelibrary.wiley.com/doi/10.1002/art.43028/abstract.

organs showed no pathologic change, suggesting a highly acceptable MMOF biocompatibility in vivo (Supplementary Figure 7A).

DISCUSSION

Subchondral bone is the bone tissue underneath the calcified cartilage and tidemark. Altered subchondral bone remodeling in OA represents abnormal bone formation and bone resorption. Several bone anabolic or catabolic agents targeting osteoclasts and osteoblasts have been under intensive investigation to modulate subchondral bone abnormal remodeling in OA, including bisphosphonates, calcitonin, and strontium ranelate.[28] Apart from osteoblasts and osteoclasts, growing evidence indicates that matrix-embedded osteocytes also play important roles in arthritic subchondral bone remodeling. The causative role of elevated COX-2 expression has been reported in subchondral bone osteocytes in both spontaneous OA and rheumatoid arthritis.[9] COX-2 is one of the factors released by osteocytes upon mechanical stimulation, which modulates bone remodeling.[29] Interestingly, in line with this previous finding, we have found that COX-2 messenger RNA expression (*Ptgs2*) could be positively regulated by H19 during cellular and animal functional experiments. Although our clinical samples did not show a significant correlation between H19 and *Ptgs2*, *Tnfrsf11b*, and *Dmp1* levels (Supplementary Figure 1F), it is important to consider the diverse etiologies of human OA, involving a range of internal and external factors that also influence the expression level[9] of COX-2. In addition, spatial expression patterns of H19 and the target genes in clinical OA samples should be taken into consideration in correlation analysis. Therefore, the complementary role between H19 and COX-2 as well as other mechanoresponsive genes in OA development is warranted for further investigation.

The mechanosensitivity response of osteocytes on abnormal subchondral bone remodeling and OA development is further evidenced by another study ablating osteocyte transforming growth factor β (TGFβ) type II receptor.[30] In addition to the response to mechanical stimulation, the altered osteocyte function, such as matrix metalloproteinase 13–dependent perilacunar/canalicular remodeling in OA subchondral bone, has been reported.[31] This emerging evidence supports the notion of targeting osteocytes for OA treatment. Along this line, we provide fresh evidence on the novel biologic function of H19 in terms of regulating osteocyte mechanoresponse, modulating subchondral bone alteration, and maintaining cartilage homeostasis during OA progression. H19 mediates the mechanotransduction of osteocytes in response to FSS stimulation by repressing PP2A through PI3K/AKT/GSK3 signaling pathway activation. A previous in silico study suggests that H19 is a potential noncoding RNA candidate mediating mechanoresponsive signaling pathways.[32] However, the clinical implication of its mechanoresponse function in OA has not been elucidated. In this study, we identified the PI3K/AKT/GSK3 signaling pathway as one of the key downstream pathways of H19-mediated osteocyte mechanotransduction, which may regulate the downstream Wnt/β-catenin pathway to induce mechanoresponse in osteocytes[33] and lead to a series of consequences, including the release of bioactive factors and interaction with osteoblasts and osteoclasts molecules, resulting in aberrant bone formation in OA subchondral bone.[34] By using MMOF for site-specific anti-H19 ASO delivery, we demonstrated that reducing the H19 level in OA subchondral bone osteocytes is a new therapeutic target for alleviating the progression of cartilage degeneration and subchondral bone sclerosis.

PP2A is one of the major phosphatases and is ubiquitously expressed in all mammalian cells.[35] PP2A is composed of the scaffold subunit (A subunit), the catalytic subunit (C subunit), and the regulatory subunit (B subunit).[36] The PP2A scaffold subunit is encoded by *PPP2R1A*, and *PPP2R5D* encodes the regulatory subunit of PP2A. Both of their mutants have been reported to trigger the hyperphosphorylation of the AKT/GSK3 singling pathway.[37,38] Previous studies showed that inhibition of PP2A could induce apoptosis of chondrocytes through mediating TGFβ1 signaling transduction.[39] In osteocytes, PP2A can participant in 26S proteosome complex formation to maintain a low level of intracellular β-catenin, which is implicated in osteocyte function, such as transmitting signals of mechanical loading.[40] However, how PP2A is involved in osteocyte mechanical signaling transduction in the context of OA has not been reported. Our findings show that PP2A is the downstream target of H19, participating in the regulation of PI3K/AKT/GSK3 pathway activation, which is in line with a previous study showing the link between increased phosphorylation of AKT and aberrant bone formation in subchondral bone remodeling during OA progression.[41] The biologic roles of lncRNAs in epigenetics have been extensively investigated, and DNA methylation is closely linked to the changes in the nucleosome DNA scaffold by recruiting methyltransferases that coordinate individual cellular gene expression.[42] EZH2, the catalytic subunit of polycomb repressive complex 2, is closely associated with gene silencing by trimethylating lysine 27 on histone 3 (H3K27).[43] EZH2-dependent H3K27me3 was reported to influence the expression of PP2A in breast cancer.[44] In the nuclei, the interaction between H19 and EZH2 has drawn researchers' interest.[45] For instance, lncRNA H19 could accelerate bladder cancer metastasis by recruiting EZH2 and enhancing H3K27me3 interaction with target gene transcription.[46] In liver fibrosis, H19 could directly bind to EZH2 to reprogram H3K27me3 profiles and promote excess formation of the extracellular matrix from activated hepatic stellate cells.[47] By using EZH2 methyltransferase inhibitor, our findings suggest that EZH2 might participate as a negative transcriptional regulation of PP2A, thus affecting H19-mediated PP2A expression in

osteocytes. However, further in-depth mechanistic investigation is warranted to elucidate their interaction and impact on osteocytes activity.

This is the first study to investigate the potential therapeutic effect of targeted inhibition of lncRNA H19 in subchondral bone for OA treatment. Growing evidence suggests that lncRNAs can be potential drug targets by using ASOs[48]; however, undesired off-target effects and unspecific biodistribution remain technical hindrances in ASO-based treatment.[49] In recent years, the use of MOF carriers for nucleic acid delivery has emerged as an effective therapeutic strategy because of their ease of preparation, high drug-loading capacity, and good biocompatibility.[50] In addition, MOF as a carrier can be modified to be magnetic responsive,[51] providing a feasible platform to enhance the accumulation at the target site upon external magnetic field exposure, thereby promoting the delivery efficiency of the drug.[52] As far as we known, this study represents the initial endeavor to design and fabricate an MMOF carrier to deliver ASO for H19 silencing in the knee subchondral bone of an OA mouse model, which holds promise for ameliorating cartilage degradation and subchondral sclerosis in OA through a site-specific drug delivery system. The gradual releasing profile of ASO from MMOF further reduces its rapid clearance from the blood stream; thus, persistent effective concentration of ASO at the site of interest could be achieved without the requirement of multiple injections of pure ASO at high dosages.[53] However, it is important to note that our developed ASO-loaded MMOF treatment approach does not exclusively target osteocytes and may also affect other cell types, such as chondrocytes, synoviocytes, vascular cells, and osteoclasts and osteoblasts in OA subchondral bone. Therefore, more investigation is needed to assess the long-term efficacy and side effects of MMOF treatment. Future development of MMOF as a drug delivery carrier in the clinical setting should consider the specificity of site delivery mediated by the magnetic field in view of the complex geometry of the knee joint and the balance of wearing comfort and magnetic field intensity; thus, it is more reasonable to place the magnetic device adjacent to the affected side of the joints of patients.

The findings of the present study have generated additional research questions for future investigation. Firstly, although we have demonstrated that reducing the H19 expression level in subchondral bone osteocytes could ameliorate OA progression, the complicated pathologic changes caused by DMM surgery should be acknowledged, and further investigation on the effect of H19 on other joint compartment tissues during OA progression is warranted. Hence, a noninvasive loading model, such as the ulnar axial loading system and the tibial loading model, could be considered to explore the role and response of H19 in the context of the mechanical stimulation. Secondly, the epigenetic regulation of H19 is unique and complex in osteocyte mechanotransduction, which will further define the role of H19 on influencing target gene expression as an epigenetic modifier. For instance, the direct interaction between the promoter region of PP2A and histone H3K27me3 may provide a new perspective for the mechanism of H19 on PP2A expression. Finally, the biomedical safety of ASO-loaded MOFs remains unexplored, particularly in the assessment of their biologic activity, toxicity to tissue diseases, and drug damage.

ACKNOWLEDGMENTS

This work was mainly supported by the General Research Fund (Ref. No. 24121622), and partly by Area of Excellence (Ref. No. AoE/M-402/20) and Matching Grant Scheme, University Grants Committee, Hong Kong SAR, China; Start-up Fund, The Chinese University of Hong Kong, Hong Kong SAR, China; Rising Star Award provided by American Society for Bone and Mineral Research; Research fund to the Center for Neuromusculoskeletal Restorative Medicine from Health@InnoHK program launched by Innovation Technology Commission, Hong Kong SAR, China. We gratefully acknowledged the support from Nanobiotechnology Laboratory (S106b) of the Biomedical Engineering Department of the Hong Kong Polytechnic University for providing facility for DLS analysis.

AUTHOR CONTRIBUTIONS

All authors contributed to at least one of the following manuscript preparation roles: conceptualization AND/OR methodology, software, investigation, formal analysis, data curation, visualization, and validation AND drafting or reviewing/editing the final draft. As corresponding author, Drs G. Li, Chu, and Lee confirm that all authors have provided the final approval of the version to be published and take responsibility for the affirmations regarding article submission (eg, not under consideration by another journal), the integrity of the data presented, and the statements regarding compliance with institutional review board/Declaration of Helsinki requirements.

DATA AVAILABILITY STATEMENT

RNA seq source data for Figure 3E–F, Figure 4A, Supplements Figure 3D, and Supplementary Data file 1. The raw data that support the findings of this study will be openly available on publication in GEO database (GSE254053).

REFERENCES

1. Goldring SR, Goldring MB. Changes in the osteochondral unit during osteoarthritis: structure, function and cartilage-bone crosstalk. Nat Rev Rheumatol 2016;12(11):632–644.
2. Glyn-Jones S, Palmer AJ, Agricola R, et al. Osteoarthritis. Lancet 2015;386(9991):376–387.
3. Chang SH, Mori D, Kobayashi H, et al. Excessive mechanical loading promotes osteoarthritis through the gremlin-1-NF-κB pathway. Nat Commun 2019;10(1):1442.
4. Hu Y, Chen X, Wang S, et al. Subchondral bone microenvironment in osteoarthritis and pain. Bone Res 2021;9(1):20.
5. Burr DB, Gallant MA. Bone remodelling in osteoarthritis. Nat Rev Rheumatol 2012;8(11):665–673.
6. Tatsumi S, Ishii K, Amizuka N, et al. Targeted ablation of osteocytes induces osteoporosis with defective mechanotransduction. Cell Metab 2007;5(6):464–475.

7. Bonewald LF. The amazing osteocyte. J Bone Miner Res 2011;26(2): 229–238.
8. Klein-Nulend J, Bakker AD, Bacabac RG, et al. Mechanosensation and transduction in osteocytes. Bone 2013;54(2):182–190.
9. Tu M, Yang M, Yu N, et al. Inhibition of cyclooxygenase-2 activity in subchondral bone modifies a subtype of osteoarthritis. Bone Res 2019;7(1):29.
10. Kovács B, Vajda E, Nagy EE. Regulatory effects and interactions of the Wnt and OPG-RANKL-RANK Signaling at the bone-cartilage interface in osteoarthritis. Int J Mol Sci 2019;20(18):4653.
11. Zhang Q, Lin S, Liu Y, et al. *Dmp1* null mice develop a unique osteoarthritis-like phenotype. Int J Biol Sci 2016;12(10): 1203–1212.
12. Kapranov P, Cheng J, Dike S, et al. RNA maps reveal new RNA classes and a possible function for pervasive transcription. Science 2007; 316(5830):1484–1488.
13. Wang R, Shiu HT, Lee WYW. Emerging role of lncRNAs in osteoarthritis: an updated review. Front Immunol 2022;13:982773.
14. Steck E, Boeuf S, Gabler J, et al. Regulation of H19 and its encoded microRNA-675 in osteoarthritis and under anabolic and catabolic in vitro conditions. J Mol Med (Berl) 2012;90(10): 1185–1195.
15. Stuhlmüller B, Kunisch E, Franz J, et al. Detection of oncofetal h19 RNA in rheumatoid arthritis synovial tissue. Am J Pathol 2003; 163(3):901–911.
16. Chen S, Liu D, Zhou Z, et al. Role of long non-coding RNA H19 in the development of osteoporosis. Mol Med 2021;27(1):122.
17. Wu J, Zhao J, Sun L, et al. Long non-coding RNA H19 mediates mechanical tension-induced osteogenesis of bone marrow mesenchymal stem cells via FAK by sponging miR-138. Bone 2018;108: 62–70.
18. Eichaker LR, Cho H, Duvall CL, et al. Future nanomedicine for the diagnosis and treatment of osteoarthritis. Nanomedicine (Lond) 2014;9(14):2203–2215.
19. Guo L, Zhong S, Liu P, et al. Radicals scavenging MOFs enabling targeting delivery of siRNA for rheumatoid arthritis therapy. Small 2022; 18(27):e2202604.
20. Riccò R, Liang W, Li S, et al. Metal-organic frameworks for cell and virus biology: a perspective. ACS Nano 2018;12(1):13–23.
21. Bonewald LF. Mechanosensation and transduction in osteocytes. Bonekey Osteovision 2006;3(10):7–15.
22. Li X, Han L, Nookaew I, et al. Stimulation of Piezo1 by mechanical signals promotes bone anabolism. eLife 2019;8:8.
23. Riquelme MA, Gu S, Hua R, et al. Mechanotransduction via the coordinated actions of integrins, PI3K signaling and Connexin hemichannels. Bone Res 2021;9(1):8.
24. Seshacharyulu P, Pandey P, Datta K, et al. Phosphatase: PP2A structural importance, regulation and its aberrant expression in cancer. Cancer Lett 2013;335(1):9–18.
25. Du Z, Shi X, Guan A. lncRNA H19 facilitates the proliferation and differentiation of human dental pulp stem cells via EZH2-dependent LATS1 methylation. Mol Ther Nucleic Acids 2021;25:116–126.
26. Di Fusco D, Dinallo V, Marafini I, et al. Antisense oligonucleotide: basic concepts and therapeutic application in inflammatory bowel disease. Front Pharmacol 2019;10:305.
27. Sharma VK, Watts JK. Oligonucleotide therapeutics: chemistry, delivery and clinical progress. Future Med Chem 2015;7(16):2221–2242.
28. Zhu X, Chan YT, Yung PSH, et al. Subchondral bone remodeling: a therapeutic target for osteoarthritis. Front Cell Dev Biol 2021;8: 607764.
29. Choi JUA, Kijas AW, Lauko J, et al. The mechanosensory role of osteocytes and implications for bone health and disease states. Front Cell Dev Biol 2022;9:770143.
30. Bailey KN, Nguyen J, Yee CS, et al. Mechanosensitive control of articular cartilage and subchondral bone homeostasis in mice requires osteocytic transforming growth factor β signaling. Arthritis Rheumatol 2021;73(3):414–425.
31. Mazur CM, Woo JJ, Yee CS, et al. Osteocyte dysfunction promotes osteoarthritis through MMP13-dependent suppression of subchondral bone homeostasis. Bone Res 2019;7(1):34.
32. Cai J, Li C, Li S, et al. A quartet network analysis identifying mechanically responsive long noncoding RNAs in bone remodeling. Front Bioeng Biotechnol 2022;10:780211.
33. Kitase Y, Barragan L, Qing H, et al. Mechanical induction of PGE2 in osteocytes blocks glucocorticoid-induced apoptosis through both the β-catenin and PKA pathways. J Bone Miner Res 2010;25(12): 2657–2668.
34. Lin C, Shao Y, Zeng C, et al. Blocking PI3K/AKT signaling inhibits bone sclerosis in subchondral bone and attenuates post-traumatic osteoarthritis. J Cell Physiol 2018;233(8):6135–6147.
35. Shi Y. Serine/threonine phosphatases: mechanism through structure. Cell 2009;139(3):468–484.
36. Xu Y, Xing Y, Chen Y, et al. Structure of the protein phosphatase 2A holoenzyme. Cell 2006;127(6):1239–1251.
37. Haesen D, Abbasi Asbagh L, Derua R, et al. Recurrent PPP2R1A mutations in uterine cancer act through a dominant-negative mechanism to promote malignant cell growth. Cancer Res 2016;76(19): 5719–5731.
38. Papke CM, Smolen KA, Swingle MR, et al. A disorder-related variant (E420K) of a PP2A-regulatory subunit (PPP2R5D) causes constitutively active AKT-mTOR signaling and uncoordinated cell growth. J Biol Chem 2021;296:100313.
39. López-Armada MJ, Caramés B, Cillero-Pastor B, et al. Phosphatase-1 and -2A inhibition modulates apoptosis in human osteoarthritis chondrocytes independently of nitric oxide production. Ann Rheum Dis 2005;64(7):1079–1082.
40. Bonewald LF, Johnson ML. Osteocytes, mechanosensing and Wnt signaling. Bone 2008;42(4):606–615.
41. Sun K, Luo J, Guo J, et al. The PI3K/AKT/mTOR signaling pathway in osteoarthritis: a narrative review. Osteoarthritis Cartilage 2020;28(4): 400–409.
42. Houseman EA, Accomando WP, Koestler DC, et al. DNA methylation arrays as surrogate measures of cell mixture distribution. BMC Bioinformatics 2012;13(1):86.
43. Eich ML, Athar M, Ferguson JE III, et al. EZH2-targeted therapies in cancer: hype or a reality. Cancer Res 2020;80(24):5449–5458.
44. Bao Y, Oguz G, Lee WC, et al. EZH2-mediated PP2A inactivation confers resistance to HER2-targeted breast cancer therapy. Nat Commun 2020;11(1):5878.
45. Guo CJ, Xu G, Chen LL. Mechanisms of long noncoding RNA nuclear retention. Trends Biochem Sci 2020;45(11):947–960.
46. Luo M, Li Z, Wang W, et al. Long non-coding RNA H19 increases bladder cancer metastasis by associating with EZH2 and inhibiting E-cadherin expression. Cancer Lett 2013;333(2):213–221.
47. Li XJ, Zhou F, Li YJ, et al. LncRNA H19-EZH2 interaction promotes liver fibrosis via reprogramming H3K27me3 profiles. Acta Pharmacol Sin 2023;44(12):2479–2491.
48. Chen Y, Li Z, Chen X, et al. Long non-coding RNAs: from disease code to drug role. Acta Pharm Sin B 2021;11(2):340–354.
49. Nakamura A, Ali SA, Kapoor M. Antisense oligonucleotide-based therapies for the treatment of osteoarthritis: opportunities and roadblocks. Bone 2020;138:115461.

50. Cai W, Wang J, Chu C, et al. Metal-organic framework-based stimuli-responsive systems for drug delivery. Adv Sci (Weinh) 2018;6(1): 1801526.
51. Chung CW, Liao BW, Huang SW, et al. Magnetic responsive release of nitric oxide from an MOF-derived Fe_3O_4@PLGA microsphere for the treatment of bacteria-infected cutaneous wound. ACS Appl Mater Interfaces 2022;14(5):6343–6357.
52. Zhang M, Hu W, Cai C, et al. Advanced application of stimuli-responsive drug delivery system for inflammatory arthritis treatment. Mater Today Bio 2022;14:100223.
53. Miao YB, Pan WY, Chen KH, et al. Engineering a nanoscale Al-MOF-armored antigen carried by a "trojan horse"-like platform for oral vaccination to induce potent and long-lasting immunity. Adv Funct Mater 2019;29(43):1904828.

Supplementary information

Methods

Micro-CT analysis

The harvested mice knee joints and human subchondral bone were fixed in 4% paraformaldehyde overnight, then subjected to micro-CT scan and analysis (Scanco Medical, Switzerland). The resolution was set at 10 μm per voxel resolution at 114 μA current and 70 kV voltage. The region of interest was selected from the subchondral plate[1], and extending distally towards the growth plate with a region of 0.15 mm in medial tibial plateau. The sigma parameter was set at 0.8, while the lower threshold was set to 220. Bone volume fraction (BV/TV), bone mineral density (BMD), trabecular thickness (Tb.Th) and cortical thickness (Ct.Th) were measured for comparison. All measurements were performed according to the guidelines of the American Society for Bone and Mineral Research[2].

Histology analysis

The samples were decalcified for 2 weeks in 0.5M EDTA (pH 7.4), and embedded in paraffin. Embedded samples were cut into 7 μm thick sections with a rotary microtome prior to Safranin O/Fast green (S.O.) or Hematoxylin and Eosin (H&E) staining. Cartilage destruction was assessed by blinded observers using OARSI scoring system[3], the highest OARSI score for every section were recorded and the means of all scores were calculated.

Immunohistochemical (IHC) staining

The tissue sections were processed with IHC staining as before[4]. Slides were incubated overnight at 4°C with primary antibody against COX2, OPG, DMP1 (ABclonal, China). After washing, the sections were incubated with HRP-conjugated secondary antibody (Beyotime, China). Subsequently, slides were processed with a 3,3'-diaminobenzidine (DAB) horseradish peroxidase color development kit (Abcam, USA) and counterstained with hematoxylin. All of the sections were imaged with DM550 microscope (Leica Microsystems). The number of positively stained cells in mouse or human tissue sections were counted by blinded observers in two randomly selected field of views per slide. The number of positively stained cells were normalized to the percentage of positive cells of adjacent cartilage in subchondral bone (%).

Fluorescence in situ hybridization (FISH)

Customized probe was specifically developed to detect H19 (Boster, China). FISH protocol for paraffin sections and cultured adherent cells was performed according to manufacturer's instruction (Boster, China). The proportions of positive cells in human and mouse samples were quantified by two observers under blind condition. The probe sequences for human lncRNA H19 are as following: (1) 5'-TACTTCCTCCACGGAGTCGGCACACTATGGCTGCCCTCTG-3'; (2) 5'-ATGAATATGCTGCACTTTACAACCACTGCACTACCTGACT-3'; (3) 5'-

TAATTTGCACTAAGTCATTTGCACTGGTTGGAGTTGTGGA-3'. The probe sequences for mice lncRNA H19 are as following: (1) 5'-TGGTACACTGTATGCCCTAACCGCTCAGTCCCTGGGTCTG-3'; (2) 5'-TGGGCTGGCGCCTTGTCGTAGAAGCCGTCTGTTCTTTCAC-3'; (3) 5'-CTAGTCTGGAAGCAGTTCCATCATAAAGTGTTCAACATGC-3'. Then the samples were stained with DAPI (Abcam, USA) and imaged with DM550 microscope. The number of positively stained cells in human or mouse subchondral bone were counted by blinded observers in two randomly selected field of view per slide. The quantification of osteocytes expressing H19 involved counting both the total number of osteocytes and the number of osteocytes that expressed the target gene in the subchondral bone below the cartilage.

MLO-Y4 cell culture

MLO-Y4 cells were provided by Prof. Lynda F. Bonewald (Indiana University, USA) and cultured in α-MEM supplemented with 2.5% fetal bovine serum (FBS), 2.5% calf serum (CS), and 1% penicillin/streptomycin/glutamine. Cells were treated with EZH2 inhibitor GSK126 (MCE, USA) at indicated concentrations in the subsequent experiments.

Fluid shear stress (FSS)

MLO-Y4 cells (cell number 1×10^5) were seeded in a μ-Slide I Luer (0.4 mm) fluid chamber slide (IBIDI, Germany) for 24 h to reach 60–70% confluency. After pre-treatment with H19 silencing (ASO transfection), overexpression (H19 plasmid transfection), PI3K inhibitor (LY290042, 10 μM, MCE, USA), PP2A inhibitor (okadaic acid, 10 nM, MCE, USA), and PP2A activator (DT-061, 10 mM, MCE, USA), the cells were exposed to a shear stress stimulation (Figure. 3A) using a Masterflex® peristaltic pump systems (Avantor, USA). Briefly, the cells were exposed to a shear stress of 2 Pa for 4 cycles, where each cycle comprised of 15 minutes of rest and 10 minutes of fluid flow stimulation. Control samples were sealed in slides with equal volume of medium under static condition throughout the duration. Protein and mRNA samples were collected right after FSS treatment.

H19 silencing in MLO-Y4 cells was achieved by transfecting cells using lipo3000 (Invitrogen, USA) with antisense oligonucleotides (ASO, IBSBIO, China) against H19: Negative ASO (50 μM): 5'-CCTTCCCTGAAGGTTCCTCC-3'; ASO1 (50 μM): 5'-GCTGTATACATTCATACGGA-3'; ASO2 (50 μM): 5'-AGACGGACTTAAAGAAGTCC-3'. H19 overexpression was achieved by transfecting cells using lipo3000 with pcDNA3.1 plasmid (5 μg/mL, NCBI Reference Sequence: NR_130973.1, IBSBIO, China). H19 silencing and overexpression efficiency were determined by qRT-PCR.

RNA sequencing and analysis

MLO-Y4 cells transfected with control and ASO after shear stress stimulation were used for RNA-sequencing analysis (n = 4). Total RNAs were isolated for RNA-seq analysis performed by Hong Kong Genomics Institute (BGI International, Hong Kong). The sequencing data was filtered with SOAPnuke (v1.5.2) and stored in

FASTQ format[5]. Essentially, differential expression analysis was performed using the DESeq2 (v1.4.5) with Q value ≤ 0.05[6]. Phenotype changes were assessed using Encyclopedia of Genes and Genomes (KEGG, https://www.kegg.jp/) enrichment analysis of annotated different expressed gene by Phyper (https://en.wikipedia.org/wiki/Hypergeometric_distribution) based on Hypergeometric test, and the heatmap was drawn by R package ClusterProfiler (v4.1.1. Gene set enrichment analysis (GSEA) was employed to determine the potential downstream pathways using GSEA software (v4.1.0).

Real-Time Quantitative Reverse Transcription PCR (qPCR)

For human subchondral bone, the regions of interest were chosen 5 mm below the cartilage-bone boundary and was carefully carried out with saw blade tool. The method to get the RNA from bone tissues and cells was reported as previously described[4]. After the isolation, the concentration of RNA was determined using Nanodrop 2000. Subsequently, cDNA was synthesized from 1 μg RNA with reverse transcriptase (Takara, Japan). Gene expression was analyzed by ABI 7500 Sequencing Detection System (Applied Biosystems, USA) with Power SYBR Green (Thermo Fisher Scientific, USA) using the specific primers (Supplementary Table 2). The relative expression level of target genes was normalized to that of GAPDH and was analyzed by the $2^{-\Delta\Delta T}$ method.

Western Blot

RIPA lysis buffer (Solarbio, China) was used to extract the total proteins from bone and cells which were measured by BCA assay (Thermo Fisher Scientific, USA). The same amounts of proteins were separated on SDS-PAGE and transferred onto PVDF membrane (Bio-Rad, Germany). After blocking with 5% (w/v) nonfat dried milk (Solarbio, China), the membranes were probed with indicated primary antibodies overnight at 4 °C (Supplementary Table 3), followed by incubation with the appropriate secondary antibodies for 1 h at room temperature. Protein bands were developed with ECL (WBKLS0500, Millipore) and ImageJ software was used for semiquantitative analysis.

Synthesis of magnetic metal organic frameworks (MMOF)

To synthesize cystine functionalized Fe_3O_4 nanoparticles (L-cystine-Fe_3O_4 which from now on is called Fe_3O_4), equal molar amount (6 mmol) of L-cystine (Shanghai Macklin Biochemical Technology, China) and $FeSO_4.7H_2O$ (Riedel-deHaen, Germany) were dissolved each in 30 mL of DI water to form a colourless solution. Next, 48 mL of NaOH (1 M) (International Laboratory (IL), USA) was injected rapidly to the solution under sonication at room temperature and sonicated for 30 min. Later, the dark particles were separated by magnetic field and washed with DI water for several times followed by freeze drying.

To synthesize MIL-101-Fe (From now on is called MOF), solutions of 1.35 g of $FeCl_3.6H_2O$ (Shanghai Macklin Biochemical Technology, China) and 0.45 g of terephthalic acid (Sigma Aldrich, USA) each in 30 mL of dimethylformamide (DMF) (RCI Labscan, Thailand) were mixed in a 100 mL stainless steel autoclave

container, closed tightly and put in the oven at 383 K for 20 h. After cooling down, the resulted powder was collected via centrifuging at 8000 rpm for 10 min to remove by-product and unreacted agents. Then, the powder was washed for at least 3 cycles of washing with hot DMF and hot ethanol separately followed by drying in a vacuum oven at 373 K overnight.

Finally, to achieve Fe_3O_4@MIL-101-Fe (From now on is called MMOF), 100 mg of the synthesized MOF and 40 mg of Fe_3O_4 were dispersed in 30 mL of DI water, separately. To adjust the surface charge of Fe_3O_4 particles, the pH of solution was adjusted to 8.5-9 by adding 1mM NaOH dropwise. Consequently, these two solutions were mixed by ultrasonication for 20 min. The as-synthesized MMOF were collected through external magnetic field, washed with DI water for multiple times, followed by drying in a vacuum oven at 60 °C overnight.

The powders morphology was examined by scanning electron microscopy (SEM, Zeiss 300, Germany) and transmission electron microscopy (TEM, FEI Talos F200x, USA). The powders size distribution and zeta potential were measured by dynamic light scattering (DLS, Zetasizer nano ZS, Malvern, USA) while their pore size and the surface area were analyzed by BET surface and porosity analyser (Micromeritics ASAP2460, USA). Furthermore, their chemical states were evaluated using attenuated total reflectance Fourier transform infrared spectroscopy (ATR-FTIR, Spectrum Two, PerkinElmer, USA) and X-ray photoelectron spectroscopy (XPS, K-alpha, Thermo Fischer scientific, USA). The particles magnetic properties were assessed by a vibration sample magnetometer (VSM, Quantum design PPMS DynaCool, USA).

***In Vitro* ASO Release Assay**

Briefly, 5 μL of ASO1 aqueous solution (100 μM) was added into the MMOF solutions (45 μL, 5 mg/mL) under ultrasonication, then placed in Thermo-shaker (Thermo Fischer scientific, USA) at 1000 rpm and room temperature overnight. After centrifugation at 15000 rpm for 15 min, both the supernatant and precipitate were collected. Then, the obtained ASO-loaden MMOF were dispersed into 50 μL DI water while being placed in a shaking incubator at 200 rpm and 37 °C followed by ultrasonication to test the samples at predetermined time intervals. To do so, the samples were centrifuged at 15000 rpm for 15 min to collect the supernatant for measuring the percentage of the released ASO using a Quant-iT™ OliGreen™ ssDNA assay kit (Thermo Fisher Scientific, USA).

To detect silencing effect of released ASO, MLO-Y4 cells (cell number 2×10^5) were seeded in 6-well plates one day before ASO/MMOF treatment. The indicated negative ASO (150 μM), MMOF (25 μL, 5 mg/mL), and ASO-MMOF (25 μL, 5 mg/mL) were placed in transwell inserts (0.4 μm Pore Polyester Membrane, Corning, USA) with lipo3000 transfection system for 6h treatment. After changed to cell culture media for 24h, the cells were lysed to perform RNA extraction, cDNA synthesis, and qRT-PCR as described previously.

***In Vivo* Biodistribution**

Under general anesthesia by ketamine and xylazine mixture, the C57BL/6 mice were injected with ICG-labeled MMOF intravenously at 5 mg/kg^{-1}, and then exposed to external magnetic guidance for 6 h. To apply an external magnetic field, a 5×2×1 cm magnet was placed near the targeted knee joint. Then, the mice were anesthetized by isoflurane at 0, 1,3, 6 and 24 h post administration, respectively, and imaged with Xenogen IVIS200 (California, USA). Additionally, the major organs including knee joints, heart, liver, spleen, lung, and kidneys were collected at 24 h post administration and imaged by IVIS200.

Statistical analysis

All data are presented as mean ± SD, with n as the number of tissue preparations, cells, or animals. In vitro experiments were performed in triplicates. Paired two-tailed Student's t test was used for comparison between injured and uninjured groups of human bone samples. Unpaired two-tailed Student's t test was used for comparison between two groups when data are normally distributed. One-way ANOVA with relevant post-hoc tests were used for multiple-group comparisons. A value of $p<0.05$ was considered to be statistically significant using the GraphPad Prism software.

Results

Characterization of MMOF

Zeta potential is an important parameter which can affect the efficacy of cellular uptake and adsorption[7; 8]. Normally it is believed that due to the negative charge of cell membrane, nanoparticles with positive charge have greater cellular affinity and chance for adsorption[9; 10]. However, as the charge on the cell membrane doesn't distribute evenly, particles with negative charge can also be attracted to the cells via the cationic sites of the membrane and localized[11; 12]. Therefore, due to the higher zeta potential of ASO-loaded MMOF compared to the pure ASO[13; 14], the chance of ASO uptake by cells would be higher. According to the XRD results, the main representative peaks of Fe_3O_4 particles, can be seen which are located at 35.7, 43.3, 54.4 and 63.2 degree, corresponding to 311, 400, 422 and 440 planes, respectively. After synthesizing MMOF, the main peaks of both Fe_3O_4 and MOF can be distinguished in the spectrum, where the peaks in the red and blue areas are related to the MOF and Fe_3O_4 nanoparticles, respectively (Figure 5E).

Characterization by means of FTIR reveals more information of MMOF about synthesized Fe_3O_4 and its incorporation with MOF (Figure 5G). The peak at 540 cm^{-1} is attributed to Fe-O bond which can be seen in as-received and as-synthesized Fe_3O_4 nanoparticles[15]. The comparison between L-cystine and synthesized Fe_3O_4 particles, shows that the peaks related to S-H stretching and bending vibrations located at 538 cm^{-1}, 2082 cm^{-1} and 2552 cm^{-1} are diminished or weaken significantly, therefore it can be assumed that L-cystine is bonded to the Fe_3O_4 nanoparticles through Fe-S bond[16]. Also, the two peaks located at 780±20 cm^{-1} and 880±20 cm^{-1} are attributed to the C-H bending of L-cystine. In the case of MOF, the characteristic peak of Fe-O is located at 555 cm^{-1} while 746 cm^{-1} representing the C-H bond. The peak located at 1020 cm^{-1} represents C-O-C bond and symmetric and asymmetric peaks of O-C=O are located at 1388 cm^{-1} and 1602 cm^{-1}, respectively[17; 18; 19]. After synthesizing MMOF, there are few differences between FTIR spectrums of MOF and MMOF. The first one is related to Fe-O bond, which is different among synthesized Fe_3O_4 and MOF and in this case, two close peaks at 538 cm^{-1} and 555 cm^{-1} are detected. Another one is related to the blue shift of O-C=O which can be as a result of the repelling effect between O-C=O from MOF with negative charge and negatively charged Fe_3O_4 nanoparticles.

According to the Fe2p spectrums, it can be seen that the intensity of peak at 712.1 eV in Fe_3O_4 and MMOF is higher than MOF and it is due to the presence of Fe-S bond. As it was suggested based on FTIR analysis, Fe_3O_4 was bonded with L-cystine through Fe-S bond and superimposing of its representing peak at 712.1 eV in XPS spectrum[20] with the characteristic peak of Fe^{3+} of MOF at the same bonding energy[21], resulted in higher intensity for this peak in MMOF spectrum. Also, C-S bond in C1s spectrum of MMOF compared to the one of MOF at 285.2 eV, stemmed from presence of Fe_3O_4 nanoparticles. It can be seen from O1s spectrum that Fe-O bond has higher intensity at MMOF spectrum compared to the MOF alone indicating the successful

formation of MMOF.

Reference

1. Zhu X., Cao M., Li K., Chan Y.T., Chan H.F., Mak Y.W., Yao H., Sun J., Ong M.T., Ho K.K., Lee C.W., Lee O.K., Yung P.S., and Jiang Y., Intra-articular sustained-release of pirfenidone as a disease-modifying treatment for early osteoarthritis. Bioact Mater. 2024: 39: 255-272.
2. Bouxsein M.L., Boyd S.K., Christiansen B.A., Guldberg R.E., Jepsen K.J., and Muller R., Guidelines for assessment of bone microstructure in rodents using micro-computed tomography. J Bone Miner Res. 2010: 25: 1468-86.
3. Glasson S.S., Chambers M.G., Van Den Berg W.B., and Little C.B., The OARSI histopathology initiative - recommendations for histological assessments of osteoarthritis in the mouse. Osteoarthritis Cartilage. 2010: 18 Suppl 3: S17-23.
4. Li Q., Wang R., Zhang Z., Wang H., Lu X., Zhang J., Kong A.P., Tian X.Y., Chan H.F., Chung A.C., Cheng J.C., Jiang Q., and Lee W.Y., Sirt3 mediates the benefits of exercise on bone in aged mice. Cell Death Differ. 2023: 30: 152-167.
5. Li R., Li Y., Kristiansen K., and Wang J., SOAP: short oligonucleotide alignment program. Bioinformatics. 2008: 24: 713-4.
6. Love M.I., Huber W., and Anders S., Moderated estimation of fold change and dispersion for RNA-seq data with DESeq2. Genome Biol. 2014: 15: 550.
7. Rasmussen M.K., Pedersen J.N., and Marie R., Size and surface charge characterization of nanoparticles with a salt gradient. Nat Commun. 2020: 11: 2337.
8. Schwegmann H., Feitz A.J., and Frimmel F.H., Influence of the zeta potential on the sorption and toxicity of iron oxide nanoparticles on S. cerevisiae and E. coli. J Colloid Interface Sci. 2010: 347: 43-8.
9. Patil S., Sandberg A., Heckert E., Self W., and Seal S., Protein adsorption and cellular uptake of cerium oxide nanoparticles as a function of zeta potential. Biomaterials. 2007: 28: 4600-7.
10. Bernfield M., Gotte M., Park P.W., Reizes O., Fitzgerald M.L., Lincecum J., and Zako M., Functions of cell surface heparan sulfate proteoglycans. Annu Rev Biochem. 1999: 68: 729-77.
11. Limbach L.K., Li Y., Grass R.N., Brunner T.J., Hintermann M.A., Muller M., Gunther D., and Stark W.J., Oxide nanoparticle uptake in human lung fibroblasts: effects of particle size, agglomeration, and diffusion at low concentrations. Environ Sci Technol. 2005: 39: 9370-6.
12. Win K.Y., and Feng S.S., Effects of particle size and surface coating on cellular uptake of polymeric nanoparticles for oral delivery of anticancer drugs. Biomaterials. 2005: 26: 2713-22.
13. Di Fusco D., Dinallo V., Marafini I., Figliuzzi M.M., Romano B., and Monteleone G., Antisense Oligonucleotide: Basic Concepts and Therapeutic Application in Inflammatory Bowel Disease. Front Pharmacol. 2019: 10: 305.
14. Sharma V.K., and Watts J.K., Oligonucleotide therapeutics: chemistry, delivery and clinical progress. Future Med Chem. 2015: 7: 2221-42.
15. Gadgeel. A.A., Mhaske. S.T., Duerr. C., and Liu. K.L., In-Situ Preparation and Characterization of Aconitic Acid Capped Fe3O4 Nanoparticle by Using Citric Acid as a Reducing Agent. Journal of Inorganic and Organometallic Polymers and Materials. 2019: 29: 1688–1700.
16. Shen. X., Wang. Q., Chen. W., and Pang. Y., One-step synthesis of water-dispersible cysteine functionalized magnetic Fe3O4 nanoparticles for mercury(II) removal from aqueous solutions. Applied Surface Science. 2014: 317: 1028-1034.
17. Xie Q., Li Y., Lv Z., Zhou H., Yang X., Chen J., and Guo H., Effective Adsorption and Removal of Phosphate from Aqueous Solutions and Eutrophic Water by Fe-based MOFs of MIL-101. Sci Rep. 2017: 7: 3316.
18. Jarrah. A., and Farhadi. S., Encapsulation of K6P2W18O62 into magnetic nanoporous Fe3O4/MIL-101 (Fe) for highly enhanced removal of organic dyes. Journal of Solid State Chemistry. 2020: 285: 1-14.
19. Hamedia. A., Mahmood Borhani Zarandia, and Nateghi. M.R., Highly efficient removal of dye pollutants by MIL-101(Fe) metal-organic framework loaded magnetic particles mediated by Poly L-Dopa. Journal of Environmental Chemical Engineering. 2019: 7.
20. Li L., Ma P., Hussain S., Jia L., Lin D., Yin X., Lin Y., Cheng Z., and Wang L., FeS2/carbon hybrids on carbon cloth: a highly efficient and stable counter electrode for dye-sensitized solar cells. Sustainable Energy & Fuels. 2019: 3: 1749-1756.
21. Qian Tang X., Dan Zhang Y., Wei Jiang Z., Mei Wang D., Zhi Huang C., and Fang Li Y., Fe(3)O(4) and metal-organic framework MIL-101(Fe) composites catalyze luminol chemiluminescence for sensitively sensing hydrogen peroxide and glucose. Talanta. 2018: 179: 43-50.

Supplementary Materials

Supplementary Table 1. List of Primer Sequences used for genotype

Gene	Forward (5'-3')	Reverse (5'-3')
Dmp1-Cre	TTGCCTTTCTCTCCACAGGT	CATGTCCATCAGGTTCTTGC
Internal positive control	CTAGGCCACAGAATTGAAAGATCT	GTAGGTGGAAATTCTAGCATCATCC
H19 Flox	CTCTGTGTACGTCCATTGGGACTC	TACCCAGGAAGGACATGGGTATAG

Supplementary Table 2. List of Primer Sequences used for qRT-PCR

Gene	Forward (5'-3')	Reverse (5'-3')
Human-18S	ACCCGTTGAACCCCATTCGTGA	GCCTCACTAAACCATCCAATCGG
Human-H19	GAGTCTGGCAGGAGTGATGA	AAAGTGACCGGGATGAATGC
Human-Gapdh	GTCTCCTCTGACTTCAACAGCG	ACCACCCTGTTGCTGTAGCCAA
Human-Ptgs2	ATGCTGACTATGGCTACAAAAGC	TCGGGCAATCATCAGGCAC
Human- Tnfrsf11b	CACAAATTGCAGTGTCTTTGGTC	TCTGCGTTTACTTTGGTGCCA
Human-Dmp1	GAGCAGTGAGTCATCAGAAGGC	GAGAAGCCACCAGCTAGCCTAT
Mice-β-actin	GGCTGTATTCCCCTCCATCG	CCAGTTGGTAACAATGCCATGT
Mice-18S	TAGAGGGACAAGTGGCGTTC	CGCTGAGCCAGTCAGTGT
Mice-Gapdh	AGGTCGGTGTGAACGGATTTG	GGGGTCGTTGATGGCAACA
Mice-H19	CCTCAAGATGAAAGAAATGGTGCTA	TCAGAACGAGACGGACTTAAAGAA
Mice-Ptgs2	TTCAACACACTCTATCACTGGC	AGAAGCGTTTGCGGTACTCAT
Mice-Tnfrsf11b	CCTTGCCCTGACCACTCTTAT	CACACACTCGGTTGTGGGT
Mice-Tnfsf11	GCTCCGAGCTGGTGAAGAAA	CCCCAAAGTACGTCGCATCT
Mice-Dmp1	GCACAGGCAAATAGTGACCA	TACTGGCCTCTGTCGTAGCC
Mice-Ppp2r1a	GACGGTGACGATTCGCTCTAT	CTGGTCCGTTCAACCCCAAG
Mice-Ppp2r5d	CCCAGTCTCAGTCACCATCAT	GCGTCGTTCTTTCTTGACAATC

Supplementary Table 3. Antibodies list

Target	Supplier	Catalog	Molecular weight (kDa)
COX2/PTGS2	ABclonal	A1253	69
OPG/ TNFRSF11B	ABclonal	A2100	48
DMP1	ABclonal	A16832	102
GAPDH	CST	5174	37
P-AKT	CST	4060	60
AKT	CST	4691	60
P-GSK	CST	9331	46/51
GSKα	CST	4337	51
GSKβ	CST	9315	46
PPP2R1A	ABclonal	A5799	65
PPP2R5D	CST	5687	66/69
Histone H3	CST	4499	17
H3K27me3	ABCAM	Ab6002	17

Supplementary Table 4. Atomic percentage of Fe, C and O acquired from XPS full spectrums of Fe_3O_4, MOF and MMOF

	Fe	C
Fe_3O_4	8.5	60.7
MOF	7.8	67
MMOF	8.9	59.2

Supplementary Figure 1.

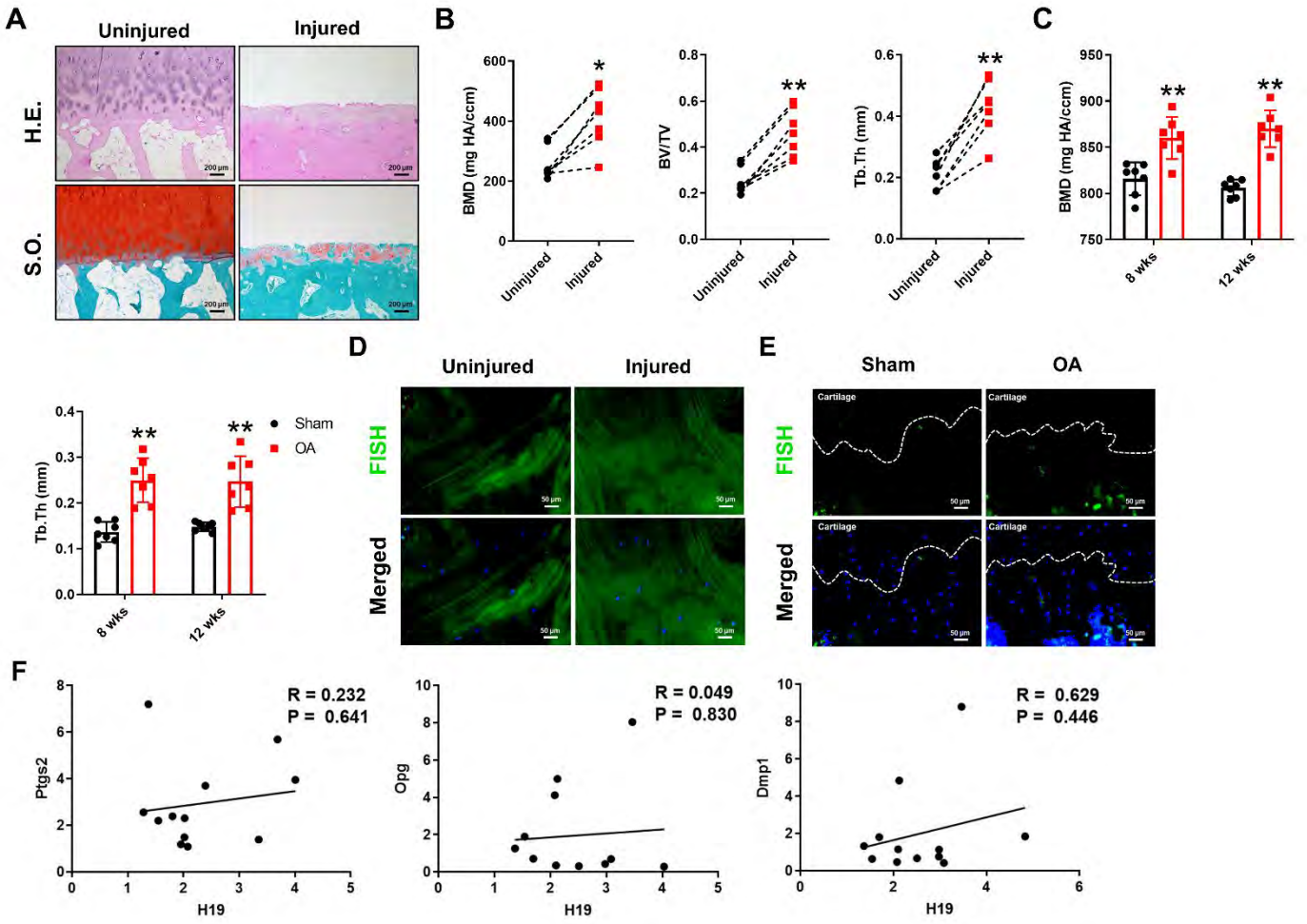

(A) Representative H.E. and S.O staining of human OA subchondral bone. (Scare bar = 200 μm).

(B) Quantitation of human OA subchondral bone parameters (BMD, BV/TV, and Tb.Th). *n* = 7 in each group.

(C) Quantitation of subchondral bone parameters (BMD and Tb.Th) for C57BL/6 mice subjected to Sham or DMM operation for 8 and 12 weeks. *n* = 7 in each group.

(D) Representative FISH staining of negative control in human OA subchondral. Cells were counterstained with DAPI to visualize nuclei (blue). (Scare bar = 20 μm)

(E) Representative FISH staining of negative control in C57BL/6 mice. Cells were counterstained with DAPI to visualize nuclei (blue). (Scare bar = 20 μm)

(F) Correlation between *H19* and *Ptgs2*, *Tnfrsf11b*, *Dmp1* levels in human OA subchondral bone from Injured group was assessed by qPCR. n = 12 in each group.

Supplementary Figure 2.

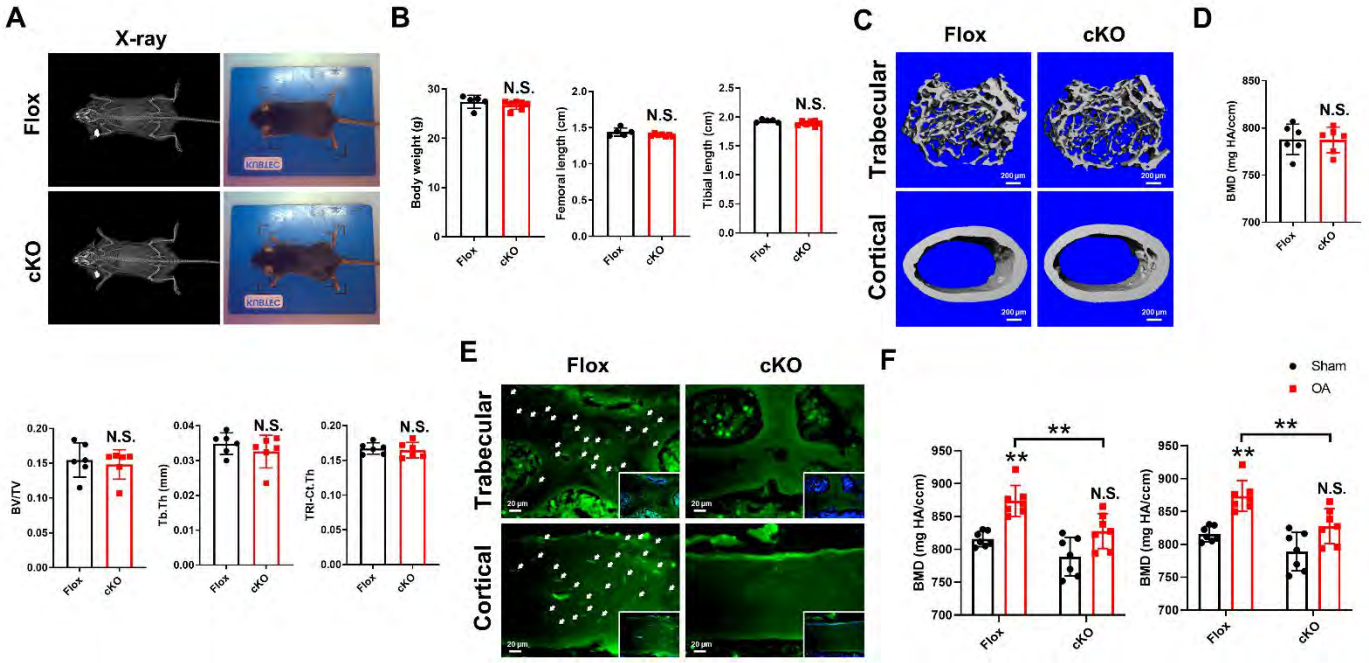

(A) Representative X-ray (left panel) and gross images (right panel) of 3 months male Flox and cKO mice.

(B) Body weight, femoral length and tibial length of 3 months male Flox and cKO mice. $n > 5$ in each group.

(C) Representative micro-CT images of trabecular bone and cortical bone (Scare bar = 200 μm) in the proximal femur of 3 months male Flox and cKO mice.

(D) Quantitation of subchondral bone parameters (BMD, BV/TV, Tb.Th and Ct.Th) of 12-week-old male Flox and cKO mice. $n = 7$ in each group.

(E) Representative FISH staining of osteocytes in trabecular bone and cortical bone of 3 months Flox and cKO mice. Osteocytes were stained with a mice H19-probe and visualized with FITC-conjugated secondary (green). Cells were counterstained with DAPI to visualize nuclei (blue). (Scare bar = 20 μm)

(F) Quantitation of subchondral bone parameters (BMD and Tb.Th) for 3 months male Flox and cKO mice subjected to Sham or DMM operation for 8 weeks. $n = 7$ in each group.

Supplementary Figure 3.

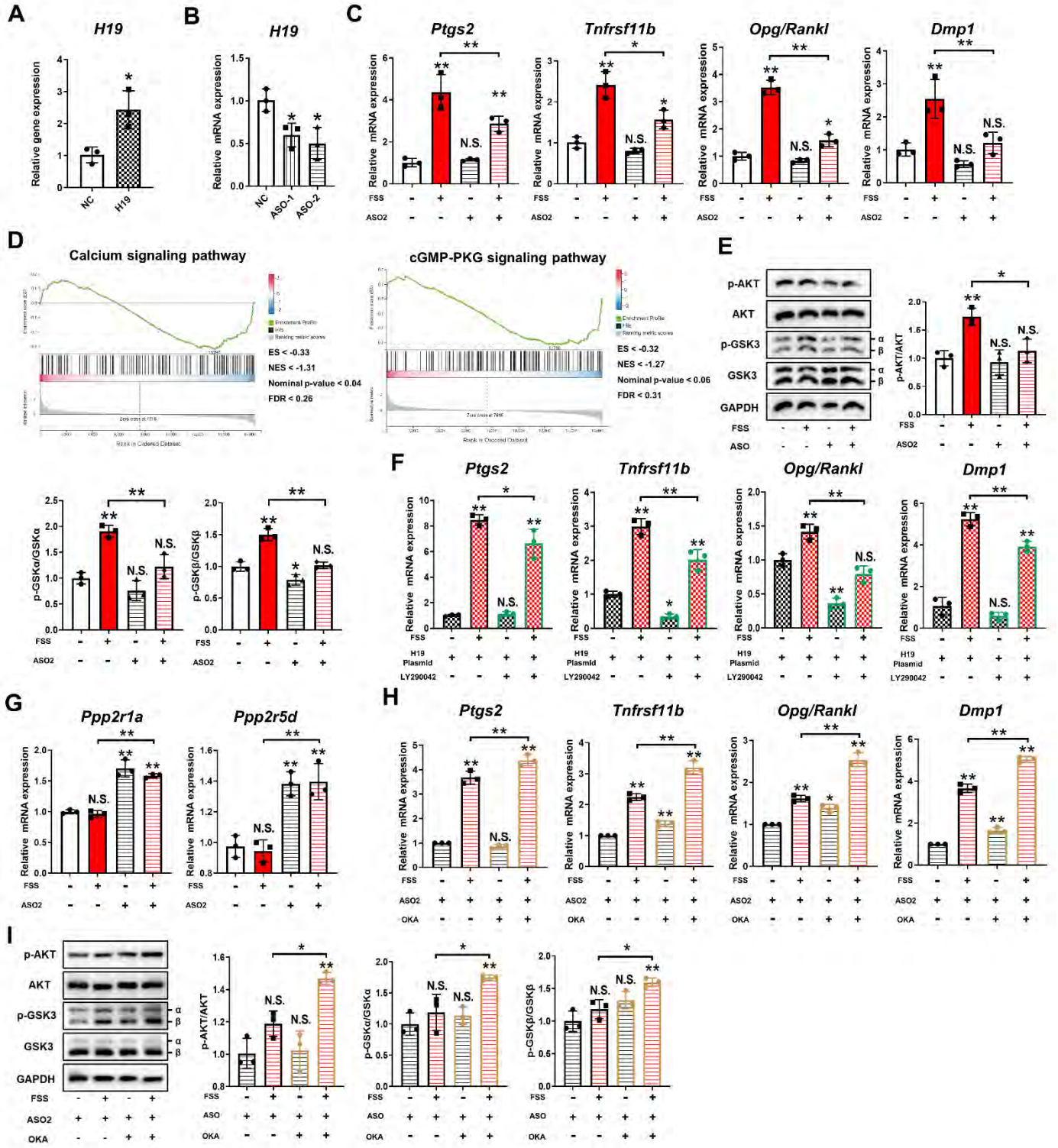

(A) The *H19* expression was assessed by qPCR in MLO-Y4 cells transfected with control (NC) and H19 plasmid. $n = 3$ in each group.

(B) The *H19* expression was assessed by qPCR in MLO-Y4 cells transfected with control (NC), ASO1, and ASO2. $n = 3$ in each group.

(C) The expression of *Ptgs2*, *Tnfrsf11b*, *Opg/Rankl* ratio, and *Dmp1* were assessed by qPCR in control or H19 silenced (ASO2) MLO-Y4 cells cultured under FSS conditions. $n = 3$ per group.

(D) GSEA showing the enrichment of Calcium signaling pathway and cGMP-PKG signaling pathway in

MLO-Y4 cells transfected with control and ASO after FSS stimulation. *n* = 4 per group.

(E) The protein levels of AKT-GSK signaling in control or H19 silenced (ASO2) MLO-Y4 cells were analyzed by western blot under FSS conditions. *n* = 3 per group.

(F) The expression of *Ptgs2*, *Tnfrsf11b*, *Opg/Rankl* ratio, and *Dmp1* were assessed by qPCR in H19 over-expressed MLO-Y4 cells cultured under FSS conditions with or without pretreatment of LY290042 (10 μM) for 30 min. *n* = 3 per group.

(G) The expression of *Ppp2r1a* and *Ppp2r5d* were assessed by qPCR in H19 silenced (ASO2) MLO-Y4 cells cultured under FSS conditions. *n* = 3 per group.

(H) The expression of *Ptgs2*, *Tnfrsf11b*, *Opg/Rankl* ratio, and *Dmp1* were assessed by qPCR in H19 silenced (ASO2) MLO-Y4 cells cultured under FSS conditions with or without pretreatment of OKA (10 nM) for 30 min. n = 3 per group.

(I) The protein levels of AKT-GSK signaling in H19 silenced (ASO2) MLO-Y4 cells were analyzed by western blot under FSS conditions with or without pretreatment of OKA (10 nM) for 30 min. n = 3 per group.

Supplementary Figure 4.

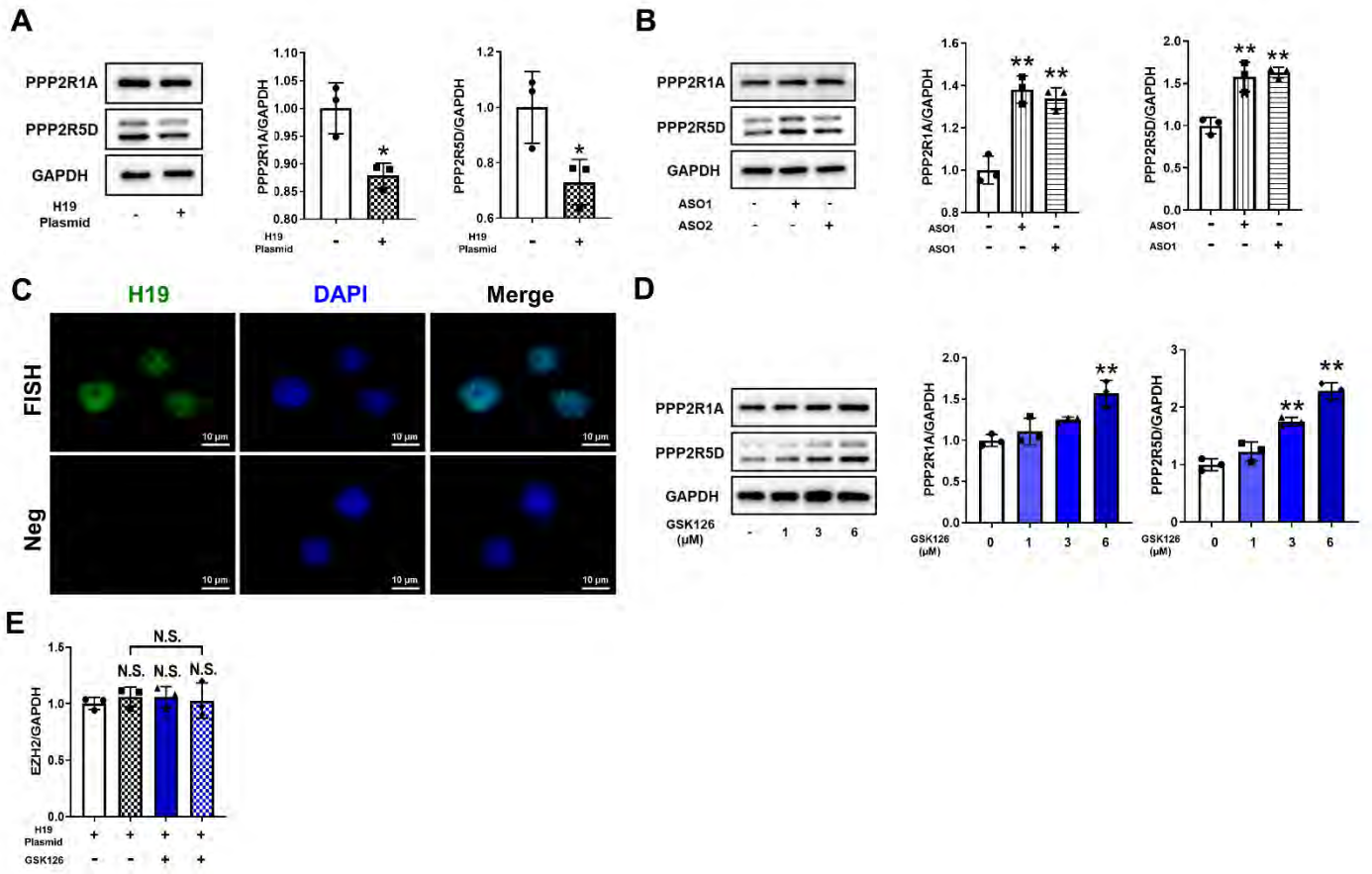

(A) The protein levels of PPP2R1A and PPP2R5D were analyzed by western blot in control or H19 over-expressed MLO-Y4 cells. *n* = 3 per group.

(B) The protein levels of PPP2R1A and PPP2R5D were analyzed by western blot in control or H19 silenced MLO-Y4 cells. *n* = 3 per group.

(C) Representative FISH staining in MLO-Y4 cells. Osteocytes were stained with a mice H19-probe and visualized with FITC-conjugated secondary (green). Cells were counterstained with DAPI to visualize nuclei (blue). (Scare bar = 10 μm)

(D) The protein levels of PPP2R1A and PPP2R5D were analyzed by western blot in MLO-Y4 cells treated with GSK126 of various concentrations (0, 1, 3, 6 μM) for 24 h. *n* = 3 per group.

(E) The protein level of EZH2 were analyzed by western blot in control or H19 over-expressed MLO-Y4 cells with/without GSK126 (6 μM) treatment for 24 h. *n* = 3 per group.

Supplementary Figure 5.

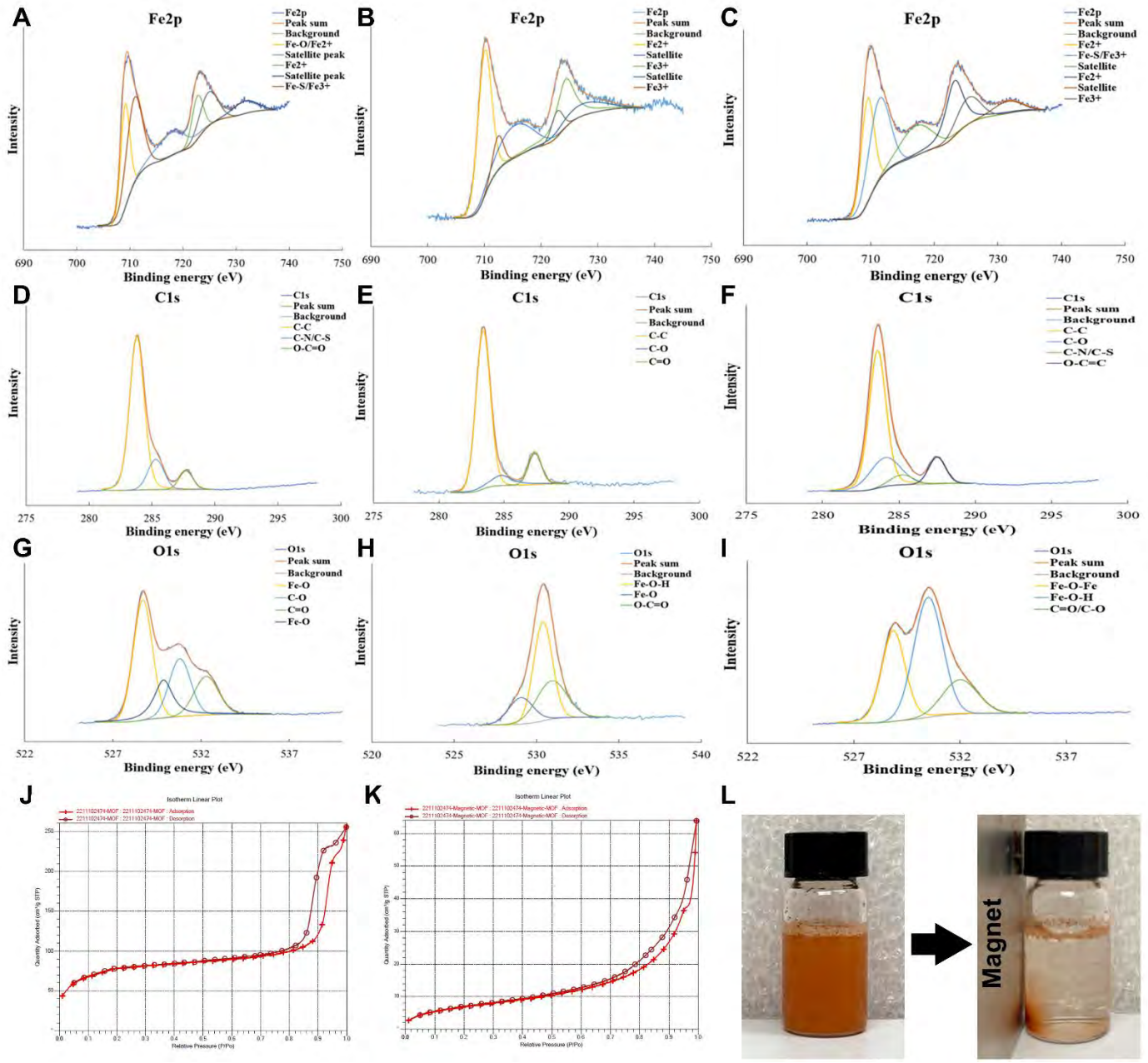

(A-I) XPS high resolution spectra of Fe 2p, C1s and O1s of Fe_3O_4 (A, D, G), MIL-101-Fe (B, E, H) and Fe_3O_4@MIL-101-Fe (C, F, I).

(J, K) BET spectrums of MOF and MMOF.

(L) Suspension and the magnet-driven separation of the MMOF in deionized water.

Supplementary Figure 6.

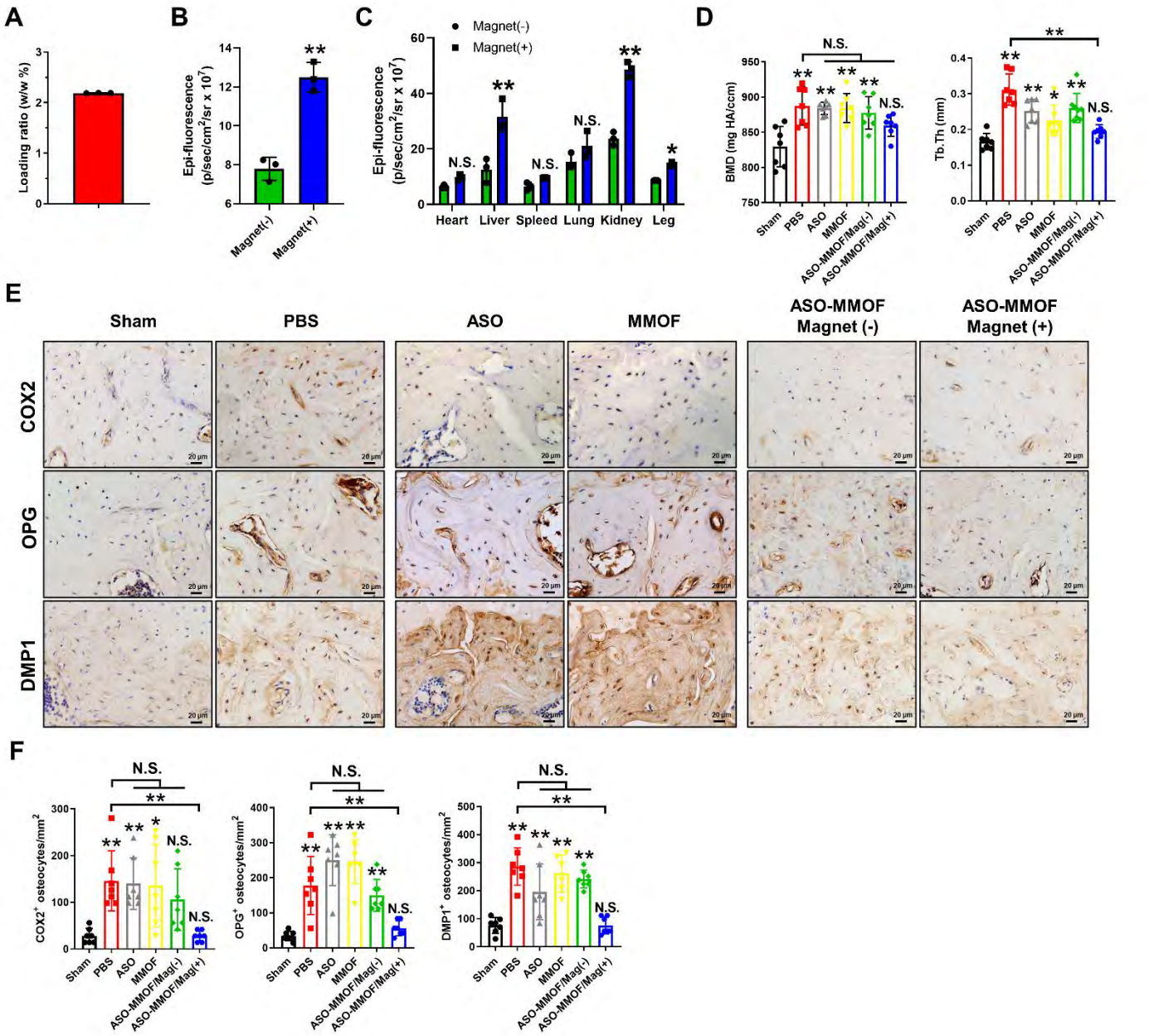

(A) ASO loading ratio of MMOFs.

(B) Fluorescence quantitative assessment of isolated knee joints from C57BL/6 mice at 6 h post i.v. injection of ICG-labeled MMOF with or without 6-hour external magnetic field exposure. n = 3 in each group.

(C) Fluorescence quantitative assessment of isolated major organs and knee joints from C57BL/6 mice at 24 h post i.v. injection of ICG-labeled MMOF with or without 6-hour external magnetic field exposure. *n* = 3 in each group.

(D) Quantitation of subchondral bone parameters (BMD and Tb.Th) for C57BL/6 mice following the indicated treatments for seven consecutive weeks. *n* = 7 in each group.

(E) Representative IHC staining of subchondral bone for COX2, OPG and DMP1 in osteocytes from C57BL/6 mice following the indicated treatments for seven consecutive weeks. (Scare bar = 20 μm)

(F) The percentage number for COX2, OPG and DMP1-positive osteocytes in subchondral bone for C57BL/6

mice following the indicated treatments for seven consecutive weeks. $n = 7$ in each group.

Supplementary Figure 7.

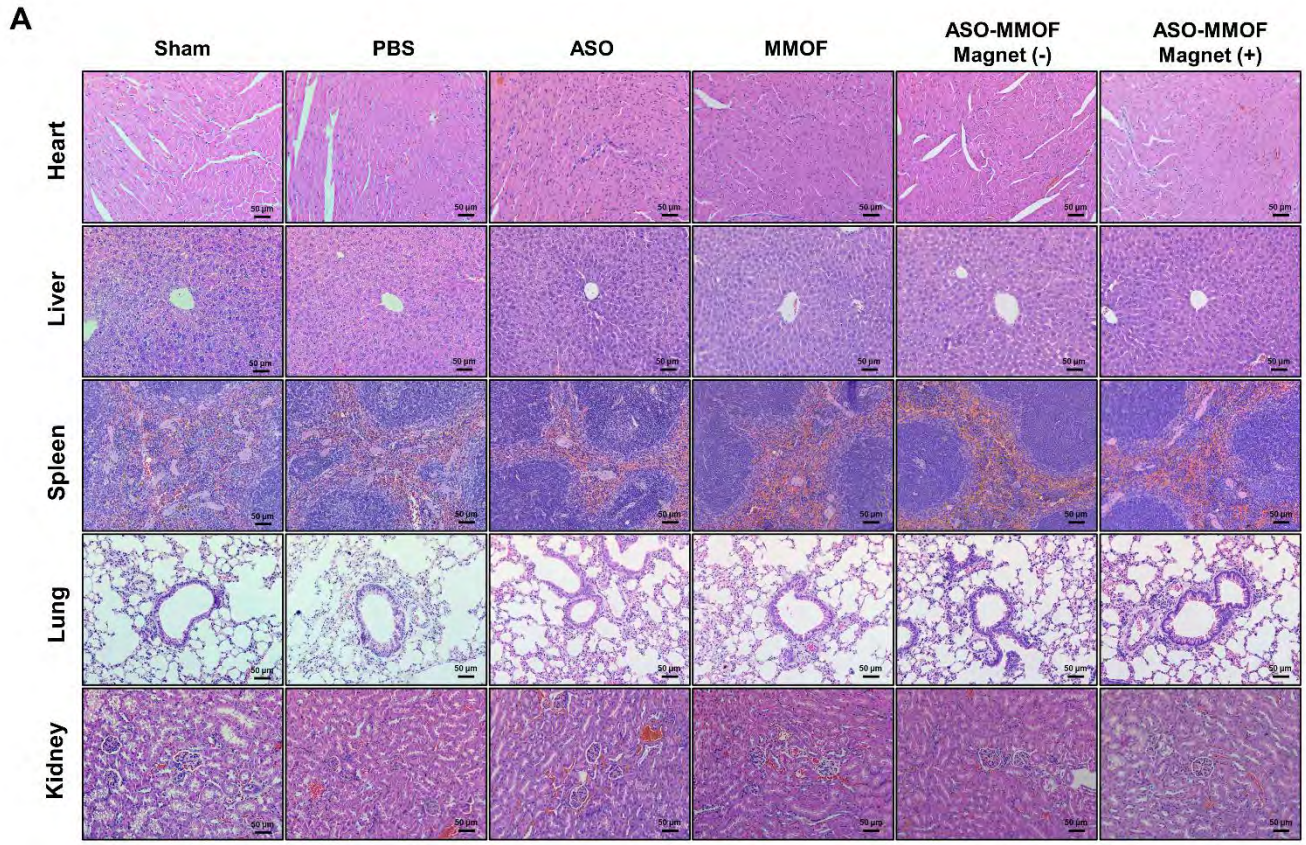

(A) Representative images of H&E staining in major organs from C57BL/6 mice following the indicated treatments for seven consecutive weeks. (Scare bar = 20 μm)

Gene ID	Gene Syml	Type	log2 (ASO	Qvalue (ASO / NC)
100017	'Ldlrap1'	mRNA	-0.17417	0.042728
100038882	'Isg15'	mRNA	0.286271	0.012889
100039796	'Tgtp2'	mRNA	-0.38485	2.55E-07
100043272	'Inafm2'	mRNA	-0.28275	0.035265
100043813	'Rps27rt'	mRNA	-0.31174	0.00569
100044509	'Tgfbr3l'	mRNA	1.257673	2.34E-06
100463512	'Gm20594'	mRNA	-0.49069	0.03969
100502766	'Kifc1'	mRNA	0.382455	2.83E-04
100502841	'Epg5'	mRNA	-0.25527	0.006776
100503353	'Gm14440'	mRNA	-0.40175	0.032793
100678	'Psph'	mRNA	0.358035	0.006612
100689	'Spon2'	mRNA	-1.1083	6.37E-09
100702	'Gbp6'	mRNA	-0.37096	2.39E-04
100862085	'Gm16867'	mRNA	-0.39351	0.018837
101055758	'Gm7592'	mRNA	0.268759	0.011583
101055939	'Gm4869'	mRNA	1.690189	2.50E-08
101056205	'Gm29797'	mRNA	1.101355	8.84E-05
101187	'Parp11'	mRNA	0.335616	0.001475
101476	'Plekha1'	mRNA	-0.26437	0.009077
101497	'Plekhg2'	mRNA	-0.51808	6.42E-05
101685	'Spty2d1'	mRNA	-0.26974	0.033174
102103	'Mtus1'	mRNA	-0.52339	0.001939
102278	'Cpne7'	mRNA	1.983123	1.16E-05
102570	'Slc22a13'	mRNA	1.399236	0.001803
102595	'Plekho2'	mRNA	-0.40518	9.30E-05
102626	'Mapkapk3	mRNA	0.283793	0.047946
102632737	'Gm30732'	mRNA	1.065318	0.012655
102636082	'Gm8251'	mRNA	1.857827	1.27E-13
102638882	'Gm35339'	mRNA	0.952027	0.002943
102639105	'Gm35498'	mRNA	-0.43497	0.001691
102693	'Phldb1'	mRNA	-0.31086	0.020103
102857	'Slc6a8'	mRNA	-0.27129	0.025264
103080	'Septin10'	mRNA	0.399657	0.031607
103135	'Pan2'	mRNA	-0.21539	0.031623
103284	'Zc3h10'	mRNA	0.384597	7.30E-04
103466	'Nt5dc3'	mRNA	-0.32292	1.88E-04
103573	'Xpo1'	mRNA	0.242965	0.024785
103724	'Tbc1d10a'	mRNA	-0.22481	0.013069
103768	'Tubg2'	mRNA	-0.81842	0.017034
104079	'Nxph3'	mRNA	-0.8308	0.01189
104156	'Etv5'	mRNA	-0.40383	3.30E-05
104174	'Gldc'	mRNA	0.671087	0.034062
104215	'Rhoq'	mRNA	-0.30308	0.005927
104263	'Kdm3a'	mRNA	-0.2061	0.032018
104394	'E2f4'	mRNA	0.230554	0.014181
104759	'Pld4'	mRNA	1.078814	0.030909
104806	'Fancm'	mRNA	-0.32476	0.010622
104884	'Tdp1'	mRNA	0.342799	0.009759
104943	'Fam110c'	mRNA	-0.46789	8.59E-07
105171	'Arrdc3'	mRNA	-0.35725	0.008605
105203	'Tasor2'	mRNA	-0.24646	0.046696
105244831	'Gm40367'	mRNA	-0.84437	0.002057
105245342	'Gm40814'	mRNA	0.76869	1.04E-04
105246572	'Gm41844'	mRNA	0.792933	0.001892
105247234	'Gm42368'	mRNA	-0.22194	0.04705
105298	'Epdr1'	mRNA	-0.27258	0.004577
105387	'Akr1c14'	mRNA	-1.42653	0.014691

105522	'Ankrd28'	mRNA	-0.50416	2.01E-11
105734	'Tigd5'	mRNA	-0.71543	5.93E-04
105988	'Espl1'	mRNA	0.422621	1.08E-05
106572	'Rab31'	mRNA	-0.21525	0.006424
106582	'Nrm'	mRNA	0.367714	0.026358
106628	'Trip10'	mRNA	0.208849	0.032055
106763	'Ttbk1'	mRNA	1.748687	0.03041
107022	'Gramd3'	mRNA	-0.34507	0.008928
107239	'Carns1'	mRNA	-0.51211	0.00756
107351	'Kank1'	mRNA	-0.47057	3.19E-04
107368	'Pdzd8'	mRNA	-0.2531	0.003958
107392	'Brms1'	mRNA	0.265396	0.021665
107508	'Eprs'	mRNA	0.245477	5.28E-04
107527	'Il1rl2'	mRNA	2.677521	1.18E-07
107589	'Mylk'	mRNA	-0.76596	8.77E-07
107686	'Snrpd2'	mRNA	0.285247	0.029895
107732	'Mrpl10'	mRNA	0.191306	0.040731
107767	'Scamp1'	mRNA	-0.25708	0.043443
107770	'Tm6sf2'	mRNA	1.183464	0.009793
107869	'Cth'	mRNA	0.186364	0.046791
107995	'Cdc20'	mRNA	0.490886	1.48E-04
108000	'Cenpf'	mRNA	0.601013	2.98E-13
108037	'Shmt2'	mRNA	0.346154	0.026923
108068	'Grm2'	mRNA	2.587398	4.92E-06
108075	'Ltbp4'	mRNA	-0.28751	0.041889
108089	'Rnf144a'	mRNA	-0.2452	0.034388
108097	'Prkab2'	mRNA	-0.17984	0.032034
108101	'Fermt3'	mRNA	1.762887	1.27E-13
108154	'Adamts6'	mRNA	0.346898	0.034169
108167347	'Gm2619'	mRNA	7.644924	0.023998
108167434	'Gm45988'	mRNA	1.67517	0.01735
108167725	'Gm46156'	mRNA	0.444174	0.004411
108167918	'Gm46290'	mRNA	1.344639	0.010709
108168003	'Gm46353'	mRNA	0.972697	4.74E-05
108168208	'Gm45521'	mRNA	2.143477	0.036237
108169043	'Gm46911'	mRNA	0.452234	2.57E-04
108670	'Epsti1'	mRNA	0.69413	1.38E-04
108829	'Jmjd1c'	mRNA	-0.34701	0.023998
108899	'2700081O	mRNA	-0.25281	0.038987
108907	'Nusap1'	mRNA	0.541907	0.001237
108911	'Rcc2'	mRNA	0.240821	0.026651
108912	'Cdca2'	mRNA	0.324394	0.008485
108961	'E2f8'	mRNA	0.295276	0.013103
109032	'Sp110'	mRNA	0.222302	0.008171
109095	'Rbm15b'	mRNA	-0.2686	0.031985
109212	'Pimreg'	mRNA	0.651548	1.43E-05
109246	'Tspan9'	mRNA	0.224071	0.009716
110012	'Tpgs1'	mRNA	0.366373	2.62E-05
110033	'Kif22'	mRNA	0.597355	5.90E-06
110147	'Ehmt2'	mRNA	0.232427	1.97E-04
110213	'Tmbim6'	mRNA	0.291308	0.005413
110524	'Dgkq'	mRNA	-0.40944	0.002406
110532	'Adarb1'	mRNA	-0.53434	2.63E-06
110542	'Amhr2'	mRNA	1.415316	2.58E-05
110809	'Srsf1'	mRNA	-0.15289	0.01138
110956	'D17H6S56	mRNA	0.271593	0.001124
110960	'Tars'	mRNA	0.210212	0.038224
112418	'1700102P	mRNA	1.123059	0.007644

11305	'Abca2'	mRNA	-0.30192	0.034726
114128	'Laptm4b'	mRNA	-0.20598	0.013782
114249	'Npnt'	mRNA	-0.54418	0.003208
114479	'Slc5a5'	mRNA	1.606026	2.86E-15
114584	'Clic1'	mRNA	0.199612	0.001451
11459	'Acta1'	mRNA	-1.13631	1.71E-05
114601	'Ehbp1l1'	mRNA	-0.23122	0.025689
114644	'Slc13a3'	mRNA	-0.7845	0.032893
114679	'Selenom'	mRNA	-0.27347	0.02061
11468	'Actg2'	mRNA	-0.54794	3.90E-04
114713	'Rasa2'	mRNA	-0.25387	0.040908
114716	'Spred2'	mRNA	-0.34106	0.016172
11477	'Acvr1'	mRNA	-0.25584	0.020196
114874	'Ddhd1'	mRNA	-0.36056	0.001032
11492	'Adam19'	mRNA	-0.50215	1.23E-05
11535	'Adm'	mRNA	-0.52263	8.82E-08
11541	'Adora2b'	mRNA	-0.48762	0.035025
11548	'Adra1b'	mRNA	-0.70402	0.012464
115486432	'LOC11548	mRNA	2.323504	0.006406
115487803	'Gm51918'	mRNA	0.475035	1.01E-05
115488029	'LOC11548	mRNA	0.40464	0.023148
115489118	'Gm52429'	mRNA	4.808459	0.003417
115489304	'Gm52481'	mRNA	1.418401	0.006851
115490111	'Gm52768'	mRNA	0.555262	3.72E-07
11552	'Adra2b'	mRNA	2.277286	1.32E-12
11567	'Avil'	mRNA	0.964462	8.33E-09
11596	'Ager'	mRNA	0.606815	0.019353
11600	'Angpt1'	mRNA	-0.39076	6.17E-07
11601	'Angpt2'	mRNA	-0.80109	0.02641
11606	'Agt'	mRNA	-1.70384	6.32E-11
11622	'Ahr'	mRNA	-0.51317	1.93E-04
11632	'Aip'	mRNA	0.169397	0.018589
11634	'Aire'	mRNA	-0.95094	0.002423
11647	'Alpl'	mRNA	0.367004	1.25E-04
11670	'Aldh3a1'	mRNA	-1.07426	1.08E-06
116701	'Fgfrl1'	mRNA	-0.29166	0.036243
11676	'Aldoc'	mRNA	0.682576	0.043662
11705	'Amh'	mRNA	0.699489	5.89E-04
117167	'Steap4'	mRNA	-0.56494	0.031682
117198	'Ivns1abp'	mRNA	-0.26743	0.0017
11732	'Ank'	mRNA	-0.84431	2.67E-09
11747	'Anxa5'	mRNA	-0.16871	0.029895
11761	'Aox1'	mRNA	-0.50505	3.17E-04
11764	'Ap1b1'	mRNA	0.215892	0.004106
11769	'Ap1s1'	mRNA	0.232675	0.008183
11773	'Ap2m1'	mRNA	0.199711	0.002858
11778	'Ap3s2'	mRNA	0.265294	0.005931
11799	'Birc5'	mRNA	0.58301	1.72E-08
11804	'Aplp2'	mRNA	-0.2368	0.009611
11806	'Apoa1'	mRNA	2.081227	1.10E-04
11820	'App'	mRNA	-0.17984	0.033427
11838	'Arc'	mRNA	-0.22133	0.047674
11844	'Arf5'	mRNA	0.230895	0.00164
11852	'Rhob'	mRNA	-0.33566	0.001136
11855	'Arhgap5'	mRNA	-0.24741	0.004855
11856	'Arhgap6'	mRNA	-0.33257	0.017762
11865	'Arntl'	mRNA	-1.34145	2.67E-19
11875	'Art5'	mRNA	4.740506	0.001885

11898	'Ass1'	mRNA	0.233098	0.012734
11907	'Ate1'	mRNA	-0.26279	0.020136
11932	'Atp1b2'	mRNA	-1.42122	9.05E-04
11937	'Atp2a1'	mRNA	1.545397	0.002182
11938	'Atp2a2'	mRNA	-0.17683	0.02733
11947	'Atp5b'	mRNA	0.220361	0.002764
11966	'Atp6v1b2'	mRNA	-0.21199	0.040121
11982	'Atp10a'	mRNA	0.237609	0.008124
11988	'Slc7a2'	mRNA	-0.78737	2.09E-07
12014	'Bach2'	mRNA	0.463092	8.59E-04
12018	'Bak1'	mRNA	0.327915	6.10E-06
12028	'Bax'	mRNA	0.342941	0.003167
12035	'Bcat1'	mRNA	0.436148	5.38E-08
12051	'Bcl3'	mRNA	0.309218	0.011494
12053	'Bcl6'	mRNA	-0.30225	0.00214
12061	'Bdkrb1'	mRNA	0.47201	0.006311
12096	'Bglap'	mRNA	-0.60018	0.003417
12097	'Bglap2'	mRNA	-0.7246	1.61E-05
121021	'Cspg4'	mRNA	-0.43722	0.012389
121022	'Mrps6'	mRNA	-0.21023	0.017945
12142	'Prdm1'	mRNA	-0.7009	0.018319
12168	'Bmpr2'	mRNA	-0.22673	0.021883
12215	'Bsg'	mRNA	-0.27129	0.006164
12224	'Klf5'	mRNA	-0.50141	0.002293
12235	'Bub1'	mRNA	0.407063	0.007504
12236	'Bub1b'	mRNA	0.489424	6.56E-05
12257	'Tspo'	mRNA	0.472306	4.72E-05
12258	'Serping1'	mRNA	-0.66698	2.22E-04
12287	'Cacna1b'	mRNA	2.252944	0.034635
12297	'Cacnb3'	mRNA	-0.27513	0.024867
12304	'Pdia4'	mRNA	0.442937	6.23E-07
12306	'Anxa2'	mRNA	0.178595	0.029895
12315	'Calm3'	mRNA	0.305242	2.08E-08
12316	'Aspm'	mRNA	0.426874	0.009077
12317	'Calr'	mRNA	0.58915	1.95E-11
12322	'Camk2a'	mRNA	-0.52099	0.038246
12332	'Capg'	mRNA	0.170277	0.008458
12333	'Capn1'	mRNA	0.207507	0.012769
12338	'Capn6'	mRNA	0.294682	0.008214
12368	'Casp6'	mRNA	0.523143	1.43E-08
12387	'Ctnnb1'	mRNA	-0.20784	1.77E-04
12406	'Serpinh1'	mRNA	0.272369	3.97E-04
12418	'Cbx4'	mRNA	0.764683	0.003845
12428	'Ccna2'	mRNA	0.385382	0.00182
12442	'Ccnb2'	mRNA	0.57324	1.35E-06
12445	'Ccnd3'	mRNA	0.263035	1.45E-04
12450	'Ccng1'	mRNA	0.251495	0.011376
12452	'Ccng2'	mRNA	0.601984	0.040259
12457	'Noct'	mRNA	-0.33193	1.53E-04
12505	'Cd44'	mRNA	0.187546	0.004439
12514	'Cd68'	mRNA	1.535774	6.33E-26
12530	'Cdc25a'	mRNA	-0.21498	0.032917
12531	'Cdc25b'	mRNA	0.615931	2.67E-09
12532	'Cdc25c'	mRNA	0.625281	7.26E-05
12534	'Cdk1'	mRNA	0.421806	0.008183
12549	'Arhgap31	mRNA	-0.34569	0.017287
12554	'Cdh13'	mRNA	-0.81857	7.21E-08
12571	'Cdk6'	mRNA	0.298771	0.017771

12575	'Cdkn1a'	mRNA	-0.21042	0.009693
12581	'Cdkn2d'	mRNA	0.588354	0.001623
12583	'Cdo1'	mRNA	-1.01429	4.28E-05
12606	'Cebpa'	mRNA	-0.46428	6.42E-05
12607	'Cebpz'	mRNA	-0.20516	0.038099
12613	'Cel'	mRNA	2.087098	7.85E-07
12615	'Cenpa'	mRNA	0.545054	2.63E-06
12660	'Chka'	mRNA	-0.2645	0.014062
12672	'Chrm4'	mRNA	1.501326	5.53E-05
12675	'Chuk'	mRNA	-0.21192	0.043275
12696	'Cirbp'	mRNA	0.33541	0.021804
12704	'Cit'	mRNA	0.377949	1.85E-04
12723	'Clcn1'	mRNA	1.551805	1.97E-04
12753	'Clock'	mRNA	-0.34027	0.001297
12794	'Cnih2'	mRNA	-0.24948	0.044928
12803	'Cntf'	mRNA	1.339306	4.27E-04
12813	'Col10a1'	mRNA	-0.93435	1.31E-05
12814	'Col11a1'	mRNA	-0.66786	2.86E-04
12818	'Col14a1'	mRNA	-1.4135	0.035804
12824	'Col2a1'	mRNA	-1.07648	0.028797
12825	'Col3a1'	mRNA	-0.32129	4.16E-04
12826	'Col4a1'	mRNA	-0.53818	9.12E-07
12827	'Col4a2'	mRNA	-0.41175	8.59E-06
12830	'Col4a5'	mRNA	-0.68088	8.86E-04
12832	'Col5a2'	mRNA	-0.1843	0.02061
12861	'Cox6a1'	mRNA	0.173517	0.010998
12864	'Cox6c'	mRNA	0.240311	0.040731
12865	'Cox7a1'	mRNA	-0.52771	0.026301
12870	'Cp'	mRNA	-0.43042	1.10E-07
12876	'Cpe'	mRNA	-0.62585	1.37E-21
12890	'Cplx2'	mRNA	-1.11694	1.90E-07
12892	'Cpox'	mRNA	0.220841	0.04113
12895	'Cpt1b'	mRNA	0.573013	0.013782
12896	'Cpt2'	mRNA	0.36938	0.008801
12925	'Crip1'	mRNA	-0.23595	0.011132
12931	'Crlf1'	mRNA	0.223281	0.042162
12952	'Cry1'	mRNA	-0.51079	3.96E-05
12953	'Cry2'	mRNA	0.59135	6.15E-06
12955	'Cryab'	mRNA	-0.31333	0.016196
12983	'Csf2rb'	mRNA	-0.45552	2.63E-04
12985	'Csf3'	mRNA	2.149346	1.64E-04
13003	'Vcan'	mRNA	-0.36745	0.001266
13007	'Csrp1'	mRNA	-0.23956	0.024916
13008	'Csrp2'	mRNA	-0.41105	0.004903
13010	'Cst3'	mRNA	-0.34065	2.70E-05
13026	'Pcyt1a'	mRNA	-0.21724	0.026096
13032	'Ctsc'	mRNA	0.372063	0.005078
13057	'Cyba'	mRNA	-0.56248	0.002352
13079	'Cyp21a1'	mRNA	2.488449	0.010575
13107	'Cyp2f2'	mRNA	-1.65838	2.47E-06
13132	'Dab2'	mRNA	-0.3306	1.02E-04
13144	'Dapk3'	mRNA	0.279882	0.013738
13170	'Dbp'	mRNA	1.181817	5.66E-21
13179	'Dcn'	mRNA	-0.34984	0.018212
13180	'Pcbd1'	mRNA	-0.53431	8.35E-06
13198	'Ddit3'	mRNA	-0.32305	0.022916
13199	'Ddn'	mRNA	2.703941	1.93E-07
13205	'Ddx3x'	mRNA	-0.24934	0.003492

13207	'Ddx5'	mRNA	-0.19775	0.008801
13346	'Des'	mRNA	-0.55289	0.011616
13371	'Dio2'	mRNA	-1.32631	0.006178
13406	'Dmp1'	mRNA	-1.46768	0.00247
13423	'Dnase2a'	mRNA	-0.39849	0.001026
13435	'Dnmt3a'	mRNA	-0.49249	2.12E-05
13549	'Dyrk1b'	mRNA	0.430239	3.42E-06
13595	'Ebp'	mRNA	0.264863	0.031189
13602	'Sparcl1'	mRNA	-0.53412	5.95E-07
13605	'Ect2'	mRNA	0.415068	5.97E-04
13610	'S1pr3'	mRNA	-0.42789	0.018293
13641	'Efnb1'	mRNA	-0.37462	0.013853
13642	'Efnb2'	mRNA	-0.27936	0.019973
13649	'Egfr'	mRNA	-0.17677	0.024227
13650	'Rhbdf1'	mRNA	-0.23439	0.028237
13654	'Egr2'	mRNA	-0.40323	0.002737
13685	'Eif4ebp1'	mRNA	0.359522	0.001441
13710	'Elf3'	mRNA	2.15667	0.005647
13717	'Eln'	mRNA	-1.46225	6.63E-05
13803	'Enc1'	mRNA	-0.30909	0.011239
13806	'Eno1'	mRNA	0.160159	0.005766
13809	'Enpep'	mRNA	-0.91284	2.09E-09
13819	'Epas1'	mRNA	-1.1293	7.83E-08
13836	'Epha2'	mRNA	0.284282	4.44E-05
13852	'Stx2'	mRNA	0.168864	0.039687
13982	'Esr1'	mRNA	-0.30408	0.041135
14009	'Etv1'	mRNA	-0.27786	0.019446
14027	'Evpl'	mRNA	1.930538	1.09E-12
14042	'Ext1'	mRNA	0.153449	0.046048
140481	'Man2a2'	mRNA	-0.27605	5.68E-04
140570	'Plxnb2'	mRNA	0.203955	0.001044
14062	'F2r'	mRNA	-0.22523	0.005078
140629	'Ubox5'	mRNA	0.431202	0.010828
14065	'F2rl3'	mRNA	1.128624	0.040107
14066	'F3'	mRNA	-0.61123	0.033332
140742	'Sesn1'	mRNA	-0.38897	0.002484
140792	'Colec12'	mRNA	-0.29883	0.008408
14114	'Fbln1'	mRNA	-0.29223	0.03199
14148	'Fdx1'	mRNA	0.368243	4.57E-04
14154	'Fem1a'	mRNA	-0.28565	0.026667
14155	'Fem1b'	mRNA	-0.22636	0.009514
14164	'Fgf1'	mRNA	-0.60007	6.96E-04
14172	'Fgf18'	mRNA	1.784322	4.09E-06
14173	'Fgf2'	mRNA	-0.53375	3.11E-04
14200	'Fhl2'	mRNA	-0.38624	4.64E-05
14204	'Il4i1'	mRNA	3.967248	0.001124
14205	'Vegfd'	mRNA	0.36304	3.97E-04
14219	'Ccn2'	mRNA	-0.53122	0.028632
14228	'Fkbp4'	mRNA	0.334223	4.92E-05
14232	'Fkbp8'	mRNA	0.2311	1.65E-04
14234	'Foxc2'	mRNA	-0.44383	0.006157
14235	'Foxm1'	mRNA	0.329466	8.81E-05
14239	'Foxs1'	mRNA	-0.74329	0.00569
14241	'Foxl1'	mRNA	-0.47593	0.040731
14251	'Flot1'	mRNA	0.245997	0.020392
14260	'Fmn1'	mRNA	0.466979	2.18E-05
142682	'Zcchc14'	mRNA	-0.47423	9.14E-04
14360	'Fyn'	mRNA	0.186127	0.018402

14362	'Fzd1'	mRNA	-0.33124	0.013155
14367	'Fzd5'	mRNA	-0.47565	1.04E-04
14370	'Fzd8'	mRNA	-0.41489	0.004574
14387	'Gaa'	mRNA	-0.19185	0.02437
14431	'Gamt'	mRNA	-0.44815	0.001026
14538	'Gcnt2'	mRNA	-0.37775	5.01E-05
14573	'Gdnf'	mRNA	0.440403	0.002744
14588	'Gfra4'	mRNA	-0.85825	0.022753
14594	'Ggta1'	mRNA	0.36142	0.029891
14622	'Gjb5'	mRNA	1.095697	0.003756
14630	'Gclm'	mRNA	0.245305	0.037042
14667	'Gm2a'	mRNA	-0.48447	2.13E-04
14681	'Gnao1'	mRNA	-0.41081	0.012017
14685	'Gnat1'	mRNA	2.292508	6.27E-04
14688	'Gnb1'	mRNA	0.160229	0.020763
14705	'Bscl2'	mRNA	0.245869	0.015566
14712	'Gnpat'	mRNA	0.191842	0.024227
14714	'Gnrh1'	mRNA	1.415405	0.028237
14718	'Got1'	mRNA	0.305885	7.64E-05
14726	'Pdpn'	mRNA	0.218916	0.011599
14729	'Gp5'	mRNA	1.284073	7.54E-10
14733	'Gpc1'	mRNA	0.369229	7.70E-13
14758	'Gpm6b'	mRNA	-0.97113	2.08E-08
14793	'Cdca3'	mRNA	0.609961	1.44E-05
14815	'Nr3c1'	mRNA	-0.31262	2.99E-05
14824	'Grn'	mRNA	0.195766	0.023628
14827	'Pdia3'	mRNA	0.282871	0.001153
14860	'Gsta4'	mRNA	-0.46213	0.010232
14862	'Gstm1'	mRNA	-0.52296	6.26E-05
14863	'Gstm2'	mRNA	-0.32332	6.63E-05
14866	'Gstm5'	mRNA	-0.22494	0.038872
14958	'H1f0'	mRNA	0.231357	0.037931
15002	'H2-Ob'	mRNA	4.414812	0.011639
15042	'H2-T24'	mRNA	0.462059	0.011298
15064	'Mr1'	mRNA	-0.25673	0.035804
15161	'Hcfc1'	mRNA	0.22386	0.005927
15163	'Hcls1'	mRNA	2.084568	1.25E-06
15170	'Ptpn6'	mRNA	0.800249	3.42E-04
15184	'Hdac5'	mRNA	0.252497	0.002721
15185	'Hdac6'	mRNA	0.225633	0.004254
15186	'Hdc'	mRNA	2.091981	2.43E-05
15191	'Hdgf'	mRNA	0.201181	0.019597
15200	'Hbegf'	mRNA	-0.25614	0.005861
15201	'Hells'	mRNA	-0.21839	0.025857
15205	'Hes1'	mRNA	0.244043	0.03669
15211	'Hexa'	mRNA	-0.18877	0.004182
15212	'Hexb'	mRNA	-0.24866	0.004551
15228	'Foxg1'	mRNA	-1.4341	0.004376
15234	'Hgf'	mRNA	-0.41011	9.72E-05
15239	'Hgs'	mRNA	0.163991	0.034656
15251	'Hif1a'	mRNA	-0.33211	2.37E-07
15267	'H2ac18'	mRNA	-0.66251	4.16E-04
15270	'H2ax'	mRNA	0.336516	0.006099
15331	'Hmgn2'	mRNA	0.446056	1.11E-05
15354	'Hmgb3'	mRNA	0.738633	4.96E-05
15366	'Hmmr'	mRNA	0.543243	9.67E-09
15368	'Hmox1'	mRNA	-0.57888	0.025607
15369	'Hmox2'	mRNA	0.183744	0.039914

15370	'Nr4a1'	mRNA	0.38672	0.002831
15374	'Jpt1'	mRNA	0.258859	0.021845
15388	'Hnrnpl'	mRNA	0.231361	0.007656
15399	'Hoxa2'	mRNA	0.819039	0.025616
15400	'Hoxa3'	mRNA	0.482148	0.005078
15401	'Hoxa4'	mRNA	0.420696	0.018561
15404	'Hoxa7'	mRNA	0.559895	0.029506
15405	'Hoxa9'	mRNA	0.391398	2.19E-04
15423	'Hoxc4'	mRNA	0.422563	0.002937
15424	'Hoxc5'	mRNA	0.85238	0.028651
15425	'Hoxc6'	mRNA	0.375667	0.006657
15426	'Hoxc8'	mRNA	0.926377	0.005162
15451	'Hpn'	mRNA	1.149632	0.019952
15460	'Hr'	mRNA	-0.50424	0.003645
15473	'Rida'	mRNA	-0.45898	3.99E-05
15490	'Hsd17b7'	mRNA	-0.20715	0.046619
15507	'Hspb1'	mRNA	-0.3376	0.001404
15511	'Hspa1b'	mRNA	-0.32221	0.046496
15516	'Hsp90ab1	mRNA	0.327788	1.45E-08
15528	'Hspe1'	mRNA	0.271329	0.030057
15586	'Hyal1'	mRNA	-0.46353	0.037486
15944	'Irgm1'	mRNA	-0.23026	0.00418
15950	'Ifi203'	mRNA	-0.30384	8.85E-05
16149	'Cd74'	mRNA	-0.52254	0.00193
16159	'Il12a'	mRNA	-1.70319	0.027953
16170	'Il16'	mRNA	-0.24853	0.018909
16181	'Il1rn'	mRNA	-1.16401	1.15E-12
16182	'Il18r1'	mRNA	3.530309	7.95E-66
16185	'Il2rb'	mRNA	0.434695	2.52E-08
16194	'Il6ra'	mRNA	-0.46243	0.001678
16195	'Il6st'	mRNA	-0.30276	0.011652
16201	'Ilf3'	mRNA	0.203579	0.034092
16206	'Lrig1'	mRNA	-0.33532	9.16E-04
16319	'Incenp'	mRNA	0.425898	2.47E-04
16323	'Inhba'	mRNA	-0.63891	5.98E-12
16332	'Inppl1'	mRNA	-0.36437	1.37E-04
16399	'Itga2b'	mRNA	0.658745	1.10E-05
16402	'Itga5'	mRNA	-0.35313	0.0291
16404	'Itga7'	mRNA	-0.33777	0.002719
16412	'Itgb1'	mRNA	-0.15606	0.037713
16414	'Itgb2'	mRNA	-0.56712	3.36E-04
16421	'Itgb7'	mRNA	0.315687	0.032893
16425	'Itih2'	mRNA	-0.88027	5.10E-24
16438	'Itpr1'	mRNA	-0.34356	0.010232
16449	'Jag1'	mRNA	-0.61443	0.004176
16451	'Jak1'	mRNA	-0.3335	8.28E-04
16468	'Jarid2'	mRNA	0.531362	2.63E-04
16529	'Kcnk5'	mRNA	0.294971	4.16E-04
16551	'Kif11'	mRNA	0.33458	0.025905
16559	'Kif17'	mRNA	1.411262	0.001198
16571	'Kif4'	mRNA	0.347201	0.012698
16581	'Kifc2'	mRNA	-0.71514	0.014691
16644	'Kng1'	mRNA	-1.07214	0.018437
16647	'Kpna2'	mRNA	0.336997	0.005056
16649	'Kpna4'	mRNA	-0.2259	8.37E-04
16728	'L1cam'	mRNA	1.077911	7.74E-04
16768	'Lag3'	mRNA	0.807511	0.002103
16776	'Lama5'	mRNA	-0.88679	8.86E-16

16777	'Lamb1'	mRNA	-0.31244	5.57E-05
16782	'Lamc2'	mRNA	-0.40136	4.94E-06
16790	'Anpep'	mRNA	-0.66055	0.045212
16803	'Lbp'	mRNA	-0.49123	0.01455
16828	'Ldha'	mRNA	0.145673	0.004497
16855	'Lgals4'	mRNA	0.58013	0.005861
16859	'Lgals9'	mRNA	0.3239	3.01E-05
16871	'Lhx3'	mRNA	2.598721	0.018837
16878	'Lif'	mRNA	0.533412	1.64E-04
16880	'Lifr'	mRNA	-0.46848	9.39E-05
16891	'Lipg'	mRNA	-0.85475	1.94E-13
16905	'Lmna'	mRNA	0.22697	7.30E-04
16907	'Lmnb2'	mRNA	0.202237	0.023762
16913	'Psmb8'	mRNA	0.178195	0.031081
16923	'Sh2b3'	mRNA	-0.29092	5.01E-04
16948	'Lox'	mRNA	-0.29596	8.23E-05
16950	'Loxl3'	mRNA	0.418503	8.60E-14
16975	'Lrp8'	mRNA	0.315541	0.014968
16978	'Lrrfip1'	mRNA	-0.20071	0.040607
16997	'Ltbp2'	mRNA	0.559247	2.34E-06
170574	'Sp7'	mRNA	0.427775	0.019067
170625	'Snx18'	mRNA	-0.29315	0.002
170644	'Ubn1'	mRNA	-0.32653	0.009381
17069	'Ly6e'	mRNA	0.509185	3.38E-07
170732	'Trhr2'	mRNA	-1.19628	0.021234
170737	'Znrf1'	mRNA	-0.29754	0.001908
17101	'Lyst'	mRNA	-0.40112	9.89E-04
171095	'Il17rc'	mRNA	0.246634	7.48E-05
17119	'Mxd1'	mRNA	0.48834	8.37E-04
17121	'Mxd3'	mRNA	0.470145	0.016396
17125	'Smad1'	mRNA	-0.26406	0.004872
17131	'Smad7'	mRNA	0.264818	1.87E-04
17133	'Maff'	mRNA	-0.35877	3.26E-04
171388	'Bnipl'	mRNA	1.350493	7.08E-04
171567	'Nme7'	mRNA	0.371879	0.001266
171580	'Mical1'	mRNA	-0.33611	0.045365
17159	'Man2b1'	mRNA	-0.22968	0.008019
17160	'Man2b2'	mRNA	-0.2497	0.037902
17174	'Masp1'	mRNA	-0.24462	0.006612
17179	'Matk'	mRNA	-1.02959	0.045859
17192	'Mbd3'	mRNA	0.254569	0.004574
17219	'Mcm6'	mRNA	-0.15725	0.005078
17242	'Mdk'	mRNA	1.17318	0.048614
17258	'Mef2a'	mRNA	-0.56804	9.24E-08
17279	'Melk'	mRNA	0.353232	0.030909
17289	'Mertk'	mRNA	-0.50691	1.85E-04
17300	'Foxc1'	mRNA	-0.21855	0.036011
17311	'Kitl'	mRNA	-0.45222	4.67E-05
17329	'Cxcl9'	mRNA	1.069103	0.004509
17341	'Bhlha15'	mRNA	1.301731	0.010971
17345	'Mki67'	mRNA	0.365198	1.16E-04
17386	'Mmp13'	mRNA	-1.02402	2.65E-18
17390	'Mmp2'	mRNA	-0.31195	3.50E-05
17454	'Mov10'	mRNA	0.477163	5.72E-15
17472	'Gbp4'	mRNA	-0.5674	8.05E-05
17523	'Mpo'	mRNA	1.538967	0.006026
17524	'Mpp1'	mRNA	0.284997	0.00431
17540	'Mrvi1'	mRNA	-1.06909	9.15E-07

17688	'Msh6'	mRNA	-0.1936	0.019378
17691	'Sik1'	mRNA	0.460076	5.47E-04
17755	'Map1b'	mRNA	0.312453	0.006116
17910	'Myo15'	mRNA	1.599318	8.12E-09
17929	'Myom1'	mRNA	-0.70484	0.045729
17965	'Nbl1'	mRNA	-0.32546	3.78E-04
17992	'Ndufa4'	mRNA	0.243102	0.006695
18002	'Nedd8'	mRNA	0.344629	3.90E-04
18005	'Nek2'	mRNA	0.394897	8.44E-04
18008	'Nes'	mRNA	-0.52773	2.63E-06
18010	'Neu1'	mRNA	-0.42217	1.62E-04
18024	'Nfe2l2'	mRNA	0.173396	0.007822
18029	'Nfic'	mRNA	0.17473	0.025689
18030	'Nfil3'	mRNA	-0.449	1.71E-05
18036	'Nfkbib'	mRNA	0.307551	0.019066
18044	'Nfya'	mRNA	-0.22322	0.037906
18049	'Ngf'	mRNA	0.321073	0.015624
18073	'Nid1'	mRNA	-0.44887	1.53E-08
18074	'Nid2'	mRNA	-0.28565	0.008519
18081	'Ninj1'	mRNA	-0.24172	0.003417
18102	'Nme1'	mRNA	0.375271	0.001087
18103	'Nme2'	mRNA	0.251333	0.017287
18128	'Notch1'	mRNA	-0.38276	0.006762
18131	'Notch3'	mRNA	-0.40282	0.04705
18142	'Npas1'	mRNA	4.115628	0.031204
18143	'Npas2'	mRNA	-1.21759	0.012414
18160	'Npr1'	mRNA	-0.60024	0.001475
18218	'Dusp8'	mRNA	0.37578	0.012383
18220	'Nucb1'	mRNA	-0.21431	0.023564
18221	'Nudc'	mRNA	0.229455	0.024884
18263	'Odc1'	mRNA	0.237141	0.025894
18286	'Odf2'	mRNA	0.39931	5.43E-05
18295	'Ogn'	mRNA	-0.97598	1.56E-27
18301	'Fxyd5'	mRNA	0.225464	0.005708
18302	'Oit3'	mRNA	0.981495	8.03E-04
18383	'Tnfrsf11b'	mRNA	-0.81011	2.93E-04
18392	'Orc1'	mRNA	-0.25087	0.029895
18414	'Osmr'	mRNA	-0.29269	3.16E-04
18483	'Palm'	mRNA	0.19492	0.032893
18507	'Pax5'	mRNA	0.471625	0.025759
18515	'Pbx2'	mRNA	0.333923	0.004091
18519	'Kat2b'	mRNA	-0.26261	0.035139
18538	'Pcna'	mRNA	-0.19679	0.028382
18541	'Pcnt'	mRNA	0.276399	3.83E-04
18574	'Pde1b'	mRNA	-0.58012	0.030008
18578	'Pde4b'	mRNA	0.464162	0.022488
18582	'Pde6d'	mRNA	0.288108	1.00E-03
18583	'Pde7a'	mRNA	-0.23753	0.021452
18590	'Pdgfa'	mRNA	-0.33379	0.02197
18595	'Pdgfra'	mRNA	-0.25421	1.28E-04
18596	'Pdgfrb'	mRNA	-0.28589	0.025857
18605	'Enpp1'	mRNA	-0.8038	1.09E-12
18606	'Enpp2'	mRNA	-0.50339	4.93E-05
18619	'Penk'	mRNA	0.873875	0.002
18626	'Per1'	mRNA	0.49865	1.14E-04
18628	'Per3'	mRNA	0.603713	0.005102
18641	'Pfkl'	mRNA	0.196044	0.034672
18643	'Pfn1'	mRNA	0.260329	0.001636

18648	'Pgam1'	mRNA	0.175095	0.001827
18710	'Pik3r3'	mRNA	-0.29077	0.016548
18746	'Pkm'	mRNA	0.174584	0.003968
18750	'Prkca'	mRNA	0.260896	3.85E-04
18751	'Prkcb'	mRNA	-1.16543	0.003766
18752	'Prkcg'	mRNA	-0.50059	0.011583
18763	'Pkd1'	mRNA	-0.34765	0.018264
18791	'Plat'	mRNA	-0.35973	4.74E-05
18816	'Serpinf2'	mRNA	0.927791	0.025689
18817	'Plk1'	mRNA	0.738495	8.31E-14
18846	'Plxna3'	mRNA	-0.38798	0.008458
18854	'Pml'	mRNA	0.149054	0.014691
18933	'Prrx1'	mRNA	0.189184	0.048845
18938	'Ppp1r14b'	mRNA	0.308616	0.037184
18971	'Pold1'	mRNA	0.157652	0.038987
18972	'Pold2'	mRNA	0.207807	0.033136
19025	'Ctsa'	mRNA	-0.21526	0.006162
19039	'Lgals3bp'	mRNA	0.431254	4.22E-08
19044	'Ppox'	mRNA	-0.32125	8.67E-04
19060	'Ppp5c'	mRNA	0.210895	0.015148
19072	'Prep'	mRNA	0.242151	0.019952
19089	'Prkcsh'	mRNA	0.200829	0.004423
19124	'Procr'	mRNA	0.266286	0.033891
19134	'Prpf4b'	mRNA	-0.21211	0.006631
19155	'Npepps'	mRNA	0.200362	0.043094
19156	'Psap'	mRNA	-0.28295	3.76E-04
19171	'Psmb10'	mRNA	0.380106	0.019433
19179	'Psmc1'	mRNA	0.276841	0.026301
19182	'Psmc3'	mRNA	0.190608	0.037109
19186	'Psme1'	mRNA	0.203007	0.036607
19188	'Psme2'	mRNA	0.211798	0.012033
19200	'Pstpip1'	mRNA	0.466462	0.002115
19204	'Ptafr'	mRNA	2.143235	0.007218
19205	'Ptbp1'	mRNA	0.201737	0.002
19206	'Ptch1'	mRNA	0.386307	0.04714
192169	'Ufsp2'	mRNA	0.229389	0.022233
19218	'Ptger3'	mRNA	0.370926	0.040737
192185	'Nadk'	mRNA	0.18528	0.047056
192187	'Stab1'	mRNA	0.70481	0.041283
19220	'Ptgfr'	mRNA	0.405908	0.003604
192287	'Slc25a36'	mRNA	-0.32632	0.003835
19231	'Ptma'	mRNA	0.307945	3.56E-05
19241	'Tmsb4x'	mRNA	-0.60089	1.52E-07
19245	'Ptp4a3'	mRNA	0.226586	0.002963
192653	'Ttc36'	mRNA	2.082546	0.001638
192663	'Abcg4'	mRNA	1.066903	0.014304
19275	'Ptprn'	mRNA	0.896875	0.004574
19305	'Pex5'	mRNA	0.403644	1.45E-08
19332	'Rab20'	mRNA	-0.65842	6.84E-04
19345	'Rab5c'	mRNA	0.230076	0.00623
19348	'Kif20a'	mRNA	0.538671	1.85E-07
19353	'Rac1'	mRNA	0.170577	0.002839
19357	'Rad21'	mRNA	0.255644	0.009077
19378	'Aldh1a2'	mRNA	-0.38813	9.30E-05
19384	'Ran'	mRNA	0.259685	0.044278
19386	'Ranbp2'	mRNA	-0.27922	0.007577
19387	'Rangap1'	mRNA	0.327264	5.20E-04
19411	'Rarg'	mRNA	0.199426	0.012403

194952	'Jmjd4'	mRNA	-0.28553	0.022233
195434	'Utp14b'	mRNA	-0.34923	0.038208
19647	'Rbbp6'	mRNA	0.202575	0.034672
19659	'Rbp1'	mRNA	-0.65366	6.00E-06
19679	'Pitpnm2'	mRNA	-0.31661	0.006841
19700	'Rem1'	mRNA	-0.54281	5.81E-05
19714	'Rev3l'	mRNA	-0.50516	1.04E-05
19731	'Rgl1'	mRNA	-0.51154	1.75E-10
19735	'Rgs2'	mRNA	0.705657	0.003621
19736	'Rgs4'	mRNA	-1.12007	0.013707
20020	'Polr2a'	mRNA	0.171862	0.046795
20132	'Rrh'	mRNA	2.253477	9.89E-04
20166	'Rtkn'	mRNA	0.238929	0.030833
20174	'Ruvbl2'	mRNA	0.386912	2.10E-04
20193	'S100a1'	mRNA	-0.26282	0.029891
20194	'S100a10'	mRNA	0.186519	0.009452
20197	'S100a3'	mRNA	-0.53241	0.016584
20215	'Sag'	mRNA	1.423884	1.39E-04
20229	'Sat1'	mRNA	-0.25687	0.017533
20249	'Scd1'	mRNA	-0.17436	0.039049
20304	'Ccl5'	mRNA	0.244461	0.017763
20306	'Ccl7'	mRNA	-0.42428	7.94E-04
20311	'Cxcl5'	mRNA	0.832582	0.005615
20312	'Cx3cl1'	mRNA	-0.40105	0.020411
20336	'Exoc4'	mRNA	0.252597	0.007068
20341	'Selenbp1'	mRNA	-0.58939	7.27E-06
20347	'Sema3b'	mRNA	-0.20732	0.039203
20348	'Sema3c'	mRNA	-0.80775	5.56E-08
20353	'Sema4c'	mRNA	0.493591	0.016084
20356	'Sema5a'	mRNA	-0.29762	0.041165
20360	'Sema6c'	mRNA	-0.48643	2.75E-04
20361	'Sema7a'	mRNA	-0.37769	4.26E-04
20363	'Selenop'	mRNA	-0.55924	4.72E-05
20379	'Sfrp4'	mRNA	-0.71081	1.02E-15
20393	'Sgk1'	mRNA	-0.49578	1.51E-04
20397	'Sgpl1'	mRNA	-0.15798	0.032793
20409	'Ostf1'	mRNA	0.37503	1.60E-04
20419	'Shcbp1'	mRNA	0.397385	0.030334
20422	'Sem1'	mRNA	0.335655	5.90E-04
20446	'St6galnac2	mRNA	-0.45157	5.58E-04
20448	'St6galnac4	mRNA	-0.36723	0.022256
20454	'St3gal5'	mRNA	-0.41771	0.016344
20462	'Tra2b'	mRNA	-0.2303	0.017876
20463	'Cox7a2l'	mRNA	-0.24835	5.81E-04
20475	'Six5'	mRNA	-0.3626	0.030127
20480	'Clpb'	mRNA	0.294029	6.09E-05
20481	'Ski'	mRNA	-0.36599	0.001266
20492	'Slbp'	mRNA	-0.26057	0.002442
20497	'Slc12a3'	mRNA	3.08784	6.91E-04
20498	'Slc12a4'	mRNA	-0.18156	0.027872
20504	'Slc17a1'	mRNA	-1.6432	0.03732
20514	'Slc1a5'	mRNA	0.327266	0.010304
20515	'Slc20a1'	mRNA	-0.699	4.80E-08
20536	'Slc4a3'	mRNA	-0.35961	0.005078
20538	'Slc6a2'	mRNA	-0.71569	0.037486
20539	'Slc7a5'	mRNA	0.139233	0.043456
20568	'Slpi'	mRNA	0.685347	5.83E-07
20586	'Smarca4'	mRNA	0.187626	0.007826

20620	'Plk2'	mRNA	-0.39648	9.46E-05
20621	'Snn'	mRNA	-0.22096	0.044299
20637	'Snrnp70'	mRNA	0.163501	0.029326
20661	'Sort1'	mRNA	1.183601	1.73E-05
20670	'Sox15'	mRNA	1.780483	7.35E-04
20682	'Sox9'	mRNA	-0.44542	0.002573
20684	'Sp100'	mRNA	0.247854	0.00588
20698	'Sphk1'	mRNA	-0.69918	8.86E-16
20716	'Serpina3n	mRNA	-0.47971	0.006164
20719	'Serpinb6a	mRNA	0.155949	0.025788
207214	'Larp4'	mRNA	-0.15907	0.040737
20744	'Strbp'	mRNA	0.368064	0.047937
207495	'Baiap2l2'	mRNA	2.780578	0.003645
207686	'Cfap69'	mRNA	0.304055	0.040737
207742	'Rnf43'	mRNA	2.880991	4.84E-04
207777	'Tspoap1'	mRNA	0.733378	1.27E-04
207785	'Csrnp2'	mRNA	-0.27724	0.028541
20787	'Srebf1'	mRNA	0.176669	0.043662
20807	'Srf'	mRNA	-0.27302	0.003592
208080	'Ubap1l'	mRNA	1.455174	0.004703
208084	'Pif1'	mRNA	0.644722	3.03E-04
208104	'Mlxip'	mRNA	-0.23811	0.034352
208198	'Btbd2'	mRNA	0.282524	1.15E-04
208228	'Mob3a'	mRNA	-0.30347	1.58E-05
208431	'Shroom4'	mRNA	0.401058	0.002376
20846	'Stat1'	mRNA	0.196425	0.002783
208650	'Cblb'	mRNA	-0.37852	4.54E-04
20869	'Stk11'	mRNA	0.293319	1.92E-08
208718	'Dis3l2'	mRNA	0.362627	0.008605
20877	'Aurkb'	mRNA	0.572167	8.05E-05
208777	'Sned1'	mRNA	-0.54517	2.47E-04
20878	'Aurka'	mRNA	0.551571	1.06E-05
208820	'Triqk'	mRNA	-0.49713	0.041739
208836	'Fanci'	mRNA	0.362557	0.002222
208943	'Myo5c'	mRNA	-0.50087	0.025342
209032	'Zc3hav1l'	mRNA	1.119085	1.09E-13
209039	'Tns2'	mRNA	0.45358	9.24E-08
20908	'Stx3'	mRNA	-0.40144	0.012838
209334	'Gen1'	mRNA	0.488257	0.004372
209378	'Itih5'	mRNA	-0.36487	0.021292
209448	'Hoxc10'	mRNA	0.350354	2.99E-07
209558	'Enpp3'	mRNA	-0.72139	5.19E-07
20970	'Sdc3'	mRNA	0.367697	0.003795
20971	'Sdc4'	mRNA	-0.27381	1.02E-04
210094	'Iglon5'	mRNA	-0.45897	0.002
210105	'Zfp719'	mRNA	-0.39783	0.001417
210108	'D130043K	mRNA	2.088616	1.65E-07
210148	'Slc30a6'	mRNA	0.320637	0.046619
210293	'Dock10'	mRNA	-0.71298	0.003264
210582	'Coq10a'	mRNA	-0.24564	0.036353
210925	'Ints9'	mRNA	0.310217	0.001297
211232	'Cpne9'	mRNA	2.279736	1.00E-05
211401	'Mtss1'	mRNA	0.395047	0.001908
211480	'Kcnj14'	mRNA	0.711029	4.57E-04
211548	'Nomo1'	mRNA	0.346256	2.70E-05
211623	'Plac9a'	mRNA	-0.46461	0.028469
212032	'Hk3'	mRNA	4.446319	0.004634
212168	'Zswim4'	mRNA	-0.3801	1.73E-04

212439	'AA98686(	mRNA	0.991476	9.37E-04
212483	'Fam193b'	mRNA	-0.34935	0.006957
212728	'Tarbp1'	mRNA	-0.41015	0.037633
212919	'Kctd7'	mRNA	0.642525	2.18E-04
213019	'Pdlim2'	mRNA	-0.32207	1.77E-04
213081	'Wdr19'	mRNA	0.338161	0.046618
213119	'Itga10'	mRNA	-0.45458	0.001908
213211	'Rnf26'	mRNA	0.397971	0.001703
213272	'Txndc2'	mRNA	1.213122	1.11E-04
21335	'Tacc3'	mRNA	0.342378	0.002939
21345	'Tagln'	mRNA	-0.81772	3.01E-05
21346	'Tagln2'	mRNA	0.256223	0.001388
21354	'Tap1'	mRNA	0.273006	0.012729
213556	'Plekhh2'	mRNA	-0.53858	7.43E-08
21356	'Tapbp'	mRNA	0.405629	5.38E-08
213582	'Map9'	mRNA	0.359494	0.025516
21375	'Tbr1'	mRNA	2.289674	5.94E-08
21385	'Tbx2'	mRNA	1.370958	8.45E-04
21390	'Tbxa2r'	mRNA	0.988342	3.47E-04
21393	'Tcap'	mRNA	1.831677	5.89E-04
21452	'Tcn2'	mRNA	-0.58259	9.62E-07
214642	'Cped1'	mRNA	-0.55919	2.94E-05
214855	'Arid5a'	mRNA	-0.22931	0.008214
214951	'Rhbdl1'	mRNA	-0.48582	0.036442
215001	'Wfikkn1'	mRNA	1.196861	2.94E-07
215095	'Astl'	mRNA	2.093431	9.87E-08
215418	'Csrnp1'	mRNA	0.247628	0.036392
215493	'A3galt2'	mRNA	1.783085	2.01E-04
215494	'Pomgnt2'	mRNA	-0.35496	0.034105
215615	'Rnpep'	mRNA	0.252691	0.007635
215653	'Rassf2'	mRNA	0.320051	0.004393
215693	'Zmat1'	mRNA	-0.50537	0.007201
215999	'Mcu'	mRNA	0.238596	0.026961
216019	'Hkdc1'	mRNA	1.083897	0.010382
216134	'Pdxk'	mRNA	0.328265	1.56E-04
216188	'Aldh1l2'	mRNA	0.382759	6.64E-04
216190	'Appl2'	mRNA	-0.32771	0.024227
216198	'Tcp11l2'	mRNA	-0.44542	3.63E-04
216238	'Eea1'	mRNA	-0.37879	3.11E-04
216343	'Tph2'	mRNA	1.557322	0.023564
216456	'Gls2'	mRNA	0.386181	0.01735
216725	'Adamts2'	mRNA	-0.37685	0.004505
216742	'Fnip1'	mRNA	-0.34953	0.001094
21678	'Tead3'	mRNA	-0.40426	5.89E-04
216805	'Flcn'	mRNA	-0.38099	0.00598
21682	'Tec'	mRNA	-1.46113	0.031293
21683	'Tecta'	mRNA	2.294301	0.001254
21685	'Tef'	mRNA	0.562828	4.02E-10
216858	'Kctd11'	mRNA	-0.46365	1.57E-04
217154	'Stac2'	mRNA	0.291186	0.002207
217166	'Nr1d1'	mRNA	0.782328	0.015132
217198	'Plekhh3'	mRNA	-0.35249	0.004176
217216	'Hrob'	mRNA	0.742721	3.30E-11
217304	'Cd300lb'	mRNA	-0.41296	0.002931
217310	'Hid1'	mRNA	-0.47758	4.80E-08
217333	'Trim47'	mRNA	-0.3102	0.036011
217340	'Rnf157'	mRNA	-0.23547	0.036353
217371	'Rab40b'	mRNA	-0.99804	3.31E-04

217410	'Trib2'	mRNA	-0.81923	2.49E-06
21743	'Inmt'	mRNA	-1.84237	0.008301
21749	'Terf1'	mRNA	0.344394	0.040737
21754	'Tesk1'	mRNA	-0.22412	0.039071
217578	'Baz1a'	mRNA	-0.25977	0.040105
217653	'Mis18bp1'	mRNA	0.541694	0.001331
217664	'Mgat2'	mRNA	-0.24494	0.007036
21770	'Ppp2r5d'	mRNA	0.14758	0.035025
217737	'Ahsa1'	mRNA	0.237415	0.013025
217830	'Dglucy'	mRNA	0.338285	0.00511
217864	'Rcor1'	mRNA	-0.18364	0.019694
217893	'Pacs2'	mRNA	-0.34543	0.038542
21809	'Tgfb3'	mRNA	-0.48987	1.88E-07
21812	'Tgfbr1'	mRNA	-0.39247	0.031456
21815	'Tgif1'	mRNA	-0.40241	0.004819
21817	'Tgm2'	mRNA	-0.35944	9.02E-05
218203	'Mylip'	mRNA	-0.3307	0.049632
218210	'Nup153'	mRNA	-0.17847	0.014272
218232	'Ptpdc1'	mRNA	-0.36776	6.14E-04
21825	'Thbs1'	mRNA	-0.38816	3.95E-05
21826	'Thbs2'	mRNA	-0.20651	0.010895
21832	'Thpo'	mRNA	-1.89655	0.014691
218397	'Rasa1'	mRNA	-0.28388	0.012017
218454	'Lhfpl2'	mRNA	-0.36893	0.004228
218461	'Pde8b'	mRNA	-1.91724	0.040144
218518	'Marveld2'	mRNA	2.323093	1.93E-08
218581	'Depdc1b'	mRNA	0.581988	0.018451
21872	'Tjp1'	mRNA	-0.28032	0.002649
218756	'Slc4a7'	mRNA	-0.4631	2.13E-07
218772	'Rarb'	mRNA	-0.30944	0.010766
21888	'Tle4'	mRNA	-0.59205	7.51E-05
218952	'Fermt2'	mRNA	-0.2841	3.88E-04
218977	'Dlgap5'	mRNA	0.541637	5.26E-05
219105	'Zmym5'	mRNA	-0.22091	0.040545
219114	'Ska3'	mRNA	0.280159	0.016196
21924	'Tnnc1'	mRNA	-0.91659	6.25E-04
21926	'Tnf'	mRNA	-0.33343	0.044994
21928	'Tnfaip2'	mRNA	-0.27711	3.86E-04
21929	'Tnfaip3'	mRNA	-0.54404	2.67E-09
21938	'Tnfrsf1b'	mRNA	-0.30287	0.006612
21960	'Tnr'	mRNA	-0.84734	3.09E-04
21961	'Tns1'	mRNA	-0.4687	0.008019
21969	'Top1'	mRNA	-0.18785	0.041793
21973	'Top2a'	mRNA	0.399902	3.78E-04
21981	'Ppp1r13b'	mRNA	-0.35221	0.022791
21991	'Tpi1'	mRNA	0.143041	0.022381
22022	'Tpst2'	mRNA	0.229784	0.032504
22027	'Hsp90b1'	mRNA	0.345252	8.55E-04
22033	'Traf5'	mRNA	-0.37877	0.001266
22061	'Trp63'	mRNA	-0.50046	0.022916
22083	'Ctr9'	mRNA	-0.31619	1.37E-04
22123	'Psmd3'	mRNA	0.245069	0.041889
22134	'Tgoln1'	mRNA	-0.29531	0.00261
22137	'Ttk'	mRNA	0.462493	6.96E-04
22151	'Tubb2a'	mRNA	-0.19446	0.015997
22163	'Tnfrsf4'	mRNA	0.855226	3.90E-04
22166	'Txn1'	mRNA	0.505281	1.03E-04
22187	'Ubb'	mRNA	0.266172	0.003353

22192	'Ube2m'	mRNA	0.239374	0.022345
22195	'Ube2l3'	mRNA	0.175207	0.031066
22201	'Uba1'	mRNA	0.211425	0.003113
22241	'Ulk1'	mRNA	-0.24509	0.037358
22256	'Ung'	mRNA	-0.43282	0.007704
22273	'Uqcrc1'	mRNA	0.270436	4.61E-06
22321	'Vars'	mRNA	0.260622	4.33E-04
223254	'Farp1'	mRNA	0.197092	0.001474
223272	'Itgbl1'	mRNA	-0.52412	0.01527
22330	'Vcl'	mRNA	-0.64958	1.33E-06
22361	'Vnn1'	mRNA	0.504571	6.15E-06
223626	'Them6'	mRNA	0.442272	0.008859
223645	'Mroh6'	mRNA	1.138477	0.01603
223649	'Nrbp2'	mRNA	-0.47705	0.006841
22365	'Vps45'	mRNA	0.355629	9.96E-04
223672	'Apol9a'	mRNA	0.15095	0.020125
22370	'Vtn'	mRNA	-1.09922	1.51E-16
223723	'Ttll12'	mRNA	0.299	0.007846
223752	'Gramd4'	mRNA	-0.33231	2.25E-06
22377	'Wbp1'	mRNA	-0.33392	5.50E-04
22390	'Wee1'	mRNA	-0.26866	0.02387
223978	'Cpped1'	mRNA	0.28445	7.30E-04
224024	'Scarf2'	mRNA	-0.26962	0.004903
224088	'Atp13a3'	mRNA	-0.39751	2.63E-04
224105	'Pak2'	mRNA	-0.15259	0.025192
224171	'Cip2a'	mRNA	0.293443	0.039418
224224	'Impg2'	mRNA	1.032324	0.001193
224273	'Crybg3'	mRNA	-0.52189	1.35E-04
22433	'Xbp1'	mRNA	-0.40106	1.20E-04
224697	'Adamts10'	mRNA	-0.53143	9.29E-04
224796	'Clic5'	mRNA	-0.39219	0.030812
224805	'Aars2'	mRNA	0.318337	0.030641
224829	'Trerf1'	mRNA	0.332332	0.002905
225027	'Srsf7'	mRNA	-0.18297	0.039963
225049	'Ttc7'	mRNA	0.258218	0.002466
225055	'Fbxo11'	mRNA	-0.20647	0.038004
225339	'Ammecr1l'	mRNA	-0.18371	0.044964
225594	'Gm4841'	mRNA	-0.80151	1.87E-04
225872	'Npas4'	mRNA	-0.45088	0.003301
225888	'Kmt5b'	mRNA	-0.26999	0.01064
22592	'Ercc5'	mRNA	0.255623	0.045652
225997	'Trpm6'	mRNA	0.46179	0.002065
226089	'Ric1'	mRNA	-0.44497	3.20E-06
226122	'Ubtd1'	mRNA	-0.37019	0.001031
226143	'Cyp2c23'	mRNA	1.165452	0.005736
226153	'Twnk'	mRNA	-0.29174	0.021726
22627	'Ywhae'	mRNA	0.243784	9.88E-04
22634	'Plagl1'	mRNA	-0.38311	1.05E-09
226413	'Lct'	mRNA	1.768399	5.05E-29
226421	'Rab7b'	mRNA	-0.21794	0.019699
226422	'Rab29'	mRNA	0.296096	0.043663
226442	'Zfp281'	mRNA	-0.23519	0.036011
22658	'Pcgf2'	mRNA	0.221417	0.021134
226641	'Atf6'	mRNA	-0.28188	7.85E-07
226747	'Ahctf1'	mRNA	-0.17599	0.031079
22682	'Zfand5'	mRNA	-0.27306	9.89E-04
226841	'Vash2'	mRNA	-0.42584	0.030127
226844	'Flvcr1'	mRNA	-0.59186	5.32E-13

226856	'Lpgat1'	mRNA	-0.2431	0.008777
226970	'Arhgef4'	mRNA	-0.89878	0.006264
227157	'Mpp4'	mRNA	3.672293	0.024092
22722	'Zfp64'	mRNA	0.221968	0.00489
227333	'Dgkd'	mRNA	-0.32114	4.32E-05
227377	'Farp2'	mRNA	0.350836	0.021883
227449	'Zcchc2'	mRNA	-0.27227	0.004176
22761	'Zfpm1'	mRNA	-0.41374	0.014054
227620	'Uap1l1'	mRNA	-0.48175	1.53E-05
227622	'Paxx'	mRNA	-0.37468	0.04891
227634	'Camsap1'	mRNA	-0.20647	0.015773
227753	'Gsn'	mRNA	-0.50262	0.001087
22785	'Slc30a4'	mRNA	-0.26921	0.003115
22793	'Zyx'	mRNA	-0.25599	0.027889
227937	'Pkp4'	mRNA	0.234281	0.041283
228033	'Atp5g3'	mRNA	0.213231	0.032893
228357	'Lrp4'	mRNA	-0.48603	0.015472
228714	'Kat14'	mRNA	0.233235	0.044879
228836	'Dlgap4'	mRNA	-0.32254	0.008153
228880	'Zmynd8'	mRNA	0.227354	0.041084
228998	'Arfgap1'	mRNA	-0.24928	0.02602
229473	'Tmem131	mRNA	-0.29291	0.002352
229512	'Smg5'	mRNA	0.150121	0.040685
229588	'Gm128'	mRNA	1.287274	1.11E-04
229595	'Adamtsl4'	mRNA	0.17106	0.013103
229599	'Ciart'	mRNA	0.505416	0.039469
229603	'Otud7b'	mRNA	-0.20396	0.046381
229658	'Vangl1'	mRNA	0.209738	0.009733
229665	'Ampd1'	mRNA	1.52212	3.67E-04
229709	'Ahcyl1'	mRNA	-0.1739	0.012383
229731	'Slc25a24'	mRNA	0.224295	0.009134
229841	'Cenpe'	mRNA	0.432419	3.37E-06
230073	'Ddx58'	mRNA	0.212743	0.005185
230098	'Arhgef39'	mRNA	-0.65631	4.02E-04
230099	'Car9'	mRNA	-0.95226	2.22E-04
230259	'E130308A	mRNA	-0.39695	0.009011
230587	'Glis1'	mRNA	0.451384	0.013762
230674	'Kdm4a'	mRNA	0.309803	0.001052
230738	'Zc3h12a'	mRNA	0.317568	0.003466
230751	'Oscp1'	mRNA	0.346028	0.030879
230761	'Zfp362'	mRNA	-0.32827	0.046702
230863	'Sh2d5'	mRNA	2.124603	1.22E-17
231151	'Tada2b'	mRNA	-0.25078	0.045745
231430	'Cox18'	mRNA	0.538935	0.002719
231633	'Tmem119	mRNA	-0.32045	0.002421
231655	'Oasl1'	mRNA	0.345821	4.26E-05
231672	'Fbxw8'	mRNA	0.157316	0.030641
231798	'Lrch4'	mRNA	0.200226	0.037109
231834	'Snx8'	mRNA	-0.28072	0.024785
231863	'Fbxl18'	mRNA	0.346967	8.58E-04
231887	'Pdap1'	mRNA	0.269842	0.021994
232087	'Mat2a'	mRNA	-0.37656	4.77E-06
232314	'Ppp4r2'	mRNA	-0.20053	0.008458
232431	'Gprc5a'	mRNA	0.155875	0.048488
232440	'H2aj'	mRNA	0.284374	0.007844
232441	'Rerg'	mRNA	-1.12234	8.96E-04
232560	'Caprin2'	mRNA	-0.48587	2.45E-04
232791	'Cnot3'	mRNA	0.177892	0.028541

232889	'Pla2g4c'	mRNA	0.456	0.024452
233066	'Syne4'	mRNA	1.316286	0.043486
233199	'Mybpc2'	mRNA	1.819665	0.00415
233315	'Mtmr10'	mRNA	-0.24199	0.001026
233406	'Prc1'	mRNA	0.288379	0.022757
233489	'Picalm'	mRNA	-0.14986	0.034726
233490	'Crebzf'	mRNA	-0.27897	0.001031
233726	'Ipo7'	mRNA	-0.20724	9.29E-04
233863	'Gtf3c1'	mRNA	0.243204	7.53E-04
233878	'Sez6l2'	mRNA	1.223095	4.10E-04
234365	'Yjefn3'	mRNA	1.237076	0.019293
234388	'Ccdc124'	mRNA	0.306882	0.008408
234396	'Ankle1'	mRNA	0.555451	0.024785
234695	'Carmil2'	mRNA	1.363325	2.28E-14
234788	'Slc38a8'	mRNA	3.727462	0.020813
234797	'6430548M	mRNA	-0.66102	0.002024
234967	'Slc36a4'	mRNA	-0.28998	0.030008
235044	'Plppr2'	mRNA	-0.41864	0.00861
235312	'C1qtnf5'	mRNA	-0.49287	1.54E-04
235416	'Lman1l'	mRNA	1.941182	0.017287
235431	'Coro2b'	mRNA	-0.5578	0.026232
235493	'Fam214a'	mRNA	-0.50819	0.002839
235497	'Leo1'	mRNA	-0.30605	0.010241
236643	'Sytl5'	mRNA	-0.83204	1.83E-06
237320	'Aldh8a1'	mRNA	1.729818	0.038224
237459	'Cdk17'	mRNA	-0.35677	0.001233
237611	'Stac3'	mRNA	0.732658	0.045705
237898	'Usp32'	mRNA	-0.24071	0.029626
237928	'Phospho1	mRNA	-0.57836	2.22E-07
23794	'Adamts5'	mRNA	-0.37427	1.37E-04
237940	'Aoc2'	mRNA	0.642253	0.028617
23806	'Arih1'	mRNA	-0.20001	0.046406
238130	'Dock4'	mRNA	-0.76712	2.59E-06
23821	'Bace1'	mRNA	-0.30941	0.036243
23825	'Banf1'	mRNA	0.259557	0.035151
238276	'Akap5'	mRNA	1.090735	0.012814
23830	'Capn10'	mRNA	0.300002	0.016194
23849	'Klf6'	mRNA	-0.26344	0.001661
23857	'Dmtf1'	mRNA	-0.1966	0.045388
23872	'Ets2'	mRNA	-0.25787	0.040358
23874	'Farsb'	mRNA	0.248914	0.030761
23876	'Fbln5'	mRNA	-0.48386	1.69E-04
23887	'Ggt5'	mRNA	-0.31983	0.003776
239027	'Arhgap22	mRNA	-0.3198	1.68E-04
239337	'Adamts12	mRNA	-0.58756	2.90E-04
239393	'Lrp12'	mRNA	-0.21957	0.003848
239552	'Apol8'	mRNA	1.155006	1.71E-11
23956	'Neu2'	mRNA	0.678618	1.76E-05
23960	'Oas1g'	mRNA	0.49348	9.89E-04
23971	'Papss1'	mRNA	-0.18193	0.022245
239759	'Liph'	mRNA	-0.61016	0.037137
23980	'Pebp1'	mRNA	0.159204	0.018837
239833	'Lmln'	mRNA	0.502989	0.009694
239857	'Cadm2'	mRNA	0.37234	0.003783
23989	'Med24'	mRNA	0.26639	9.29E-04
23994	'Dazap2'	mRNA	0.154848	0.036392
24000	'Ptpn21'	mRNA	-0.28697	8.25E-05
240023	'Pnldc1'	mRNA	1.128348	0.002115

240047	'Mmp25'	mRNA	2.329656	0.028651
240055	'Neurl1b'	mRNA	0.757641	0.043443
24030	'Mrps12'	mRNA	0.349104	3.66E-04
240334	'Pcyox1l'	mRNA	0.549149	0.008171
24059	'Slco2a1'	mRNA	0.473676	0.010304
24064	'Spry2'	mRNA	-0.34254	7.65E-05
240641	'Kif20b'	mRNA	0.387369	0.015591
240672	'Dusp5'	mRNA	-0.35394	0.018134
240753	'Plekha6'	mRNA	-0.59138	8.56E-05
240892	'Dusp27'	mRNA	-1.15971	3.83E-04
240913	'Adamts4'	mRNA	-1.11874	9.79E-12
241274	'Pnpla7'	mRNA	0.329108	4.65E-04
241296	'Lrrc8a'	mRNA	-0.4047	0.001153
241327	'Olfml2a'	mRNA	-1.50892	3.00E-06
241452	'Dhrs9'	mRNA	-0.61542	3.03E-04
242050	'Igsf10'	mRNA	-0.36861	0.005644
242235	'Lrit3'	mRNA	1.853905	2.48E-04
242584	'Wdr78'	mRNA	0.721428	0.02387
243369	'Sspo'	mRNA	-1.029	4.86E-04
243529	'H1f10'	mRNA	0.481727	8.52E-08
243725	'Ppp1r9a'	mRNA	0.731908	0.043002
243822	'Fam71e2'	mRNA	2.671696	0.002906
243842	'Bicra'	mRNA	0.293094	0.021452
243961	'Shank1'	mRNA	-0.67071	0.013069
244059	'Chd2'	mRNA	0.49645	1.61E-05
244329	'Mcph1'	mRNA	0.332005	0.001939
244418	'Prag1'	mRNA	-0.68949	0.041926
244595	'Ces1a'	mRNA	-1.46337	7.27E-06
244654	'Mtss2'	mRNA	-0.46603	1.87E-04
244871	'Zc3h12c'	mRNA	-0.33331	0.014555
244879	'Npat'	mRNA	-0.21455	0.019994
244895	'Peak1'	mRNA	-0.22279	0.022313
245240	'9930111J2	mRNA	-1.22851	3.57E-04
245527	'Eda2r'	mRNA	0.410591	0.046529
245865	'Spag4'	mRNA	-0.91997	0.0012
245884	'Fam71f2'	mRNA	0.791904	8.33E-04
246154	'Vasn'	mRNA	-0.27457	3.65E-04
246190	'Otoa'	mRNA	2.219383	0.002115
246229	'Bivm'	mRNA	0.460211	0.009322
246727	'Oas3'	mRNA	0.536556	1.95E-06
246730	'Oas1a'	mRNA	0.404304	1.25E-04
257633	'Acsf3'	mRNA	0.300772	0.028797
260305	'Nphp4'	mRNA	0.268039	0.023564
260409	'Cdc42ep3	mRNA	-0.52559	0.023564
26362	'Axl'	mRNA	0.146373	0.009888
263803	'Pkn3'	mRNA	0.455525	2.58E-04
26388	'Ifi202b'	mRNA	4.734974	0.004497
26390	'Mapkbp1'	mRNA	-0.25361	0.044115
26408	'Map3k5'	mRNA	-0.31825	0.001237
26416	'Mapk14'	mRNA	-0.18214	0.048886
26423	'Nr5a1'	mRNA	2.529422	0.00815
26432	'Plod2'	mRNA	-0.41289	1.11E-04
26433	'Plod3'	mRNA	0.294023	1.59E-06
26442	'Psma5'	mRNA	0.268963	0.0291
26448	'Mok'	mRNA	0.410068	0.028267
26456	'Sema4g'	mRNA	-0.66062	5.71E-04
26457	'Slc27a1'	mRNA	-0.5182	7.85E-07
26465	'Zfp146'	mRNA	-0.21214	0.02926

26561	'Mmp23'	mRNA	-0.28449	0.003889
26568	'Slc27a3'	mRNA	0.276972	0.004369
266692	'Cpne1'	mRNA	0.34418	7.65E-05
268512	'Slc26a11'	mRNA	-0.48104	0.011394
268697	'Ccnb1'	mRNA	0.504617	3.84E-04
26885	'Casp8ap2	mRNA	-0.31174	0.003776
268859	'Rbfox1'	mRNA	-0.49235	0.036073
268934	'Grm4'	mRNA	3.967295	0.013461
26896	'Med14'	mRNA	-0.27987	0.003794
268977	'Ltbp1'	mRNA	0.39401	3.12E-06
26912	'Gcat'	mRNA	0.323808	0.0017
269198	'Nbeal1'	mRNA	-0.36042	0.003661
26920	'Cntrl'	mRNA	0.283735	0.016282
26922	'Mecr'	mRNA	0.313766	0.018526
269336	'Ccdc32'	mRNA	0.397472	0.010993
26934	'Racgap1'	mRNA	0.392433	3.30E-06
269523	'Vcp'	mRNA	0.23038	0.006454
269589	'Sytl1'	mRNA	0.87613	0.004903
269593	'Luzp1'	mRNA	-0.26104	6.96E-04
269608	'Plekhg5'	mRNA	-0.35947	0.017763
26968	'Islr'	mRNA	-0.65052	0.028218
269704	'Zfp664'	mRNA	-0.30866	1.03E-04
269799	'Clec4a1'	mRNA	2.514852	0.022916
269997	'Zfp747'	mRNA	-0.43749	0.034169
270210	'Zfp651'	mRNA	0.489144	0.001584
27029	'Sgsh'	mRNA	-0.45921	0.004063
27047	'Omd'	mRNA	-1.26719	4.38E-09
27053	'Asns'	mRNA	0.450049	0.00514
270627	'Taf1'	mRNA	-0.1859	0.048535
270685	'Mthfd1l'	mRNA	0.273324	5.48E-04
270906	'Prr11'	mRNA	0.530488	3.73E-04
271127	'Adamts16	mRNA	-0.53328	0.016647
271508	'Brd8dc'	mRNA	1.843721	0.002222
271844	'Pla2g4f'	mRNA	2.661153	8.03E-04
272382	'Spib'	mRNA	1.588463	6.88E-05
27273	'Pdk4'	mRNA	-0.56168	0.022233
27360	'Add3'	mRNA	-0.33598	0.001669
27362	'Dnajb9'	mRNA	-0.34687	0.012145
27364	'Srr'	mRNA	-0.2267	0.013738
27369	'Dguok'	mRNA	0.315712	0.025654
27373	'Csnk1e'	mRNA	-0.21663	0.018319
27409	'Abcg5'	mRNA	4.000003	0.041905
27426	'Nagpa'	mRNA	0.284898	0.039367
27528	'Nrep'	mRNA	-0.66458	2.45E-05
276770	'Eif5a'	mRNA	0.317005	0.019433
277414	'Trp53i11'	mRNA	-0.97496	0.039799
277939	'C2cd3'	mRNA	0.324885	8.33E-04
278507	'Wfikkn2'	mRNA	-1.28705	0.012117
28010	'Miip'	mRNA	0.386609	0.048393
28018	'Ubfd1'	mRNA	0.292289	0.020934
28109	'D10Wsu1(	mRNA	-0.27141	0.002831
286942	'Kif19a'	mRNA	2.430979	0.009941
29815	'Bcar3'	mRNA	-0.43021	1.87E-06
29864	'Rnf11'	mRNA	-0.26764	5.34E-04
29867	'Cabp1'	mRNA	0.909695	0.031676
29870	'Gtse1'	mRNA	0.387754	1.13E-05
29873	'Cspg5'	mRNA	1.337466	1.49E-04
30045	'Dnajc12'	mRNA	0.803869	0.043536

30055	'Timm13'	mRNA	0.315495	0.006273
30791	'Slc39a1'	mRNA	0.159522	0.037713
30805	'Slc22a4'	mRNA	-0.42226	0.028353
30937	'Lmcd1'	mRNA	-0.80604	1.27E-14
30938	'Fgd3'	mRNA	-0.71767	7.66E-06
30939	'Pttg1'	mRNA	0.541267	6.37E-05
30941	'Usp21'	mRNA	0.264616	0.008301
30951	'Cbx8'	mRNA	0.405755	0.0285
30953	'Schip1'	mRNA	-0.47979	0.004901
317677	'C1s2'	mRNA	-0.61619	1.68E-07
319171	'H2ac24'	mRNA	0.415811	0.008801
319195	'Rpl17'	mRNA	-0.22915	0.002071
319322	'Sf3b2'	mRNA	0.16856	0.012814
319370	'Ubald2'	mRNA	0.47311	4.97E-04
319448	'Fndc3a'	mRNA	-0.35541	0.009534
319477	'Insyn1'	mRNA	-0.36191	0.007406
319520	'Dusp4'	mRNA	-0.60387	1.16E-04
319530	'Zfp750'	mRNA	-1.42653	0.018037
319552	'Spx'	mRNA	1.171436	0.001424
319670	'Eml5'	mRNA	-0.3193	0.001019
319710	'Frmd6'	mRNA	-0.24585	0.00756
319719	'Simc1'	mRNA	-0.28821	0.003303
319909	'Ism1'	mRNA	-0.42176	2.22E-04
320078	'Olfml2b'	mRNA	-0.58566	3.33E-12
320111	'Prr18'	mRNA	2.018492	0.008657
320159	'Togaram2	mRNA	4.167837	3.55E-04
320183	'Msrb3'	mRNA	-0.32469	1.49E-04
320213	'Senp5'	mRNA	-0.25035	0.004516
320435	'Rinl'	mRNA	1.24635	0.009452
320534	'Tmem104	mRNA	0.430308	6.91E-04
320604	'Ccdc169'	mRNA	2.0207	1.62E-11
320661	'D5Ertd579	mRNA	-0.2106	0.042963
320678	'Iffo1'	mRNA	0.257906	0.033373
320712	'Abi3bp'	mRNA	-0.49966	1.16E-04
320795	'Pkn1'	mRNA	-0.24443	0.005375
320799	'Zhx3'	mRNA	-0.42167	6.36E-05
320924	'Ccbe1'	mRNA	0.279143	3.40E-04
327766	'Tmem26'	mRNA	-0.62538	2.73E-04
327900	'Ubtd2'	mRNA	-0.22529	0.029326
327987	'Med13'	mRNA	-0.41434	5.58E-08
327992	'Hsf5'	mRNA	2.765805	9.67E-09
328440	'Npm2'	mRNA	1.15748	0.015132
329154	'Ankrd44'	mRNA	-0.4249	0.039388
329252	'Lgr6'	mRNA	0.338382	0.00574
329575	'Gm14325'	mRNA	-0.33979	0.022479
329628	'Fat4'	mRNA	-0.58938	3.79E-04
329679	'Fnip2'	mRNA	-0.4937	7.65E-05
330122	'Cxcl3'	mRNA	0.93683	0.017533
330192	'Vps37b'	mRNA	0.242454	0.032903
330660	'Btbd16'	mRNA	1.748831	0.010709
330723	'Htra4'	mRNA	-0.37517	0.002504
331026	'Gmppb'	mRNA	-0.44279	0.010394
331461	'Il1rapl1'	mRNA	-0.94796	0.00181
331623	'Bend3'	mRNA	-0.30526	0.026923
332359	'Tigd3'	mRNA	0.654825	0.035359
333193	'Proser3'	mRNA	0.401602	0.037571
333473	'Zfp36l3'	mRNA	0.710956	0.003804
333789	'N4bp2'	mRNA	-0.36192	0.018319

338523	'Kdm7a'	mRNA	-0.50934	0.001417
353172	'Gars'	mRNA	0.262001	0.013231
353187	'Nr1d2'	mRNA	0.673285	3.24E-07
353188	'Adam32'	mRNA	1.324729	0.034726
353502	'Hcfc1r1'	mRNA	-0.42611	6.07E-05
380755	'Lsmem1'	mRNA	2.657272	9.82E-30
380967	'Tmem106	mRNA	-0.22297	0.015999
381113	'Cdkl4'	mRNA	3.926543	1.05E-04
381201	'Ap5b1'	mRNA	-0.47566	0.003419
381204	'Naaladl1'	mRNA	0.861409	0.025607
381293	'Kif14'	mRNA	0.430159	0.006653
381406	'Trp53rka'	mRNA	-0.37917	0.002
381410	'Zfp408'	mRNA	-0.24418	0.031599
381489	'Rxfp1'	mRNA	-0.4882	0.022757
381493	'S100a7a'	mRNA	0.517064	0.034656
381678	'Zcwpw1'	mRNA	-0.44275	0.020359
381801	'Tatdn2'	mRNA	-0.41145	2.16E-04
381845	'Rnf225'	mRNA	1.001792	1.19E-12
381990	'Zbtb2'	mRNA	-0.41483	7.60E-04
383592	'Kif28'	mRNA	4.114767	0.037109
385643	'Kng2'	mRNA	-0.97686	2.62E-09
394436	'Ugt1a1'	mRNA	-2.91374	0.014062
399510	'Map4k5'	mRNA	-0.38167	0.001257
403187	'Opa3'	mRNA	0.198482	0.036408
404710	'Iqgap3'	mRNA	0.469398	1.08E-06
407790	'Ndufa4l2'	mRNA	-0.64765	4.42E-05
407800	'Ecm2'	mRNA	-0.88119	1.89E-05
432516	'Myo1a'	mRNA	0.990998	0.003845
432763	'Prr7'	mRNA	0.302272	0.034512
433256	'Acsl5'	mRNA	0.301274	0.005481
433813	'Pusl1'	mRNA	-0.41753	0.022922
433956	'Dnaaf5'	mRNA	0.237523	0.037461
434246	'Trim72'	mRNA	1.797214	0.037053
504186	'Chrna10'	mRNA	2.974358	1.16E-13
50492	'Thop1'	mRNA	0.1979	0.01735
50493	'Txnrd1'	mRNA	-0.20156	0.025607
50501	'Prok2'	mRNA	-2.20319	0.035224
50765	'Tfr2'	mRNA	-1.116	2.08E-04
50766	'Crim1'	mRNA	-0.49637	1.74E-06
50772	'Mapk6'	mRNA	-0.21048	0.035586
50780	'Rgs3'	mRNA	-0.26819	0.03069
50781	'Dkk3'	mRNA	-0.21468	0.023148
50783	'Lsm4'	mRNA	0.391294	2.17E-04
50785	'Hs6st1'	mRNA	-0.31595	0.010828
50868	'Keap1'	mRNA	0.209172	0.019197
50908	'C1s1'	mRNA	-0.69882	1.31E-10
50909	'C1ra'	mRNA	-0.17832	0.02402
51792	'Ppp2r1a'	mRNA	0.193323	0.019507
51798	'Ech1'	mRNA	-0.25668	0.001029
51812	'Mcrs1'	mRNA	0.225861	0.001388
51902	'Rnf24'	mRNA	-0.27239	0.013329
51944	'Knstrn'	mRNA	0.365199	5.71E-04
52004	'Cdk2ap2'	mRNA	0.195328	0.005783
52118	'Pvr'	mRNA	-0.2452	1.77E-04
52132	'Ccdc97'	mRNA	0.20173	0.009585
52276	'Cdca8'	mRNA	0.507812	8.13E-05
52331	'Stbd1'	mRNA	-0.28947	0.03573
52372	'D6Ertd527	mRNA	0.884475	0.006104

52552	'Parp8'	mRNA	-0.2467	0.033591
52585	'Dhrs1'	mRNA	0.184401	0.042934
52635	'Esyt2'	mRNA	-0.27147	1.51E-04
52668	'Ifi27'	mRNA	-0.4859	0.008495
52683	'Ncaph2'	mRNA	0.225695	0.001094
52815	'Ldhd'	mRNA	-0.60425	0.019197
53321	'Cntnap1'	mRNA	-0.72775	5.01E-06
53374	'Chst3'	mRNA	-0.73049	1.14E-05
53376	'Usp2'	mRNA	0.464504	0.032878
53381	'Prdx4'	mRNA	-0.20141	0.041075
53599	'Cd164'	mRNA	-0.19432	0.001044
53612	'Vti1b'	mRNA	0.269322	0.018384
53625	'B3gnt2'	mRNA	-0.41582	6.83E-05
54123	'Irf7'	mRNA	0.279672	0.004376
54137	'Acrbp'	mRNA	0.456077	0.016361
54141	'Spag5'	mRNA	0.329574	3.98E-05
54189	'Rabep1'	mRNA	-0.24733	0.005182
54216	'Pcdh7'	mRNA	-0.17306	0.026961
54218	'B3galt4'	mRNA	0.725218	0.012336
54338	'Slc23a2'	mRNA	-0.28251	0.002215
54343	'Atf7ip'	mRNA	0.209635	0.013782
54366	'Ctnnal1'	mRNA	-0.39599	0.001872
54375	'Azin1'	mRNA	-0.27479	5.21E-05
54381	'Cpq'	mRNA	-0.41801	1.96E-06
54392	'Ncapg'	mRNA	0.425101	0.007475
54409	'Ramp2'	mRNA	-0.72216	0.002593
54445	'Unc93b1'	mRNA	0.278308	0.022126
54446	'Nfat5'	mRNA	-0.32837	0.005927
545192	'Baiap3'	mRNA	1.86422	5.81E-04
545260	'Arsi'	mRNA	-0.68916	0.013038
54598	'Calcrl'	mRNA	-0.55039	0.001477
54608	'Abhd2'	mRNA	-0.32017	0.006439
54615	'Npff'	mRNA	1.478514	0.023468
54723	'Tfip11'	mRNA	0.204773	0.025342
55932	'Gbp3'	mRNA	0.299972	0.019434
55993	'Msh4'	mRNA	2.353796	9.38E-07
56018	'Stard10'	mRNA	-0.48797	0.005056
56068	'Ammecr1'	mRNA	-0.2859	0.005644
56087	'Dnah10'	mRNA	1.915019	3.75E-11
56177	'Olfm1'	mRNA	-0.3134	0.003156
56210	'Rev1'	mRNA	-0.2249	0.017736
56229	'Thsd1'	mRNA	1.011984	0.03636
56273	'Pex14'	mRNA	0.250819	8.67E-04
56280	'Mrpl37'	mRNA	0.241177	0.008557
56312	'Nupr1'	mRNA	-0.22692	0.030798
56318	'Acpp'	mRNA	-0.81827	2.42E-05
56327	'Arl2'	mRNA	0.30247	0.003072
56330	'Pdcd5'	mRNA	0.179852	0.038395
56332	'Amotl2'	mRNA	0.161045	0.033792
56347	'Eif3c'	mRNA	0.196102	0.028188
56353	'Rybp'	mRNA	-0.28709	1.70E-04
56371	'Fzr1'	mRNA	0.369717	3.03E-04
56376	'Pdlim5'	mRNA	-0.59199	7.22E-11
56419	'Diaph3'	mRNA	0.299107	3.66E-04
56431	'Dstn'	mRNA	-0.24928	4.67E-04
56440	'Snx1'	mRNA	0.269192	0.009156
56454	'Aldh18a1'	mRNA	0.366349	5.46E-04
56458	'Foxo1'	mRNA	-0.31347	0.022901

56459	'Sae1'	mRNA	0.194387	0.019157
56464	'Ctsf'	mRNA	-0.64022	0.034797
56468	'Socs5'	mRNA	-0.53035	1.65E-04
56490	'Zbtb20'	mRNA	-0.42705	0.04456
56505	'Ruvbl1'	mRNA	0.275241	0.021234
56506	'Cib2'	mRNA	-0.25867	0.002494
56526	'Septin6'	mRNA	-0.43657	5.35E-04
56527	'Mast1'	mRNA	3.243402	0.02061
56613	'Rps6ka4'	mRNA	0.222359	0.046348
56626	'Poll'	mRNA	0.319274	0.012438
56642	'Ankrd2'	mRNA	1.520429	0.012856
56692	'Lamtor3'	mRNA	-0.22162	0.032893
56699	'Cdc42ep4	mRNA	0.377466	0.001495
56703	'Pigo'	mRNA	0.305016	0.023983
56722	'Litaf'	mRNA	-0.24649	8.49E-04
56737	'Alg2'	mRNA	-0.21734	0.045729
56742	'Psrc1'	mRNA	0.320688	9.16E-04
56743	'Lat2'	mRNA	1.370244	4.40E-05
56791	'Ube2l6'	mRNA	0.326535	9.59E-05
56847	'Aldh1a3'	mRNA	-0.81945	2.23E-05
56857	'Slc37a2'	mRNA	-0.88845	0.04304
56876	'Nsmf'	mRNA	-0.27682	0.00175
57257	'Vav3'	mRNA	-0.96555	8.31E-14
57259	'Tob2'	mRNA	0.212005	0.020083
57265	'Fzd2'	mRNA	0.270499	0.00261
57267	'Apba3'	mRNA	0.17208	0.038689
57294	'Rps27'	mRNA	-0.28488	5.89E-04
57320	'Park7'	mRNA	0.209532	0.040192
57444	'Isg20'	mRNA	0.224464	0.034767
57746	'Piwil2'	mRNA	0.997797	0.036422
57784	'Bin3'	mRNA	0.421991	1.07E-04
57785	'Rangrf'	mRNA	0.386114	0.03969
57810	'Cdon'	mRNA	-0.52806	1.50E-04
57890	'Il17re'	mRNA	4.855399	3.79E-04
57905	'Isy1'	mRNA	0.292905	1.19E-04
58172	'Sertad2'	mRNA	-0.26278	0.001237
58185	'Rsad2'	mRNA	0.40646	0.004353
58202	'Nelfb'	mRNA	0.19944	0.03098
58203	'Zbp1'	mRNA	0.22677	0.002215
58207	'Slc43a3'	mRNA	-0.22731	0.022126
58222	'Rab37'	mRNA	-0.78002	0.033081
58231	'Stk4'	mRNA	0.471351	4.57E-04
58521	'Eid1'	mRNA	-0.19719	0.016893
58805	'Mlxipl'	mRNA	-1.3132	0.02387
59013	'Hnrnph1'	mRNA	-0.19838	0.034036
59022	'Edf1'	mRNA	0.20678	0.037486
59050	'Nsa2'	mRNA	-0.24086	0.001259
59083	'Fetub'	mRNA	-0.53363	7.43E-08
59090	'Midn'	mRNA	0.370924	1.08E-05
59092	'Pcbp4'	mRNA	0.206515	0.004235
59287	'Ncstn'	mRNA	0.234053	0.001638
60321	'Wbp11'	mRNA	0.248641	6.33E-04
60364	'Donson'	mRNA	-0.22963	0.026228
60440	'Iigp1'	mRNA	-0.39839	9.18E-04
60441	'Mrpl38'	mRNA	0.266753	0.026961
60527	'Fads3'	mRNA	0.181728	0.026923
619288	'Fam71a'	mRNA	3.295575	8.69E-11
620913	'Gm12185'	mRNA	-0.57631	0.003505

621628	'Cldn20'	mRNA	1.64666	0.047809
623230	'Tmem200	mRNA	-0.35144	0.016848
623781	'Gm14137'	mRNA	0.37112	0.009209
625018	'C4a'	mRNA	1.067743	0.001098
626578	'Gbp10'	mRNA	-0.51796	4.11E-09
626848	'Zfp971'	mRNA	-0.36854	0.013655
629059	'Fam124a'	mRNA	-0.76255	3.77E-04
637079	'Iqcn'	mRNA	1.626461	3.54E-07
63953	'Dusp10'	mRNA	-0.29713	0.03669
63958	'Ube4b'	mRNA	0.161665	0.037906
64082	'Popdc2'	mRNA	1.071492	0.018437
64136	'Sdf2l1'	mRNA	0.565117	1.30E-04
64540	'Tspan4'	mRNA	0.18744	0.044292
64898	'Lpin2'	mRNA	-0.27379	0.007577
65960	'Twsg1'	mRNA	-0.34781	1.44E-07
65970	'Lima1'	mRNA	-0.32091	5.97E-04
66058	'Tmem176	mRNA	-0.53627	1.17E-04
66071	'Ethe1'	mRNA	0.190576	0.048539
66075	'Chchd3'	mRNA	0.228544	1.50E-04
66092	'Ghitm'	mRNA	0.237637	0.038224
66102	'Cxcl16'	mRNA	-0.60144	1.59E-04
66119	'Tomm6'	mRNA	0.339143	0.00193
66140	'Ska2'	mRNA	0.340091	0.022005
66141	'Ifitm3'	mRNA	0.433292	5.81E-06
66142	'Cox7b'	mRNA	0.233271	0.043456
66167	'Tma7'	mRNA	0.281244	0.029904
66168	'Grina'	mRNA	-0.20842	0.033984
66175	'Mustn1'	mRNA	-0.39809	9.29E-04
66181	'Nop10'	mRNA	0.280084	0.041614
66194	'Pycrl'	mRNA	0.187056	0.022252
66240	'Kcne1l'	mRNA	3.973317	0.001106
66245	'Hspbp1'	mRNA	0.22242	0.024785
66311	'Cenpw'	mRNA	0.410012	0.035265
66313	'Smurf2'	mRNA	-0.25946	0.00574
66341	'Eid3'	mRNA	-1.26938	0.005293
66355	'Gmpr'	mRNA	-1.00749	1.15E-09
66394	'Nosip'	mRNA	0.251327	0.015012
66399	'Tsfm'	mRNA	0.304772	0.031005
66411	'Tbcb'	mRNA	0.327412	0.003716
66427	'Cyb5b'	mRNA	0.191218	0.048535
66442	'Spc25'	mRNA	0.31874	0.048804
66459	'Pyurf'	mRNA	-0.2137	0.044964
66471	'Anp32e'	mRNA	0.216232	0.033174
66477	'Atp5md'	mRNA	0.357635	0.008322
66494	'Prelid1'	mRNA	0.173117	0.011583
664968	'Tmem238	mRNA	0.578443	0.023148
66497	'Cmss1'	mRNA	0.365623	0.011652
66505	'Zmynd11'	mRNA	-0.16982	0.040738
66532	'Rep15'	mRNA	1.054765	0.008408
665433	'H2ac23'	mRNA	1.077484	8.70E-04
66548	'Adamtsl5'	mRNA	-0.41421	2.57E-05
66559	'Metap1d'	mRNA	-0.24815	0.041174
665596	'H2bc23'	mRNA	-1.67534	0.011536
665622	'H4bc24'	mRNA	-1.65432	0.01345
66569	'Gdpd1'	mRNA	-0.70038	4.32E-04
66578	'Mis18a'	mRNA	0.284851	0.047165
66594	'Uqcr11'	mRNA	0.254312	0.026985
666190	'Gm7972'	mRNA	1.94901	1.12E-08

66642	'Ctnnbl1'	mRNA	0.260501	0.026961
66695	'Aspn'	mRNA	-1.90642	5.14E-05
667034	'Pnp2'	mRNA	1.25258	0.021563
66711	'Sbds'	mRNA	-0.19404	0.03338
66725	'Lrrk2'	mRNA	0.326332	0.02384
66734	'Map1lc3a'	mRNA	-0.2161	0.026961
66743	'Rnf220'	mRNA	0.330913	9.18E-04
66815	'Mcub'	mRNA	0.222933	0.003853
66884	'Appbp2'	mRNA	-0.21589	0.024565
66890	'Lman2'	mRNA	0.192342	0.015733
66892	'Eif4e3'	mRNA	-0.28585	0.011843
66898	'Baiap2l1'	mRNA	-0.2723	0.041911
66916	'Ndufb7'	mRNA	0.278557	0.002979
66938	'Sh3d21'	mRNA	0.564856	1.44E-04
66940	'Shisa5'	mRNA	0.29082	0.013971
66943	'Slc66a2'	mRNA	-0.38392	1.53E-04
66948	'Acad8'	mRNA	0.373141	0.002388
66949	'Trim59'	mRNA	0.261631	0.026985
66967	'Edem3'	mRNA	-0.26036	0.0457
66972	'Slc25a23'	mRNA	-0.64686	0.003611
66977	'Nuf2'	mRNA	0.372429	0.001631
67017	'Fam210b'	mRNA	-0.35352	0.020149
67023	'Use1'	mRNA	-0.37753	6.91E-04
67026	'Thap4'	mRNA	0.21477	0.019952
67035	'Dnajb4'	mRNA	-0.47531	2.46E-09
67036	'Mrpl45'	mRNA	0.172422	0.04996
67037	'Pmf1'	mRNA	0.30125	0.01783
67052	'Ndc80'	mRNA	0.467581	0.002943
67091	'Trappc6a'	mRNA	-0.30419	0.031345
67103	'Ptgr1'	mRNA	0.252643	0.014897
67119	'Ccdc159'	mRNA	-0.57367	0.030768
67121	'Mastl'	mRNA	0.401128	0.005375
67138	'Herc6'	mRNA	0.249792	0.006612
67177	'Cdt1'	mRNA	-0.25021	0.00407
67203	'Nde1'	mRNA	0.261611	0.030968
67222	'Srfbp1'	mRNA	-0.29495	0.015586
67286	'Ift22'	mRNA	0.284001	0.033362
67305	'Gpx7'	mRNA	0.349924	0.002384
67374	'Jam2'	mRNA	-0.57788	4.88E-05
67420	'Far1'	mRNA	-0.23418	0.025264
67463	'Poc5'	mRNA	0.297355	0.017289
67467	'Gpalpp1'	mRNA	0.274449	0.037849
674895	'Nek10'	mRNA	2.011389	1.20E-14
67493	'Mettl16'	mRNA	0.28452	0.025265
67557	'Larp6'	mRNA	-0.37219	0.01373
67588	'Rnf41'	mRNA	-0.22341	0.011288
67603	'Dusp6'	mRNA	-0.83504	1.85E-19
67605	'Akt1s1'	mRNA	0.174851	0.044018
67622	'Mxra7'	mRNA	-0.35759	0.001795
67629	'Spc24'	mRNA	0.480034	2.66E-04
67647	'4930523C	mRNA	-0.79753	5.32E-13
676527	'Gm12248'	mRNA	-1.00289	5.02E-21
67655	'Ctdp1'	mRNA	-0.28378	0.002539
67669	'Hikeshi'	mRNA	0.307254	0.030733
67671	'Rpl38'	mRNA	0.378467	2.43E-05
67678	'Lsm3'	mRNA	0.298113	0.006282
67693	'Hypk'	mRNA	0.251312	0.031679
67702	'Rnf149'	mRNA	-0.30321	0.001921

67712	'Slc25a37'	mRNA	-0.23815	1.03E-04
67784	'Plxnd1'	mRNA	-0.54702	0.001026
67789	'Dalrd3'	mRNA	0.265406	0.015624
67839	'Gpsm1'	mRNA	-0.3234	0.003376
67860	'S100a16'	mRNA	-0.24606	0.006612
67869	'Paip2'	mRNA	0.231337	0.007722
67886	'Camsap2'	mRNA	-0.22992	0.036385
67893	'Tmem86a	mRNA	-0.27938	0.012479
67903	'Gipc1'	mRNA	0.292311	5.03E-04
67905	'Ppm1m'	mRNA	-0.30996	0.00323
67941	'Rps27l'	mRNA	0.370529	0.043088
67956	'Kmt5a'	mRNA	0.215025	0.037571
67972	'Atp2b1'	mRNA	-0.16502	0.006658
68011	'Snrpg'	mRNA	0.405354	0.014311
68016	'Cavin4'	mRNA	-0.40954	1.27E-04
68024	'H2bc4'	mRNA	0.316658	0.005544
68031	'Rnf146'	mRNA	-0.25168	0.032921
68038	'Chid1'	mRNA	0.333243	0.003444
68041	'Mid1ip1'	mRNA	0.298597	0.021474
68047	'Mpnd'	mRNA	-0.25971	0.021814
68058	'Chd1l'	mRNA	0.321991	0.026318
68118	'Atg101'	mRNA	0.448651	0.001044
68151	'Wls'	mRNA	-0.23639	0.016396
68188	'Sympk'	mRNA	0.168103	0.008801
68201	'Ccdc34'	mRNA	0.544861	5.12E-09
68219	'Nudt21'	mRNA	0.319645	0.006596
68240	'Rpa3'	mRNA	0.280667	0.036392
68250	'Ciao2a'	mRNA	0.280485	0.037175
68251	'Babam1'	mRNA	0.174737	0.040731
68260	'Trmt12'	mRNA	-0.47853	0.025607
68273	'Pomgnt1'	mRNA	-0.28536	0.00607
68298	'Ncapd2'	mRNA	0.330319	1.30E-04
68310	'Zmym1'	mRNA	-0.27466	0.01735
68312	'Gstm7'	mRNA	-1.30595	0.003914
68339	'Ccdc88c'	mRNA	2.045336	0.001178
68404	'Nrn1'	mRNA	-0.29461	0.014691
68499	'Mrpl53'	mRNA	0.351075	2.63E-04
68514	'Micu2'	mRNA	0.19332	0.017451
68523	'Ciao2b'	mRNA	0.352013	7.04E-05
68549	'Sgo2a'	mRNA	0.374965	0.007577
68572	'Mrpl58'	mRNA	0.255096	0.045805
68576	'Lamtor5'	mRNA	0.247005	0.010382
68597	'Ccdc167'	mRNA	-0.39967	0.016344
68612	'Ube2c'	mRNA	0.524044	9.74E-09
68652	'Tab2'	mRNA	-0.13292	0.042079
68691	'Kansl1l'	mRNA	-0.46913	9.85E-06
68709	'Cilp2'	mRNA	2.899297	0.006653
68743	'Anln'	mRNA	0.300845	4.77E-04
68770	'Phtf2'	mRNA	-0.33551	0.032793
68792	'Srpx2'	mRNA	-0.26932	0.004574
68799	'Rgmb'	mRNA	-0.52084	7.83E-08
68810	'Nexn'	mRNA	-0.48208	0.048125
68813	'Dock5'	mRNA	-0.38696	1.27E-04
68817	'Ddi2'	mRNA	-0.40204	5.67E-05
68852	'Lrrn4cl'	mRNA	-0.4989	1.71E-05
68859	'Smim1'	mRNA	-0.71908	0.047173
68861	'Dipk2a'	mRNA	-0.4979	1.27E-07
68877	'Maf1'	mRNA	0.229795	0.023832

68961	'Phkg2'	mRNA	0.321642	0.017579
68968	'Cdan1'	mRNA	-0.27798	0.013864
69156	'Comtd1'	mRNA	-0.61829	0.001893
69256	'Zfp397'	mRNA	-0.2658	0.009716
69257	'Elf2'	mRNA	-0.22702	0.002436
69480	'Ttc9'	mRNA	-0.5066	0.001078
69524	'Esam'	mRNA	1.498443	0.015132
69550	'Bst2'	mRNA	0.314097	0.003961
69574	'Cmbl'	mRNA	-0.6535	6.87E-05
69577	'Fastkd3'	mRNA	-0.34475	0.003055
69582	'Plekhm2'	mRNA	-0.25753	0.028469
69660	'Tmbim1'	mRNA	-0.22034	0.004254
69663	'Ddx51'	mRNA	-0.22012	0.04745
69724	'Rnaseh2a'	mRNA	0.322042	0.001848
69740	'Dph5'	mRNA	0.324273	0.043662
69833	'Polr2f'	mRNA	0.209344	0.042505
69878	'Snrpf'	mRNA	0.325432	0.006495
69908	'Rab3b'	mRNA	-0.40629	0.034797
69926	'Dnah17'	mRNA	4.585552	0.001026
69930	'Zfp715'	mRNA	-0.26332	0.03969
70025	'Acot7'	mRNA	0.366463	1.61E-05
70099	'Smc4'	mRNA	0.228906	0.041614
70103	'Znhit1'	mRNA	0.245653	0.002274
70129	'Slc44a4'	mRNA	3.473481	0.00852
70152	'Mettl7a1'	mRNA	-0.50076	6.78E-04
70209	'Tmem143	mRNA	0.313697	0.015999
70218	'Kif18b'	mRNA	0.332586	0.002056
70248	'Dazap1'	mRNA	0.406828	7.84E-09
70333	'Cd3eap'	mRNA	-0.3709	3.42E-04
70370	'Fbln7'	mRNA	-0.46265	1.04E-04
70385	'Spdl1'	mRNA	0.412537	0.015184
70420	'Arpin'	mRNA	0.262342	0.038332
70439	'Taf15'	mRNA	0.310118	0.009452
70458	'2610318N	mRNA	0.491814	0.030034
70461	'Crtc3'	mRNA	-0.27733	0.014091
70466	'Ckap2l'	mRNA	0.377838	0.001712
70472	'Atad2'	mRNA	-0.19183	0.010969
70484	'Slc35d2'	mRNA	0.440664	0.032921
70536	'Qpct'	mRNA	-1.10525	0.005644
70560	'Wars2'	mRNA	0.273594	0.029895
70561	'Txndc16'	mRNA	-0.3451	0.030883
70584	'Pak4'	mRNA	0.220552	0.017711
70612	'Tmem230	mRNA	0.318366	0.016065
70615	'Ankrd24'	mRNA	-0.32701	0.018529
70661	'Sik3'	mRNA	0.176596	0.018437
70676	'Gulp1'	mRNA	-0.268	0.044567
70699	'Nup205'	mRNA	0.179696	0.028615
70719	'Arhgap45	mRNA	1.261657	0.002355
70897	'Fam71d'	mRNA	3.219222	1.96E-06
70967	'Eva1c'	mRNA	-0.69158	0.00735
70999	'Naa40'	mRNA	-0.27095	0.038783
71085	'Arhgap19	mRNA	0.473939	0.006162
71132	'Cabyr'	mRNA	1.862679	5.90E-04
71198	'Otud1'	mRNA	-0.25493	0.012336
71275	'Noxred1'	mRNA	1.555426	0.014763
71276	'Ccdc57'	mRNA	0.299511	0.046702
71323	'Rassf8'	mRNA	-0.50534	7.86E-13
71355	'Col24a1'	mRNA	-1.25277	0.013692

71361	'Aifm2'	mRNA	0.308783	1.44E-04
71481	'Alpk1'	mRNA	-0.42383	8.40E-05
71566	'Clmp'	mRNA	-0.42129	1.62E-04
71583	'9130008F2	mRNA	-0.51277	0.025678
71592	'Pogk'	mRNA	-0.24463	0.02694
71684	'Rbm43'	mRNA	0.27414	0.013692
71687	'Tmem25'	mRNA	1.763529	8.49E-04
71711	'Mus81'	mRNA	-0.43746	0.007722
71721	'Fam13c'	mRNA	0.324651	0.009988
71733	'Susd2'	mRNA	-0.59318	1.21E-07
71767	'Tysnd1'	mRNA	0.239676	0.020271
71768	'Vwce'	mRNA	2.326095	7.79E-05
71770	'Ap2b1'	mRNA	0.213788	0.001866
71804	'Mtfr2'	mRNA	0.534043	1.37E-04
71807	'Tars2'	mRNA	0.379266	3.97E-04
71819	'Kif23'	mRNA	0.321358	8.47E-04
71827	'Lrrc34'	mRNA	-0.88612	1.74E-06
71853	'Pdia6'	mRNA	0.35623	1.26E-06
71887	'Ppm1j'	mRNA	-0.51132	0.018037
71898	'Apol9b'	mRNA	0.216114	3.37E-05
71901	'Fam219a'	mRNA	0.546671	5.96E-04
71912	'Jsrp1'	mRNA	-0.64992	0.033229
71914	'Antxr2'	mRNA	-0.32903	6.14E-04
71932	'Ephx3'	mRNA	1.234884	1.78E-04
71947	'Tmem94'	mRNA	0.228848	0.006714
71960	'Myh14'	mRNA	-1.00481	5.70E-07
71962	'Castor1'	mRNA	0.438644	0.022908
71984	'Sars2'	mRNA	0.263394	0.037849
71994	'Cnn3'	mRNA	-0.26048	2.73E-04
72029	'Cnpy3'	mRNA	0.289532	0.003791
72046	'Urgcp'	mRNA	-0.28952	0.001555
72047	'Ddx42'	mRNA	-0.18531	0.046116
72055	'Slc38a10'	mRNA	0.195693	0.015684
72061	'Aopep'	mRNA	-0.43593	2.62E-06
72080	'Sapcd2'	mRNA	0.579527	0.014032
72082	'Cyp2c55'	mRNA	3.060003	7.95E-06
72085	'Osgepl1'	mRNA	0.428267	0.013864
72114	'Zbed3'	mRNA	0.473161	1.80E-04
72119	'Tpx2'	mRNA	0.373965	5.58E-04
72123	'Ccdc71l'	mRNA	-0.33739	0.019245
72140	'Cep89'	mRNA	0.373342	1.07E-04
72168	'Aifm3'	mRNA	1.061675	0.001192
72190	'2510009E0	mRNA	-0.37972	5.35E-04
72258	'Kcnk10'	mRNA	1.373488	0.006392
72303	'Cyp2c65'	mRNA	3.142916	0.034726
72324	'Plxdc1'	mRNA	-1.29055	0.004189
72333	'Palld'	mRNA	-0.51237	2.21E-04
72391	'Cdkn3'	mRNA	0.407066	0.045633
72401	'Slc43a1'	mRNA	-0.40444	0.044953
72454	'Ccdc71'	mRNA	0.321789	0.001404
72469	'Plcd3'	mRNA	-0.31958	4.54E-04
72472	'Slc16a10'	mRNA	-0.57435	1.17E-08
72543	'Mvb12b'	mRNA	-1.01544	5.47E-04
72549	'Reep4'	mRNA	0.555041	1.23E-06
72607	'Usp13'	mRNA	-0.28002	0.015684
72657	'Selenoh'	mRNA	0.271563	0.002
72726	'Tbcc'	mRNA	-0.41165	0.006241
72873	'Bbof1'	mRNA	0.906332	0.013256

72982	'Tmem138	mRNA	0.411162	0.016259
73086	'Rps6ka5'	mRNA	-0.5425	9.62E-04
73230	'Bmper'	mRNA	-0.25918	0.0291
73251	'Setd7'	mRNA	0.243436	0.003856
73723	'Sh3bgrl3'	mRNA	0.297137	0.018526
73737	'1110008P	mRNA	0.368118	0.007464
73739	'Cby1'	mRNA	0.224987	0.017457
73804	'Kif2c'	mRNA	0.496943	1.28E-05
73813	'Fam83e'	mRNA	1.507724	2.01E-11
73910	'Arhgap18	mRNA	-0.29807	6.42E-05
73914	'Irak3'	mRNA	0.460357	9.04E-06
74016	'Phf19'	mRNA	0.305514	0.002409
74018	'Als2'	mRNA	-0.32135	0.004855
74030	'Rin2'	mRNA	-0.56552	3.11E-07
74048	'Vsir'	mRNA	-0.41643	0.010304
74071	'Lmntd1'	mRNA	-1.40638	0.009004
74096	'Hvcn1'	mRNA	-0.87135	3.60E-07
74107	'Cep55'	mRNA	0.515649	3.90E-04
74116	'Pi16'	mRNA	-1.31308	0.002134
74127	'Krt80'	mRNA	0.350056	0.011218
74136	'Sec14l1'	mRNA	0.224921	0.002218
74155	'Errfi1'	mRNA	-0.32415	8.73E-07
74175	'Crct1'	mRNA	-1.92643	8.91E-07
74182	'Gpcpd1'	mRNA	-0.33318	0.003726
74187	'Katnb1'	mRNA	0.421951	2.47E-04
74202	'Fblim1'	mRNA	0.271398	0.023983
74241	'Chpf'	mRNA	0.178618	0.011376
74288	'Spem1'	mRNA	1.457668	0.028277
74320	'Wdr33'	mRNA	0.178662	0.032915
74337	'Palm3'	mRNA	-0.70564	0.036257
74365	'Lonrf3'	mRNA	-0.7818	5.32E-13
74386	'Rmi1'	mRNA	-0.32637	0.034726
74414	'Polr3c'	mRNA	0.275677	0.001186
74480	'Samd4'	mRNA	-0.30081	0.030909
74488	'Lrrc15'	mRNA	-0.68413	0.002134
74528	'Mgme1'	mRNA	-0.34646	0.018415
74551	'Pck2'	mRNA	0.303104	3.57E-04
74614	'Ocstamp'	mRNA	-1.03039	0.03041
74626	'Tmem81'	mRNA	1.060501	0.013794
74646	'Spsb1'	mRNA	-0.22166	0.014041
74718	'Snx16'	mRNA	-0.39961	0.005078
74732	'Stx11'	mRNA	-0.40305	0.010582
74735	'Trim14'	mRNA	0.484763	0.001541
74747	'Ddit4'	mRNA	0.378239	0.003814
74760	'Rab3il1'	mRNA	-0.45895	2.49E-06
74761	'Mxra8'	mRNA	-0.26257	3.57E-04
74843	'Mss51'	mRNA	1.298062	1.25E-04
75062	'Sf3a3'	mRNA	0.240065	0.024522
751865	'Sap25'	mRNA	0.443806	0.001421
75221	'Dpp3'	mRNA	0.318333	3.48E-04
75302	'Asxl2'	mRNA	-0.22432	0.034604
75317	'Parpbp'	mRNA	0.3472	0.0457
75423	'Arl5a'	mRNA	-0.22157	0.015999
75467	'Stpg4'	mRNA	3.140639	0.024884
75540	'Fpgt'	mRNA	-0.40555	0.005317
75608	'Chmp4b'	mRNA	0.20996	0.040336
75660	'Lin37'	mRNA	0.2474	0.049014
75678	'Ippk'	mRNA	-0.39499	0.005861

75736	'Bcl2l12'	mRNA	0.316125	0.037713
75777	'Ttc23l'	mRNA	1.019019	6.91E-04
75786	'Ckap5'	mRNA	0.20165	0.044381
76074	'Gbp8'	mRNA	-0.50254	0.045104
76179	'Usp31'	mRNA	-0.33329	0.006592
76184	'Abca6'	mRNA	-0.91852	0.048901
76252	'Atp6v0e2'	mRNA	-0.56142	0.041727
76303	'Osbp'	mRNA	-0.19513	0.037571
76308	'Rab1b'	mRNA	0.16392	0.026961
76338	'Rab2b'	mRNA	-0.29763	0.044567
76405	'1700018B	mRNA	2.672529	0.001909
76441	'Daam2'	mRNA	-0.7043	0.01112
76453	'Prss23'	mRNA	-0.39778	0.001379
76454	'Fbxo31'	mRNA	0.292424	0.0017
76464	'Knl1'	mRNA	0.440205	0.001178
76498	'Paqr4'	mRNA	-0.37555	0.004812
76566	'Rflnb'	mRNA	-0.37905	0.005581
76573	'Spatc1l'	mRNA	5.055932	0.0012
76577	'Faf2'	mRNA	0.195694	0.016879
76612	'Lrrc27'	mRNA	-0.50998	0.012425
76630	'Stambpl1'	mRNA	-0.20138	0.025607
76670	'Cfap70'	mRNA	1.307325	0.001728
76737	'Creld2'	mRNA	0.357841	0.001562
76820	'Cyria'	mRNA	-0.82942	6.86E-05
76872	'Ccdc116'	mRNA	1.579436	7.70E-13
76901	'Jade2'	mRNA	0.300244	0.048901
76917	'Flywch2'	mRNA	-0.6107	0.02977
76933	'Ifi27l2a'	mRNA	-0.37116	3.01E-05
76936	'Hnrnpm'	mRNA	0.16881	0.024227
76952	'Nt5c2'	mRNA	-0.2383	0.032986
77125	'Il33'	mRNA	0.692172	0.001072
77300	'Raph1'	mRNA	-0.2633	0.028765
77446	'Heg1'	mRNA	-0.42202	4.54E-04
77531	'Anks1b'	mRNA	0.410251	3.16E-04
77569	'Limch1'	mRNA	-0.44582	0.004583
77582	'Mboat7'	mRNA	0.354741	9.16E-04
77590	'Chst15'	mRNA	-0.61451	2.36E-09
77595	'Nup210l'	mRNA	1.140169	3.91E-11
77605	'H2az2'	mRNA	0.227171	0.016351
77652	'Zfp955a'	mRNA	-0.64756	1.44E-06
77717	'Smim41'	mRNA	2.414498	2.06E-04
77891	'Ube2s'	mRNA	0.312369	2.17E-04
77975	'Tmem50b	mRNA	-0.31993	0.004353
77976	'Nuak1'	mRNA	-0.43815	0.009373
78286	'Nav2'	mRNA	0.503527	5.03E-09
78456	'C030002A	mRNA	0.228306	0.003889
78521	'B230219D	mRNA	-0.27585	0.034546
78558	'Htra3'	mRNA	-1.0183	0.006021
78733	'Troap'	mRNA	0.445684	0.001237
78752	'Csgalnact2	mRNA	-0.18992	0.037906
78757	'Rictor'	mRNA	-0.53685	5.08E-13
78771	'Mctp1'	mRNA	-0.58464	0.019245
78772	'Hhipl2'	mRNA	1.515361	0.001939
78808	'Stxbp5'	mRNA	-0.20758	0.018174
78829	'Tsc22d4'	mRNA	0.272504	0.001035
78889	'Wsb1'	mRNA	-0.16352	0.041727
78906	'Misp'	mRNA	1.042873	0.003586
78925	'Srd5a1'	mRNA	-0.38218	0.03732

78928	'Pigt'	mRNA	0.203823	0.039388
78943	'Ern1'	mRNA	-0.3914	0.005659
80281	'Cttnbp2nl	mRNA	-0.45929	1.41E-12
80287	'Apobec3'	mRNA	0.357621	0.033984
80292	'Zxdc'	mRNA	-0.40946	1.01E-04
80733	'Car15'	mRNA	1.35684	9.05E-06
80751	'Rnf34'	mRNA	-0.26143	0.044691
80752	'Fam20c'	mRNA	-0.61519	1.67E-05
80837	'Rhoj'	mRNA	-0.51539	7.05E-06
80859	'Nfkbiz'	mRNA	-0.33407	1.69E-04
80861	'Dhx58'	mRNA	0.303619	0.013678
80910	'Gpr84'	mRNA	3.049882	2.80E-23
80914	'Uck2'	mRNA	0.325842	1.51E-04
80982	'Cemip'	mRNA	-0.52931	0.008114
81489	'Dnajb1'	mRNA	-0.24389	0.004855
81535	'Sgpp1'	mRNA	-0.26752	0.007924
83433	'Trem2'	mRNA	-0.57236	0.015354
83434	'Rsph6a'	mRNA	3.162856	4.09E-05
83671	'Sytl2'	mRNA	-0.42127	0.001703
83674	'Cnnm1'	mRNA	-1.60633	1.02E-04
83701	'Srrt'	mRNA	0.229895	0.006426
83768	'Dpp7'	mRNA	-0.23605	0.030909
83965	'Enpp5'	mRNA	-0.20795	0.007656
84094	'Plvap'	mRNA	-0.82772	1.05E-10
84095	'Pi4k2a'	mRNA	-0.1835	0.019197
89867	'Sec16b'	mRNA	-0.30952	0.020896
93689	'Lmod1'	mRNA	-0.73526	0.03338
93692	'Glrx'	mRNA	-0.50386	0.002808
93695	'Gpnmb'	mRNA	-0.39396	5.79E-05
93703	'Pcdhgb6'	mRNA	5.002917	0.002177
93835	'Amn'	mRNA	2.226827	2.62E-06
93838	'Dqx1'	mRNA	1.350793	1.24E-06
93871	'Brwd1'	mRNA	-0.23734	0.006612
93898	'Cers1'	mRNA	-0.47459	0.03303
94180	'Acsbg1'	mRNA	0.375997	0.007827
94186	'Strn3'	mRNA	-0.16148	0.032917
94216	'Col4a6'	mRNA	-0.47984	3.43E-05
94227	'Pi15'	mRNA	-1.16165	5.08E-04
94315	'Prcc'	mRNA	0.233682	0.002088
94352	'Loxl2'	mRNA	-0.38304	2.54E-05
97064	'Wwtr1'	mRNA	-0.23263	0.038131
97112	'Nmd3'	mRNA	-0.24391	0.012641
97165	'Hmgb2'	mRNA	0.373015	0.006162
97287	'Mtmr14'	mRNA	0.26649	0.03636
98415	'Nucks1'	mRNA	0.388442	0.009243
98432	'Phlpp1'	mRNA	-0.27794	0.007501
98956	'Nat10'	mRNA	0.2191	0.043755
99382	'Abtb2'	mRNA	-0.53306	0.013853
99696	'Ankrd50'	mRNA	-0.28654	0.002432
99890	'Prmt6'	mRNA	-0.35693	0.020292
99899	'Ifi44'	mRNA	0.32693	0.023998